

University of Alberta

CHARACTERIZATION OF SILICA AND DISSOLVED ORGANIC MATTER
AGGREGATION IN SAGD PRODUCED WATER

by

Jannat Fatema

A thesis submitted to the Faculty of Graduate Studies and Research in
partial fulfillment of the requirements for the degree of

Master of Science

Department of Mechanical Engineering

©Jannat Fatema
Spring 2014
Edmonton, Alberta

Permission is hereby granted to the University of Alberta Libraries to reproduce single copies of this thesis and to lend or sell such copies for private, scholarly or scientific research purposes only. Where the thesis is converted to, or otherwise made available in digital form, the University of Alberta will advise potential users of the thesis of these terms.

The author reserves all other publication and other rights in association with the copyright in the thesis and, except as herein before provided, neither the thesis nor any substantial portion thereof may be printed or otherwise reproduced in any material form whatsoever without the author's prior written permission.

To my parents and my brother

Abstract

Proper understanding of SAGD produced water and boiler blow down (BBD) water in particular is required to propose effective treatment processes for reuse and reduction in the quantity of disposable water. BBD contains high dissolved organic matter (DOM) and total dissolved solid (TDS). This study investigates the interaction of silica and DOM in BBD using different analytical techniques. The roles of different types of organics, salts, and colloids on silica-DOM co-precipitation were studied at different concentrations and pH. In order to study the effects of all factors at three levels and to determine the most influential parameters with a minimum number of experiments Taguchi orthogonal array was employed. Analysis of variance (ANOVA) was performed to evaluate the contribution of each parameter. In the presence of salt, the rate of silica organic co-precipitation varies with the nature of organics. Humic-like fractions of DOM plays a major role in the process of DOM-silica co-precipitation. Light scattering technique applied to examine the aggregation rate at low concentrations of organics and DOM also demonstrates that the presence of organics enhances silica aggregation rate.

Keywords: DLS, particle size, ANOVA, Taguchi, Humic acids, SAGD produced water

Acknowledgements

During the last two years at this university I received enormous assistance and mental support from all my colleagues and friends towards the completion of this work. I was very fortunate for the opportunity to work with such a supportive group. Therefore, I would like to take this opportunity to thank them all.

Firstly, I would like to express my gratitude and appreciation to Dr. Subir Bhattacharjee for his guidance and support throughout my masters program. His expertise, great enthusiasm and dedication to research always inspired me through various challenges regarding my research.

I would like to take the opportunity to thank Dr. Abhijit Maiti for his technical input during my experiments, for answering many of my silly questions and above all for the editing of this thesis. I am grateful to Dr. Mohtada Sadrzadeh for his conceptual contributions and valuable technical suggestions. I can not say enough to thank Ni for providing me the technical trainings required for this study. Special thanks to Josie for her love and care towards all of us. I am very grateful to Mic for all his assistance and, more importantly, his friendship. I really appreciate his patience during many of those evenings when he had to listen to my naggings about research, career and life and his ability to turn them into positive consolation. I am indebted to Hadi, Mamun, and Behnam K for their selfless help and enjoyable discussions during my research work. Thanks to Ehsan, Behnam S, Shahab, Ishita, Ahsan, Samia and all my colleagues for always being very helpful and nice. I would also like to thank my friend Mohua for giving me the feel of family far away from home, here in Edmonton.

Above all, I am very thankful to my parents and my brother for their love and support and for always being there during my difficult times.

Contents

1	Introduction	1
1.1	Background	1
1.2	Objectives	3
1.3	Organization of the Thesis	4
2	Literature Review	7
2.1	Introduction	7
2.2	SAGD process basics	8
2.3	SAGD produced water characteristics	10
2.4	Natural Organic matter	11
2.5	Dissolved organic matter (DOM) in SAGD	13
2.6	Silica chemistry	14
2.7	Theory of colloidal silica stability	15
2.8	Silica and organics mixture	16
2.9	Design of experiments	17
2.10	Analysis of variance	20
2.11	Light scattering fundamentals	21
2.12	Study of aggregation rate using light scattering	24
2.13	Measurement of fractal dimension and stability ratio using light scattering	26
2.14	Challenges of light scattering	27
2.15	Summary	28
3	Experimental Method	33
3.1	Introduction	33
3.2	Materials	34
3.3	Simultaneous multi-angle static and dynamic light scattering (SMSDLS)	35
3.3.1	Calibration	37

3.3.2	Sample preparation for humic acid and silica mixture and fractal dimension measurement	37
3.3.3	Sample preparation for particle sizes measurement with time	38
3.4	Turbidity measurement	38
3.5	UV-Vis Spectroscopy	39
3.5.1	$SUVA_{254}$	39
3.6	Scanning electron microscope (SEM)	40
3.6.1	Sample preparation	40
3.7	Atomic force microscopy (AFM)	41
3.7.1	Sample preparation	41
3.8	Design of experiments	41
3.8.1	Sample preparation	42
3.9	Total organic carbon analyzer	43
3.10	Fluorescence Spectrophotometer	43
3.10.1	Sample preparation	44
3.11	X-ray photoelectron spectroscopy (XPS)	44
3.12	Fourier transform infrared spectroscopy (FTIR)	44
3.13	pH measurement	45
3.14	Potentiometric titration	45
3.15	Summary	45
4	Results and Discussion	48
4.1	Introduction	48
4.2	Examining aggregate size and shape	50
4.2.1	Surface imaging	50
4.2.2	Light scattering	52
4.2.3	Light scattering by humic acid	54
4.2.4	Static light scattering (SLS) of humic silica mixture	54
4.2.5	Aggregation rate	58
4.3	Application of Taguchi method	63
4.3.1	Selection of appropriate experimental matrix	65
4.3.2	Preliminary screening and selection of levels	66
4.3.3	Experimental matrix and results	67
4.3.4	Predicted response obtained using MINITAB	70
4.3.5	Effects of parameters at different levels	71
4.3.6	ANOVA	79

4.3.7	Interaction between parameters	83
4.3.8	Analysis of supernatant using $SUVA_{254}$	84
4.3.9	Analysis of supernatant using fluorescence spectroscopy	85
4.3.10	Analysis of supernatant using dynamic light scattering	90
4.3.11	Analysis of precipitates using X-ray photon spectroscopy (XPS)	91
4.4	Summary	91
5	Conclusions and Future Work	93
5.1	Concluding remarks	93
5.2	Future work	96
A	Calibration of light scattering instrument	111
B	Fractal dimension	122
C	Taguchi method	126
C.1	Standard Taguchi L_{18} orthogonal array	126
C.2	Standard operating procedure	128
C.3	DOM removal through silica organic co-precipitation images	134
C.4	Minitab Prediction	137
C.5	Comparison of autocorrelation functions	146
D	XPS analysis results	148

List of Tables

3.1	Factors and levels selected for Taguchi L_{18}	42
4.1	Screening experiments (all concentrations are in mg/L)	67
4.2	Experimental matrix (all concentrations are in mg/L)	68
4.3	DOM removal	69
4.4	Optimum condition	69
4.5	ANOVA table	80
4.6	$SUVA_{254}$ values (in $Lmg^{-1}m^{-1}$) of the samples	85
4.7	Comparison of scattering intensity	91
B.1	Fractal dimension	124

List of Figures

1.1	Motivation of the study	6
2.1	Silica silica interaction at different pH [Iler, 1979]	30
2.2	Silica organics interaction at different pH [Iler, 1979, Taheri et al., 2013]	31
2.3	Schematic diagram of light scattering technique	32
3.1	Flow chart of sequential experimental progress	47
4.1	SEM image of 150 mg/L Na_2SiO_3 and 0.1M $NaCl$ at pH 8 (a) without and (b) with 50 mg/L AHA and 100 mg/L <i>Snowtex</i> [®] ZL and 0.1M $NaCl$ at pH 8 (c) without and (d) with 50 mg/L AHA	51
4.2	AFM image of 150 mg/L Na_2SiO_3 and 0.1 M $NaCl$ at pH 8 a) without and b) with 50 mg/L AHA and 100 mg/L <i>Snowtex</i> [®] 20L and 0.1M $NaCl$ at pH 8 c) without and d) with 50 mg/L AHA	52
4.3	100 mg/L <i>Snowtex</i> [®] 20L and 0.1 M $NaCl$ with and without 50 mg/L AHA	56
4.4	150 mg/L Na_2SiO_3 and 0.1 M $NaCl$ with and without 50 mg/L AHA	57
4.5	Aggregation rate of 150 mg/L Na_2SiO_3 and 0.1 M $NaCl$ at pH 8 with and without 50 mg/L AHA	59
4.6	Aggregation rate of 150 mg/L Na_2SiO_3 and 0.1 M $NaCl$ at pH 3 with and without 50 mg/L AHA	60
4.7	Aggregation rate of 150 mg/L Na_2SiO_3 with 0.1 M $NaCl$ and 50 mg/L AEO at pH 8 and 3	61
4.8	Aggregation rate of 100 mg/L <i>Snowtex</i> [®] 20L and 0. 1 M $NaCl$ at pH 3 with and without 50 mg/L AHA	62
4.9	Steps followed for design of experiments	64

4.10	Main effects plot for means	72
4.11	FTIR spectrum of AHA	73
4.12	UV-Vis spectroscopy of Polystyrene sulfate latex	75
4.13	Potentiometric titration of AHA	77
4.14	Pareto chart	82
4.15	Interaction between organics type and pH	84
4.16	Fluorescence image of a) sample 1 (100 mg/L <i>Snowtex</i> [®] , 100 mg/L AHA, 0.01M <i>NaCl</i> at pH 3), b) 2 (250 mg/L <i>Snowtex</i> [®] , 250 mg/L AHA, 0.10M <i>CaCl</i> ₂ at pH 6), c) 3 (500 mg/L <i>Snowtex</i> [®] , 500 mg/L AHA, 0.25M <i>AlCl</i> ₃ at pH 9), d) 6 (500 mg/L <i>Snowtex</i> [®] , 100 mg/L AEO, 0.01M <i>AlCl</i> ₃ at pH 6)	87
4.17	Fluorescence image of e) sample 9(100 mg/L <i>Snowtex</i> [®] , 500 mg/L BBD, 0.10M <i>AlCl</i> ₃ at pH 3), f) 12 (250 mg/L latex, 250 mg/L AHA, 0.01M <i>AlCl</i> ₃ at pH 3), g) 15 (100 mg/L latex, 250 mg/L AEO, 0.25M <i>AlCl</i> ₃ at pH 6), h) 18 (250 mg/L latex, 100 mg/L BBD, 0.10M <i>AlCl</i> ₃ at pH 9)	88
4.18	Fluorescence image of optimum condition (250 mg/L <i>Snowtex</i> [®] , 100 mg/L AHA, 0.25M <i>AlCl</i> ₃ at pH 3)	89
A.1	Scattering intensity from dynamic light scattering at 90° of <i>Snowtex</i> [®] 20L at different concentrations	112
A.2	Scattering intensity from static light scattering of <i>Snowtex</i> [®] 20L at different concentrations	113
A.3	Turbidity of <i>Snowtex</i> [®] 20L at different concentrations	114
A.4	Scattering intensity from dynamic light scattering at 90° of 100 mg/L <i>Snowtex</i> [®] 20L at different pH	115
A.5	Turbidity of 100 mg/L <i>Snowtex</i> [®] 20L at different pH	116
A.6	Comparison of normalized scattering intensity of <i>Snowtex</i> [®] 20L and <i>Na</i> ₂ <i>SiO</i> ₃	117
A.7	Scattering intensity from dynamic light scattering at 90° of <i>Na</i> ₂ <i>SiO</i> ₃ at different concentrations	118
A.8	Scattering intensity from dynamic light scattering at 90° of <i>Na</i> ₂ <i>SiO</i> ₃ (12200 mg/L) at different pH	119
A.9	Turbidity of <i>Na</i> ₂ <i>SiO</i> ₃ (12200 mg/L) at different pH	120
A.10	<i>Na</i> ₂ <i>SiO</i> ₃ (12200 mg/L) at different pH	120
A.11	Static light scattering at different angles by AHA at different pH and concentrations	121

B.1	Fractal dimension measurement of 100 <i>mg/L</i> <i>Snowtex</i> [®] 20L and 0.1 M <i>NaCl</i> with 50 <i>mg/L</i> AHA at pH 3	123
-----	---	-----

Chapter 1

Introduction

1.1 Background

In terms of worlds crude oil reserve, Alberta is in the third position after Saudi Arabia and Venezuela with initial in-place reserves of 1.73 trillion barrels [Wang and Kasperski, 2010] and ultimate potential reserve of 0.31 trillion barrels [Masliyah and Xu, 2011]. Oil sands deposit in Athabasca region is the energy center of Alberta and major alternative for declining conventional oil reserve. Crude bitumen production in Alberta is estimated to reach upto 470,000 cubic meter per day by the year 2018 from 207,600 cubic meter per day in the year 2008 [Masliyah and Xu, 2011]. This huge economy of scale of oil sands processing has some environmental impact as well, in terms of land use, water consumption, carbon dioxide emission and land reclamation. Bitumen production by both surface mining and in-situ extraction requires utilization of huge volume of water. Water as a finite natural resource requires proper management.

Most popular in-situ process used at present is steam assisted gravity drainage (SAGD) recovery process [Butler, 1998] and it requires 2.5 to 4 barrel water to produce one barrel heavy crude oil. In mining operation for every barrel of heavy crude oil 8 to 10 barrel water is required. Although in mining process 40% to 70 % and in SAGD 70% to 90% water is recycled, the volume of water consumed by oil sands industry for make up water is still a huge quantity (170 million cubic meter in 2011 [Mikula et al., 2008]). Make-up water required for per barrel of bitumen for SAGD operation is 0.5 barrel and 2.5 to 4 barrel for mining. Some water is can be lost during recycling. SAGD

profitability is subjected to steam to oil ratio i.e water usage, water quality requirement for plant and environmental regulations [Jennings and Shaikh, 2007, Pedenaud et al., 2006].

Water recycling and treatment plant at SAGD facility is consist of warm lime softening, filtration and weak acid cation exchanger. Use of mechanical vapor compression evaporation for water recycling is also under consideration by some companies [Heins, 2010]. Once through steam generator (OTSG) used for steam generation at SAGD plant, can handle higher TDS and organic content in feed water, but produces larger volume of boiler blow down (BBD) water compared to a standard boiler [Thakurta et al., 2013]. Treatment and disposal of this water imposes greater effect on SAGD economics. To make the process technically and economically feasible, proper understanding of the process and the parameters involved is important. Organics in BBD has broad molecular distribution, aromaticity and functional group [Petersen and Grade, 2011, Thakurta et al., 2013]. This characteristic made the understanding of silica and organics interaction in BBD more difficult. Although there is several research that examined organic matter present in conventional oil field produced water, there is a lack of information regarding physicochemical characteristics of SAGD produced water and BBD water.

BBD water has high dissolved solid and organic matter through leaching from oil sands. Presence of ions and change of pH during the recycling process facilitates silica and organic aggregation and scaling. So, pH and concentration of silica and salt are important factors causing silica-organic co-precipitation. At low pH and high salt concentration aggregation is higher compared to higher pH (9) and lower salt concentration [Singh and Song, 2007a]. Formation of scaling on heat exchanger, economizer, pipeline or other plant equipment surface leads to plant equipments fouling and loss of efficiency [Luo et al., 2012]. This study is an effort to understand the role of different fractions of dissolved organic matter (DOM) on silica-organic scale formation and to present a framework to quantify the magnitude of influence of each factors.

In order to address enhanced aggregation and fouling problem caused by SAGD produced water, specially BBD water, a combination of different laboratory based analytical techniques and statistical quality control tool was employed in this study. To quantify the affects of different operating conditions

on interaction between organics from BBD and silica, the parameters selected were, pH, types of salt, organics, and colloids, three concentrations of salt, organics, and colloids. Since this problem has several parameters at different levels, design of experiments was required to identify significant parameters with minimum number of experiments and cost. Taguchi L_{18} orthogonal array was selected as appropriate design for the experiments. Total organic carbon (TOC) analyzer was used to measure DOM removal. Then fluorescence excitation emission matrix and UV-Vis absorbance spectroscopy techniques were used to understand the characteristics of treated water. Light scattering technique was also used to understand the aggregation behavior of silica and organics at lower concentrations of organics and silica. The findings of this research work will provide a mean to classify the major "perpetrators" and their level of influences responsible for enhanced fouling using limited number of experiments. Quantification of contribution by each parameter will lay down the way to improved and economically efficient water treatment process.

1.2 Objectives

In the context of above discussion the aim of this work is to develop an understanding of the effect of process parameters, which are: type of organic, pH, salt concentration, coagulant dose, concentration of silica, concentration of organics on enhanced silica-organics aggregation. The specific objectives of this study are:

- Combine silica-organics chemistry with statistical tool to develop an efficient system to characterize SAGD produced water and specifically boiler blow down water with minimum number of experimental analysis and hence cost.
- Examine the role of pH, concentration of silica and organics, types of organics, concentration and type of cations to accelerate silica-organics aggregation.
- Determine which factors facilitate the silica-organics co-precipitation mostly in SAGD plant environment.
- Identify the condition at which silica organics aggregation is optimum.

- Quantify the contribution of each factor into silica-organics co-precipitation.
- Examine the role of different fractions of DOM from BBD on silica-organics aggregation.
- Examine the application of light scattering technique to understand the aggregation rate, aggregate size and shape of the silica-organics co-precipitated products at dilute concentrations.

1.3 Organization of the Thesis

In this study Aldrich humic acid (AHA) was used as model organic acid. Also acid extractable organics (AEO) prepared from BBD water, and raw BBD from SAGD plant was used as organics sample. *Snowtex*[®] ZL (100 nm) and 20L (80 nm) and polystyrene sulfate latex (100 nm) were used as representative colloids. Sodium meta silicate (Na_2SiO_3) was also used to examine affect of dissolved silica on organics precipitation. Effect of three types of salt namely $NaCl$, $CaCl_2$ and $AlCl_3$ at different concentrations was also studied. Experiments were designed using Taguchi L_{18} orthogonal array to quantify the affect of pH, concentrations, and types of organics, colloids, and salts on silica-organics aggregation. Light scattering technique, scanning electron microscope and atomic force microscopy were employed to understand the aggregation rate and particle shape of silica-organics aggregates. To determine organics removal rate after co-precipitation of silica and organics, samples were analyzed using TOC analyzer. Dynamic light scattering, $SUV A_{254}$, fluorescence spectroscopy, and X-ray photoelectron spectroscopy were applied to discover and categorize which organics fraction has precipitated and which remained in solution after aggregation.

This thesis is divided into five chapters, providing an overall idea of the background of the problem and literature review related to the area, experimental procedure, followed by results and major findings of the work and finally scope of future work.

In the present chapter, a general introduction and relevant facts related to enhanced aggregation and fouling due to presence of high silica and organics concentrations in BBD water were presented. The motivation, objectives and

scope as well as an overview of experimental work done for this research work were also outlined in this chapter.

Chapter 2 outlined the noteworthy factors related to water treatment process of present SAGD plant. This chapter also provides a detail literature review on design of experiments, Taguchi orthogonal array and analysis of variance. Light scattering technique, colloidal interaction, behavior of silica in suspension, organics and silica co-precipitation mechanism etc. were also explained briefly in this chapter.

Chapter 3 describes the details of sample preparation, materials used and experimental procedure associated with the Taguchi L_{18} and light scattering experiments. This chapter also includes description and principle of the instruments used and a flow-chart of experimental steps.

Chapter 4 comprises the experimental matrix for Taguchi L_{18} along with the discussions on the results obtained from these experiments. This chapter investigates effect of each parameter to find out the optimum condition for silica-organics co-precipitation. The quantitative contribution of each factors at each level are also documented. Aggregate shape and size of silica organic mixture is also presented in this chapter.

Finally in Chapter 5, summary of the present work is presented along with the direction of future work of the research involving further improvement in this field.

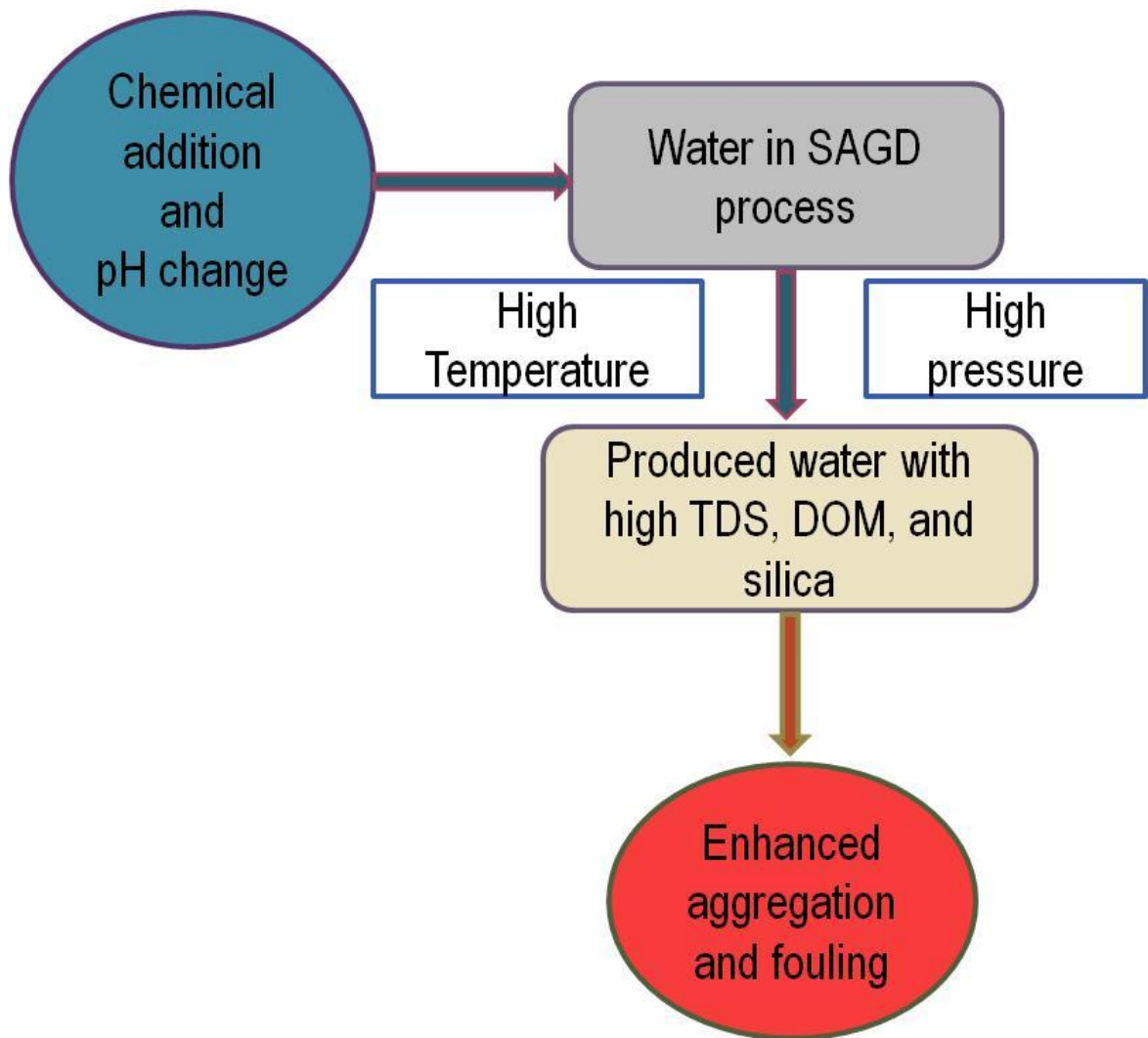


Figure 1.1 – Motivation of the study

Chapter 2

Literature Review

2.1 Introduction

Only 20% of the Canadas oil-sands deposit can be extracted by surface mining. Rest of the deposit is too deep for surface mining [Czarnecki et al., 2005]. To extract bitumen from these type of deposits different in-situ thermal recovery techniques are used by oil sands companies. Steam assisted gravity drainage (SAGD) is probably the most popular in-situ technique [Butler, 1998]. A thin film of neutral or slightly alkaline nature water called connate water separates silica sand grain from bitumen [Czarnecki et al., 2005]. This nature of Athabasca oil sands made easier to extract it using steam. In this process huge volume of water is used in boiler to produce steam. Water in a SAGD plant goes through several recycling process at high temperature and high alkaline pH operating condition. After several cycles, a large quantity of water (at least 20% of feed water) becomes unusable for boiler due to very high content of dissolved solids and organics [Thakurta et al., 2013]. Zero discharge policy imposed by the Government does not allow this water to be discharged into open environment. This has to be either treated to certain level or solidified and disposed into underground. Use of evaporative method or brine concentrator to produce distilled water and crystallizers to solidify the residue from brine concentrator is cost-intensive [Heins and Schooley, 2004]. Use of traditional water treatment process with membrane filtration is also a challenge because of combine fouling caused by silica and organics in oil sands process-affected waters (OSPW) [Kim et al., 2011]. In the presence of organics, silica can be aggregated at a certain pH to cause membrane failure. Examination of change in particle size at different pH and concentration can

give an idea about the conditions responsible for organic fouling of membrane and other equipments. Also identification of the most influential factor for silica-organics co-precipitation is required. In this study Taguchi method for design of experiments were employed to determine the optimum condition of parameters for aggregation and to examine role of humic substances on silica-DOM aggregation. Light scattering technique was used to study the aggregate size and shape at low concentration of organics and silica. This chapter gives a concise idea about SAGD process and oil sands produced water quality, silica and organics chemistry, Taguchi method followed by brief discussion on light scattering technique.

2.2 SAGD process basics

Compared to remaining conventional oil reserve, deposit of heavy oil bitumen resource is large [Butler, 2001] in Canada. There is 22 billion cubic meter bitumen reserve in three major deposits is Athabasca, cold lake, and Peace river [Prada and Cunha, 2008, Nasr and Ayodele, 2005]. Exploitation of this resource is required, otherwise oil has to be imported which will impart huge cost on country's economy. Since only 20% of the reserve can be extracted by open pit mining, for the rest 80% , with overburden greater than 200 meter different in-situ mining processes are used. There are different in situ techniques [Nasr and Ayodele, 2005] like SAGD, steam flooding, cyclic steam stimulation, in-situ combustion etc. At present, SAGD is the most popular in-situ extraction method with reduced cost and improved production Butler. In this process two horizontal wells, production and injection well, are drilled into the oil formation. Saturated steam is passed through the injection well, which is located 5 meter above the production well. Steam reduces the viscosity of bitumen (which is originally 500 Pa.s at room temperature) and it starts to flow due to gravity through the production well [Butler, 1998]. Bitumen is later separated from the bitumen water mixture. SAGD is most likely the most efficient thermal recovery method [Prada and Cunha, 2008]. Some large scale SAGD projects are, Suncor firebag project, Suncor Mackay river project, Pan Canadian Petroleum Christina lake project etc. [Butler, 2001].

There are several research work that reviewed technical aspect and performance analysis of SAGD [Edmunds et al., 1994, Heins and Schooley, 2004].

Efficiency of SAGD depends on reservoir characteristics, reservoir pressure, thickness, porosity, oil viscosity, oil thermal conductivity, methane gas mole fraction, depth to top distance etc. Depending on these factors operating pressure and maximum steam injection rate are decided. For a typical Fort McMurray reserve low pressure are favoured as they lead to low temperature and low steam consumption [Edmunds and Chhina, 2001]. According to Shin and Polikar [Shin and Polikar, 2005] optimum condition for SAGD operation is at 1500 *kPa* injection pressure and 700 m^3/d steam injection rate. Operating pressure should be higher before steam chamber contacts overburden, after contact injection pressure can be lowered to reduce heat and increase thermal efficiency [Gates and Chakrabarty, 2006]. Limitations of SAGD process are rising cost of fuel, increasing differential of heavy and light oil price, recycling and disposal of produced water [Butler, 2001]. For better recovery, alternatives under consideration are, solvent vapor extraction (VAPEX) or mixing of steam with propane low pressure [Deng, 2005].

Steam and oil ratio is used as indicator to evaluate SAGD [Shin and Polikar, 2005]. Economics of SAGD depends on steam to oil ratio. If gas price increases, steam to oil ratio increases and SAGD operation becomes unprofitable [Butler, 1998]. Steam to oil ratio is normally between 2 to 4, which means for each barrel of bitumen 2 to 4 barrel steam is required [Pedenaud et al., 2006]. High steam generation cost coupled with low bitumen price will reduce SAGD profitability. SAGD will be technically effective if steam to oil ratio is optimized [Gates and Chakrabarty, 2006]. Besides, recycling and disposal of water is another problem. Water supply and disposal can impose severe economic limitation on SAGD operation.

In SAGD process once through steam generator (OTSG) is used for steam generation. OTSG requires less maintenance and can tolerate fairly hard water with a high content of soluble solid, monovalent cation and silica. Leaching of solid and organics from oil sands deposit creates silica scale build up [Pedenaud et al., 2006] in boiler or other equipments. When feed water contains more than 100 *mg/L* silica there is a risk of silica deposition in OTSG. After several circulation silica concentration increases up to 400 *mg/L* [Pedenaud et al., 2006]. Silica can be in two forms- amorphous silicon monomer of SiO_2 and colloidal silica which cannot pass through 0.45 μ filter. When water evaporates, amorphous silica polymerize to colloidal silica and adhere inside tube.

Complete silica removal, specially colloidal or polymerized silica removal is expensive and difficult. Deposition of silica scale increases local thermal stress, which leads to tube failure and reduced efficiency [Pedenaud et al., 2006]. This will also increase steam to oil ratio.

2.3 SAGD produced water characteristics

Huge volume of water in the form of steam is used for enhanced oil recovery from the deposit which is 200-500 meter below the surface [Masliyah and Xu, 2011]. 70 to 90 % of this water is recycled as boiler feed water. Produced water recycling in SAGD is consists of de-oiling by gravity skim tanks and induced static flotation (ISF), warm lime softening (WLS) to remove silica and hardness, filtration to remove suspended solids, and weak-acid cation exchange (WAC) to remove calcium (Ca^{2+}) and magnesium (Mg^{2+}) ions. pH varies from 8 to 10 for different SAGD process water [Kawaguchi et al., 2012]. But BBD pH is generally 10 to 12. As OTSGs use high TDS feed water it produces higher volume of boiler blow down (BBD) compared to standard boilers [Thakurta et al., 2013]. Concentration of organics content increases in successive stages [Kawaguchi et al., 2012]. Dissolved organic carbon (DOC) is very high (2000 mg/L) in boiler blow down, make-up water in the process contains 4 mg/L DOC [Kawaguchi et al., 2012]. The ion exchange fractionation of BBD revealed that the DOM contains a high percentage of hydrophobic acids (39%) and hydrophilic neutrals (28.5%) [Thakurta et al., 2013]. Hydrophobic fraction of BBD is mainly humic-like organic acids. Although BBD has slightly higher Na^+ concentration (0.1M), concentration of Ca^{2+} , Mg^{2+} , Al^{3+} is less than 0.001M.

A portion of the BBD is recycled back to the WLS process and the rest is disposed. Accumulation of silica and organic contaminants in this type of water is a major problem for water treatment plants. Deposition of silica as silicates with metal ions, causes fouling of the plant equipment, affects the plant's performance and failure of the equipment. Silica and organics combined fouling is a major issue in membrane based water treatment plants [Maiti et al., 2012]. Water recycling technology is required to be developed rapidly to meet the water management needs of SAGD processes [Heins, 2010].

2.4 Natural Organic matter

Natural organic matter (NOM) has molar mass of colloidal size range and are different in functional group, elements and perhaps size depending on the source (soil, fresh water and marine system), which make them hard to eliminate completely from water [Metsmuuronen et al., 2014]. Dissolved organic matters (DOM) are referred to the portion of the NOM that passes through 0.45μ filter. In this study, all the organics samples were passed through 0.45μ filter and only DOM portion of organics were considered. Major portion of DOM is humic substances [Tipping, 2002]. There are three major fraction of humic substances: humic acids (precipitates out of solution below pH 2), Humin (water insoluble in all pH values), fulvic acid (soluble in all pH values) [Manning et al., 2000]. Aquatic humic and fulvic acids are smaller and less poly dispersed than their soil counterpart [Sutton and Sposito, 2005]. Soil humic acids are poly dispersed and have a degree of aggregation depending on pH [Sutton and Sposito, 2005]. Humic acids has aliphatic, aromatic as well as carboxylic acid, amine, carbonyl and alcohol functional group. Humic acids is soluble in base and insoluble in acid [Tipping, 2002]. Fulvic acid is hydrophilic and soluble in both acid and base, humin fraction is not soluble in base and acid. Fulvic acid forms structure more quickly than humic acids [Sutton and Sposito, 2005] as humic acid has fewer proton dissociating group than fulvic fraction. Humic acids (HA) in aqueous solution are negatively charged due to protonation of carboxylic and phenolic functional group [Tipping, 2002]. New concept of humic substances molecular structure is that, small and chemically diverse organic molecules form clusters by hydrogen bonds and hydrophobic interactions. Formation of micellar structure is also possible in aqueous solution with hydrophilic exterior shielding the hydrophobic interior under neutral to acidic pH. High molecular weight of humics represents aggregation of small monomer unit through hydrogen bonding and hydrophobic interaction. There are two types of binding in HA, site and territorial binding. In site binding ions are bound to one particular functional group. This involves electrostatic interaction between COO^- functional group and a cation. In territorial binding the species are trapped within large structure but there is no binding to a specific site [Manning et al., 2000]. Binding of ions neutralizes the negative charge of humic acids.

Humic substances are fluorescent and strongly absorb UV light [Wagoner et al., 1997]. Humic substances has two main fluorophore, one excites at 315-390 *nm* (carboxyphenol), another at 415 to 470 *nm*. Higher fluorescence means higher proton dissociation. Specific UV absorbance at 254 *nm* value greater than 4 means presence hydrophobic anionic group, less than 4 means hydrpphilic anionic group [Matilainen et al., 2011]. Some organic compounds have both hydrophobic and hydrophilic [Tipping, 2002] groups. Protein and amino acid are the dominant chemical forms of Nitrogen in humic substances [Sutton and Sposito, 2005].

Organic molecules can interact to each other through hydrophobic interaction, cation exchange, H bonding, metal cation bridging, dipole-dipole forces, van der Waals, covalent bonding [Parida et al., 2006]. Adsorption of cation occurs at pKa of organics and proton dissociation constant of surface OH group. At low pH proton binding reduces charge, hydrophobic fraction will aggregate and precipitate. At pH around 2, organics have zero charge and as a result it will precipitate by forming aggregates. However, hydrophilic fraction of organic will still be in water even if it has zero charge. Consequently, at low pH, hydrophilic fulvic acid remains in water while hydrophobic humic acid precipitates.

Humic substances have branched open network in fresh water but with increased salinity their compactness increases. Types of cations also have different effects. Compared to monovalent Na^+ , divalent Ca^{2+} is more effective. Ca^{2+} binding with organic is significant at pH 8 due to both electrostatic and non electrostatic forces [Furman et al., 2013]. Humic substances may have both hydrophobic and hydrophilic parts composed of carboxylic group [Baalousha et al., 2006]. Suwannee river humic acid (SRHA) contains 9.59 mol *C/kg* of carboxylic group, which dissociates at pH 4.42 and 4.24 mol *C/kg* phenolic group which dissociates at pH 9.68. Surface charge increases from pH 4.5 to pH 10. Presence of SRHA increase aggregation of silica as salt concentration increases [Sutton and Sposito, 2005]. This is may be due to increasing hydrophobic microsities with decreasing pH [Sutton and Sposito, 2005].

Humic acids are negatively charged poly-electrolytes and they are adsorbed on silica surface by electrostatic attraction, legand-exchange with protonated

surface hydroxyl group, cation bridging, water bridging in the presence of hydrated cations on the surface, hydrophobic interaction of uncharged macromolecules of humic acid. Main mechanism of adsorption of DOM on metal oxide is complex formation between organics legands and the surface charge site of iron oxides, but Coulombic attraction between the oppositely charges particles can also cause coagulation under suitable condition [Illes and Tombacz, 2006]. At acidic condition adsorbed humic acid on silica surface causes charge reversal that in turn causes coagulation [Majzik and Tombacz, 2007]. Magnitude of repulsive force between same charged ions is a function of distance of separation, valence, concentration of counterions and net surface charge. Mixing of silica and humic acid reduces net surface charge i.e. zeta potential [Taheri et al., 2013]. At pH around 7, zeta potential of humic acid is negative and higher than silica at same pH. But mixture of these two has less surface potential than humic acid alone. At high pH humic molecules are large, flexible and linear shape. Diffusivity of humic acids increases with decreasing pH and increasing calcium concentration, which increases compaction of humic acid molecules at low pH and high ionic strength. At low pH, high ionic strength and high humic concentration they become rigid sphere either due to neutralization of COOH and OH groups or due to complexation of humic acids with calcium ion [Wang et al., 2001]. Aggregation rate is higher at the diffusion limited regime with increase in salt concentration due to formation of complex by colloidal particles with carboxylic group of humic acids molecules through bridging by Ca^{2+} ions [Abe et al., 2011]

2.5 Dissolved organic matter (DOM) in SAGD

Dissolved organic matter (DOM) in SAGD produced water has different characteristics due to different extraction process and oil-sands characteristics [Thakurta, 2012]. There is a lack of information regarding SAGD-DOM. Previous work from the group has found that DOM in SAGD-BBD has six major fractions [Thakurta et al., 2013]. These are hydrophobic acid, base and neutral, and hydrophilic acid, base, and neutral. Among these six fractions hydrophobic acid, hydrophobic neutral, and hydrophilic neutral are the major fractions. Since there is not enough information regarding characterization techniques for SAGD-DOM available in literature, available techniques for NOM characterization were used in this study to examine SAGD-DOM. Previous works from the group has also found that these techniques are applicable to study

different concentrations of DOM in SAGD produced water [Thakurta, 2012].

2.6 Silica chemistry

Stability of soluble silica solution depends on pH and concentration [Nordström et al., 2011]. This is because solubility of silica is a function of pH and concentration [Iler, 1979]. Solubility decreases as pH decreased and increases above 9. The increase in the total soluble silica at high pH is due to formation of highly soluble silicate ions [Sheikholeslami et al., 2002, Alexander et al., 1954]. Soluble silica in water is either at monomeric state as monosilicic acid ($Si(OH)_4$) or polysilicic acid or colloidal silica particles, which are mostly un-ionized at natural pH levels. At neutral pH values, presence of metals facilitates silica polymerization [Sheikholeslami et al., 2002].

Above pH 9.0 silica solution is stable at room temperature for a long time. But at pH 9.0 silica nucleation and aggregation starts at a fast pace. At a higher temperature (80°C) aggregation occurs even below pH 8 [Baldyga et al., 2012, Tang et al., 1988, Iler, 1979]. Concentration of ionic species and their surface potential is very important parameter for aggregation. Na^+ or Ca^{2+} ions adsorbed on the surface reduces the surface charge and accelerates aggregation [Iler, 1979, Gorrepati et al., 2010]. At acidic pH H^+ build inter particle bridges [Baldyga et al., 2012]. Aggregation of silica occurs by formation of siloxane through condensation of silanol group [Iler, 1979]. Aggregates in more concentrated solution has broader particle size distribution and at pH 7.5 to 10 polymerization is also faster compared to dilute solutions [Iler, 1979]. Figure 2.1 and 2.2 shows silica-silica and silica-organics interaction at different pH.

pH and concentration dependent behavior of silica aggregation is very important phenomenon for industrial scale water treatment plants, membrane, boiler, heat exchanger or other equipments [Gill, 1993]. At higher pH values and at the presence of metal ions, silica forms aggregates, precipitates as viscous silicates on the membrane surface. As water drains out they finally forms hard cement like scales [Gorrepati et al., 2010, Sheikholeslami et al., 2002]. This leads to limited efficiency of many installations and increases operating costs. Characteristics of water specially, concentration of silica, pH, presence

of cations, operating conditions and pretreatment of water are important aspects for fouling reduction of equipments by silica bearing waters. Therefore, it is essential to understand the conditions that affect silica polymerization and identify the suitable techniques for reducing silica concentration in feed water to an acceptable limit before entering into the main treatment facility [Sheikholeslami et al., 2002].

2.7 Theory of colloidal silica stability

A system with very small particles dispersed in a continuous phase is called colloidal suspension. Small particles have large surface area, as a result, surface phenomena controls the properties of a colloidal system. In a colloidal system with water as continuous phase, colloids carries electrical charge [Masliyah and Xu, 2011]. There are several mechanism which causes change of surface charge of colloidal particles [Kobayashi et al., 2005]. Change of pH or adsorption of counter ions results in alteration of surface charge. Increase in electrolyte concentration leads to negative energy barrier and van de Waals attractive force becomes dominant. The theory of Derjaguin, Landau, Verwey, and Overbeek (DLVO) explains particle interactions in a suspension through repulsive double-layer overlap forces and an attractive dispersion (van der Waals) force. DLVO theory can also predict aggregation rate and stability ratio through critical coagulation concentration (CCC), which separates slow and fast aggregation region. However, in the slow regime the application of DLVO is restricted to weakly charged system. For example, for nano sized silica particles CCC cannot be predicted correctly through DLVO theory although it works correctly for sub-micrometer sized silica particles [Masliyah and Xu, 2011].

As opposite charged ions attracts each other there will be net excess of positive charges near a negatively charged ion as a mobile diffused layer. Negatively charged solid surface and positive charges from the bulk forms two plates which is called electric double layer (EDL) [Masliyah and Xu, 2011]. Concentration of electrolyte determines the thickness of double layer. On the other hand, double layer thickness determines range of repulsive forces resulting from surface charge. Higher surface charge means higher repulsion [Masliyah and Xu, 2011]. Since surface charge cannot be measured, zeta po-

tential of a slip plane is used as a measure of surface charge. Increase in salt concentration decreases the double layer thickness. Valence of counter ions also has a dominant effect on colloidal stability as effectiveness of counter ions increases with its valence [Masliyah and Xu, 2011]. Adsorption of counter ions alters the surface charge and particles can come closer. As a result van der Waals energy becomes dominant as separation distance reduces. So particle particle interaction energy is small and negative at larger distance. As they approach to each other van der Waals attraction becomes stronger. As a result a weak doublet forms, which does not have enough thermal energy to keep the particles together [Kobayashi et al., 2005]. But if the double layer thickness is reduced further there will be sufficient attractive force to keep them together, colloidal system will become unstable. Brownian motion imparted to the colloidal particle by the thermal motion of the solvent molecules or application of external energy increases collision frequency, particles come closer to each other and leads to the aggregation. Stability ratio of a colloidal system is the ratio of number of collisions and the number of effective collisions [Masliyah and Xu, 2011, Masliyah and Bhattacharjee, 2006].

2.8 Silica and organics mixture

In a colloidal system with silica and water, silica forms silicic acid. Silicic acid dissociates into silicic anion and H^+ ions leading to a negatively charged silica surface [Iler, 1979]. This process is reversible and charge of the silica surface varies depending on pH. At high pH concentration of H^+ is low so silica is more negatively charged. But at low pH silica surface is positively charged. On the other hand, organics acids in water also becomes negatively charged as pH reaches to the pKa values of its functional groups [Metsmuuronen et al., 2014]. So both silica and organics surface charge depends on pH [Iler, 1979, Metsmuuronen et al., 2014]. Surface charge of these two can be controlled by pH and adsorption of ions. At higher pH or surface charge, repulsive force is dominant so aggregation is reduced. As a result, at higher zeta potential lower aggregation rate and at higher ionic strength higher aggregation rate is observed [Singh and Song, 2007b]. Adsorption of Ca^{2+} or Al^{3+} ions on organics surface make them less negatively charged. Coagulants also compress double layer thickness just like electrolytes. At critical coagulation

concentration (CCC), energy barrier becomes zero and stability ratio becomes 1, which directs towards rapid coagulation and an increase in the particle average size[Masliyah and Xu, 2011, Masliyah and Bhattacharjee, 2006].

2.9 Design of experiments

Optimization can be defined as the process of finding the right design parameters at right level [Beyer and Sendhoff, 2007]. In order to identify optimum process parameter or to test a hypothesis with minimum cost and effort design of experiments is required [Kim and Shahinpoor, 2003]. A full factorial design problem with several factors at several levels will yield a large number of experiments and hence cost. Use of fractional factorial design can minimize the cost effectively. The method of fractional factorial design of experiments provided by Sir Ronald A. Fisher in his books in 1920s [Maghsoodloo et al., 2004] is consists of randomization, replication, orthogonality and factorial design. Orthogonal arrays (OAs) for factorial design were also first developed by Fisher (1920) and Tippett in 1934 [Reyhani et al., 2013, Sadrzadeh et al., 2007]. Japanese engineer Genichi Taguchi modified these OAs to user friendly standard table so that engineers with some basic knowledge in industry can customize it easily for their problem and identify significant process parameters [Maghsoodloo et al., 2004].

Loss occurs to society when a critical quality characteristic deviates from its target value. Some losses are due to control factors, some are due to uncontrollable or noise factors that causes control factors to deviate. Human error or temperature can be example of these type of factors. Quality should be addressed at the engineering stage before production. This is considered as key to achieve high quality product with low cost. Aim of quality engineering is to make products that are robust with respect to all noise factors [Ghani et al., 2004]. Through robust design and optimization, reduction of variability from target value is possible [Ghani et al., 2004]. Robust design is the selection of design parameter tolerances in such a way that the product will work under a wide variety of field conditions [Montgomery, 2013]. Objectives of robust design are a) identify control factors that affects process variability, identify signal factors that has impact on mean response and weak factors with

no impacts on mean or variability, b) to optimize levels of the control factors to reduce process variation, and finally c) move mean response towards target using signal factors. Taguchi has contributed to both quality engineering and statistical field through his robust design concept, quality loss function, signal to noise ratio (S/N) and orthogonal arrays (OA). S/N ratio measures the deviation of quality characteristics from desired value and combines both mean and standard deviation into one measure in data analysis. Taguchi loss function quantifies the quality [Maghsoodloo et al., 2004] and focuses on determining the parameter settings at the best levels of a quality characteristics [Park et al., 2006].

In order to optimize process condition Taguchi uses tighter factor tolerances which significantly reduces process variation [Maghsoodloo et al., 2004, Chen et al., 1996]. In Taguchi designs quality is determined by deviation of each factor from the target [Ng and Ng, 2006]. Taguchi is a powerful and efficient method for designing a process that operates consistently and optimally over a variety of conditions [Bhattacharya et al., 2009]. Taguchi methods are considered as quality improvement tools among other like six sigma, ISO 9000, total quality management used in manufacturing industry. Taguchi is a simple and systematic tool used for robust design to optimize design performance [Shojaeefard et al., 2013].

In this study Taguchi OA was used to simplify and standardize the experimental design by minimizing the number of parameter level combination. In full factorial design all possible combinations of two or more factors each with discrete levels are used. Experiments with multiple factors is time consuming and very expensive. Sometimes application of full factorial design is not possible when many factors and levels are involved [Mohammadi et al., 2004b] and requires factorial design in order to reduce cost and improve efficiency. Fractional design which is a subset of full factorial design utilizes a fraction of total combination to minimize time and cost [Sadeghi et al., 2012]. If we want do a full factorial design with 9 factors all at 3 levels we have to perform 19,683 experiments. But use of OA can reduce the number to 21 [Cobb and Clarkson, 1994]. In an OA, as many as parameters involved and are most likely to affect mean response are arranged at different levels. A matrix can be called orthogonal if it is diagonalized through linear transformation [Maghsoodloo et al., 2004]. All pair of combinations occurs at same number in an OA [Cobb

and Clarkson, 1994]. A balanced OA will have same number of treatment for all levels. None of the treatment are same or even mirror image [Sadrzadeh and Mohammadi, 2008].

Advantages of OAs are, significant factors and optimum condition can be identified quickly with less effort [Ramkumar and Ragupathy, 2013]. With the help of Taguchi OA it is possible to find the impact of different factors or parameters, identify most influential factors and levels, minimize effects of noise factors with minimum cost and higher process reliability [Montgomery, 2013]. Three objectives can be achieved by Taguchi OA: optimize design parameters, estimate the contribution of each parameter, predict optimal quality characteristic [Yang and Tarng, 1998] The limitation of Taguchi method is for a system with non-linear characteristic, it is not statistically efficient [Chen et al., 1996].

Taguchi has modified a number of OAs. Most frequently used OAs are L_{12} , L_{16} , L_{18} , L_{27} etc. L_{18} is a mixed level OA with one factor at two levels and seven factors at three levels. Orthogonality of L_{18} will persist even if one column is unused [Yang and Tarng, 1998]. L_{18} OA has first three columns which are written randomly. According to Kamyshny et al. [Maghsoodloo et al., 2004] rest of the columns are orthogonal although they are not unique. They showed that there are 11 possible combinations for these five columns. The L_{18} matrix has total 17 ($18-1=17$) degrees of freedom (DOF). First column with two levels can use one degree of freedom (DOF). Other seven factors will use 14 ($7 \times (3-1)=14$) DOFs, which leaves only two DOFs for interaction. So this matrix can be only used to examine interaction between column 1 and 2 [Maghsoodloo et al., 2004]. Evidently, Taguchi OAs are not designed to study interaction between factors.

In experimental design using Taguchi method, confirmation tests are performed to compare predicted results with real experiments. Robust design is achieved if prediction matches with real data. If prediction does not match with experimental results, it means selection of levels for factors were not appropriate. So same procedure has to be repeated after setting the parameters to appropriate levels. Taguchi method has been employed to optimize different problems, varying from soil erosion [Sadeghi et al., 2012] problem to manufacturing of electronic consumer products [Huang and Tai, 2001]. Reyhani et al.

[Reyhani et al., 2013] used Taguchi L_9 OA and TOC analysis to examine performance of ultra filtration membrane for produced water, which contained oil, salt, emulsifier, and dissolved solids. Quality of permeates were tested using analytical techniques which showed 100% removal of organics. Although 100% removal of organics is difficult but through application of Taguchi method identification of important factors that can reduce the concentration of organics to acceptable limit was possible. Sadeghi et al. [Sadeghi et al., 2012] was able to model soil erosion problem using L_{16} OA. To optimize design parameters as many as factors possible should be included. Use of S/N ratio as quality characteristic facilitates incorporation of noise factors into experiments and determination of key factors at their best levels for improved performance [Kim and Shahinpoor, 2003].

2.10 Analysis of variance

Since variation affects the quality, analysis of variance (ANOVA) is a suitable statistical method to interpret experimental data, detect any differences in average performance of groups of items tested and make necessary decisions. ANOVA is used as statistically based decision tool to determine the significance of different process parameter [Yang and Tarng, 1998]. It is a mathematical technique that breaks down and quantify total variation into its appropriate components [Bhattacharya et al., 2009]. Percentage contribution of each factors can also be determined using ANOVA [Gopalsamy et al., 2009]. From ANOVA error variance and effectiveness of each variation towards the performance can be evaluated [Mohammadi et al., 2004b]. Using the findings from ANOVA, mean response for all combination for all levels can be predicted [Mohammadi et al., 2004a].

ANOVA is a type of regression analysis that compares the group mean with a grand mean. ANOVA can demonstrate whether the variance is due to different levels of a factor or due to experimental error [Sadrzadeh and Mohammadi, 2008]. There are three different types of ANOVA, one way independent, two way independent and three way repeated measure. In one way ANOVA, one factor has different levels and each observation is independent [Allen, 2005]. One way ANOVA calculates sum of Squares, degree of freedom, variance, F value and p value. F value is the ratio of variance between groups and vari-

ance within the group or error variance. So large variance between groups will cause higher F value and large variance due to error will cause small F value. F value is used to identify degree of influence of each factor [Tseng et al., 2013]. If F measured value is higher than F value at 95% or 99% confidence level (extracted from F distribution table), the factor is considered to be significant. F value cannot be zero since its a ratio and if it is less then one that means error is higher than the effect variance. Factors with F values less than F extracted values are used to find out experimental errors. F distribution is a family of distribution which changes based on degree of freedom. Degree of freedom (DOF) gives estimates of data points or sample size. If a experimental matrix has n number of treatments, it is constitutes of n individual pieces of information. This means it has n-1 degrees of freedom to find out variability [Cobb and Clarkson, 1994]. p value gives the probability of occurrence of a particular F value. Smaller p value for a factor means it has more significant impact on mean response.

Parameters should be designed in such a way that a product is designed with sensitivity to noise or uncontrollable factors [Huang and Tai, 2001]. Steps in parameter design are, firstly decide quality characteristic, secondly identify effective factors and levels and finally use OAs to design experiments. Experiments should be done randomly. In this research most commonly used mixed level OA L_{18} , with total number of 18 runs was used. Use of OA effectively reduced number of experiments. Analysis of variance (ANOVA) was used to determine effective factors.

2.11 Light scattering fundamentals

With the advancement of electronics, laser and sensor technology instrumentation and data analysis technique for particle size distribution measurement has become more precise [Provdor, 1997]. Different techniques like laser diffraction, dynamic light scattering (DLS), image analysis and acoustic spectroscopy are economical and user friendly instrumentations to measure particle size. For particle in colloidal suspension DLS and acoustic spectroscopy are proper techniques. DLS instruments has been used by researchers since 1985. Particles in dilute suspension are always undergoing Brownian motion and

when an incident light is directed towards them photons are scattered from these mobile particles. Due to these quasi-elastic phenomena Dynamic light scattering (DLS) is also known as quasi-elastic light scattering (QELS) or photon correlation spectroscopy [Chang and Kaler, 1986]. The fluctuations of light scattering intensity compared to the incident light are recorded over a range of time intervals to get the autocorrelation function (ACF) [Keuren et al., 1993]. ACF is the correlation between the same signal with the delayed version of itself. Cross correlation function (CCF) which correlates two different incoming signals captured by two photon counting modules, is used for concentrated solution as it can suppress multiple scattering [Georgalis et al., 2012]. Researchers have found that particle sizes obtained for monodispersed spheres using DLS [Annunziata et al., 2005], is accurate. Moreover measurement is fast and can be used for on-line measurement of particle size for different type of system. DLS measurement of particle size is based on the assumption that particles in suspension are spherical. So for concentrated and non-spherical particle suspension, use of DLS is a challenge [Provdor, 1997].

The theory of dynamic light scattering instrument is based on Brownian motion of particles in colloidal suspension. The diffusion coefficient D of the particles is directly related to the decay rate Γ of the time-dependent correlation function [Georgalis et al., 2012]. Relation between D and Γ is [Eshuis et al., 1985, Bottero et al., 1991]:

$$D = \frac{1}{2\Gamma q^2} \quad (2.1)$$

where q is the wave vector of the scattered light, If the q^2 is related to the mean decay rate linearly that means particle structure is spherical.

$$q = \frac{4\pi n}{\lambda \sin(\Theta/2)} \quad (2.2)$$

n is the refractive index of the solvent, λ is the wavelength of the incident light in vacuum and Θ is the scattering angle. When a colloidal solution with spherical particles scatters incident light, the instrument measures the electric field autocorrelation function (g_1) which is related to autocorrelation function (g_2) through Siegert equation written below,

$$g_2(\tau) = 1 + \beta(g_1(\tau))^2 \quad (2.3)$$

where $g_1(\tau)$ is the electric field autocorrelation function, β is instrument parameter and its value varies from 0 to 1. Formation of clusters which scatters

light strongly may cause a low β . For a poly-dispersed sample

$$g_1(\tau) = \int A(\lambda) \exp(-\lambda\tau) d\lambda \quad (2.4)$$

where $A(\lambda)$ is the scattering amplitude [Camins and Russo, 1994]. In a monodispersed solution g_2 decays exponentially and it is related to D and q [Li et al., 2009] by

$$g_2(\tau) = e^{-2\Gamma D q^2} \quad (2.5)$$

Finally, the diffusion coefficient is related to apparent hydrodynamic diameter. The mean hydrodynamic radius of the particles r can be calculated using the StokesEinstein equation for spherical particles:

$$D = \frac{k_B T}{6\pi\eta r} \quad (2.6)$$

where k_B is Boltzmanns constant, T is the temperature, and μ is the shear viscosity of the solvent [Lauten et al., 2001]. The hydrodynamic radius also includes the solvent layer at the surface of the particle, which moves together with the particle [Medebach et al., 2007]. This equation is valid for non-interacting particles. If the particles are involved in an aggregation process, they will interact. However, this equation is still applicable to monitor the change of the particle size if the rate of aggregation is slower compared to the time of measurements [Ricka, 1993]. Reasonable accumulation time should be given to get a good autocorrelation. For higher concentration less accumulation time and for lower concentration longer accumulation time is required. The number of particles in scattering volume can also be obtained from integral of light intensity [Burya et al., 2001]. Figure 2.3 shows schematic diagram of dynamic light scattering instrument.

Scattering intensity also varies with angle of detection. In addition, amplitude of the correlation function decreases with decreasing angular resolution. If the angle between initial and final direction of light reflected from particle is within 90° it is called forward scattering, whereas backward scattering is the reflection backward. As a result, at lower angle when forward scattering is very strong, dust or non-spherical can create multiple scattering. At higher angles strong back reflection can cause discrepancy [Jacques et al., 1987]. At 90° contribution of multiple scattering is minimum. So 90° is a preferred angle for light scattering experiments. Greater multiple scattering reduction is possible if the detection is performed in a backward direction at 170° to 175°)

angles [Medebach et al., 2007]. But strong back reflections by bigger or poly-dispersed particles can lead to incorrect measurements of size, concentration or form factor.

2.12 Study of aggregation rate using light scattering

DLS instruments consists of laser light, usually He-Ne laser at 632.8 *nm*, a correlator, a detector that can be set at different angle and index matching sample bath. In this technique, the fluctuation of scattering intensity compared to incident gives information about dynamics of the suspension. In DLS technique the correlation functions are recorded at the real time multiple- τ mode of the correlator with more than 200 channels. The correlator is capable of covering an interval, ranging from 0.2 to almost 1 hour.

DLS measure particle hydrodynamic radius through diffusion coefficient of the scattering particles by analyzing fluctuations of the random interference pattern created by randomly moving scatterers [Ricka, 1993]. Decay rate is measured from the slope of the correlation function using CONTIN analysis. In concentrated sample neighboring particles affects particle diffusion. For this case non exponential ACF occurs which is analyzed using cumulants expansion [Nemoto and Kuwahara, 1993].

$$g^2(\tau) = 1 + \beta \exp -2\Gamma\tau + \mu\tau^2 + \dots \quad (2.7)$$

Γ and μ are the first and second cumulants. Γ can be used to define effective D which is different from free diffusion coefficient in Stokes-Einstein equation. ACF from multiple scattered light will decay more than the singly scattered light [Keuren et al., 1993]. Following decay rate measurement, diffusion coefficient is calculated using Siegert relation. Positive diffusion coefficient means repulsion and negative diffusion means attractive forces between particles. Diffusion coefficient extracted from ACF is independent of scattering angle [Keuren et al., 1993]. Weak intermolecular interaction between particles causes high diffusion coefficient. Strong interaction between particles leads to aggregation and hence lower diffusion co-efficient. Decay of correlation function is also an indication of aggregation [Lauten et al., 2001]. ACF can be

fitted with either single exponential decay if the population is mono-disperse or double exponential decay in case it has particles of two size distribution [Elhamzaoui et al., 2007]. Wider spectrum of ACF means gelation and in this case ACF does not decay to zero. Negligible decay in the correlation function means negligible aggregation. No decay indicates most molecules are still dissolved in solvent [Teklebrhan et al., 2012]. Scattered intensity of a dilute suspension is the summation of scattering of n fold cluster of particles [Holthoff et al., 1997b]. Comparison of normalized scattering intensities at different concentrations can give a qualitative idea about aggregation rate as well. Concentration of particles at a given time can fluctuate due to the formation of cross linkage within gel which reduces particle mobility [Blanco et al., 2000].

To study time dependent aggregation behavior, most widely used theory is Smoluchowski approximation. Smoluchowski rate equation provides an excellent understanding about coagulation kinetics in a dispersion [Lauten et al., 2001]. The theory explains aggregation kinetics of time dependent number concentration of particles which are entirely controlled by Brownian motion. As aggregation continues number of particle decrease and size of the particle grows. For a mono-disperse solution particle size does not vary with angle [Elhamzaoui et al., 2007]. Aggregation rate constant can be measured from the slope of straight line obtained by plotting dimer concentration against time at early stages of coagulation. But at later stage of coagulation when higher aggregates grow faster than linear measurement of aggregation rate becomes difficult [Nemoto and Kuwahara, 1993]. Besides, interference due to multiple scattering can cause incorrect measurements. Dilution of sample can be a mean to avoid multiple scattering [Elhamzaoui et al., 2007]. Affect of multiple scattering can also be neglected by reducing the separation distance between source and detector fiber. Single scattering can be achieved if the scattering mean free path is larger than the path length of light through a dispersion with low particle concentration. For a suspension containing higher concentration or bigger particles, a technique called fiber optic QELS can be used to avoid multiple scattering. This technique uses a single fiber which collects back-scattered lights from particle [Keuren et al., 1993].

Single particle light scattering and simultaneous multi-angle static and dynamic light scattering (SMSDLS) can be used to measure absolute coagulation

rate constant of more dispersed solution of spherical colloids [Yu and Borkovec, 2002]. SMSDLS measures cluster size distribution of aggregate during the coagulation process. Simultaneous DLS and SLS is a in-situ process which allows to determine average cluster size of many particle aggregate. And this process does not disturb the cluster or coagulation process. Combination of this two process can be used to determine coagulation rate through cumulant expansion of average decay rate Γ of a system containing particle aggregates without using form factor and hydrodynamic properties of dimers. In simultaneous SLS and DLS, average cluster size is determined as a function of time using Rayleigh-Gans-Debye approximation. Since this technique requires short measuring time, it works well for weak or reversible coagulation process [Holthoff et al., 1997b]. But Rayleigh-Debye-Gans approximation is valid only for diffusion limited fast coagulation regime [Holthoff et al., 1996, 1997a]. In the slow regime coagulation is reaction limited and electrostatic repulsion prevents coagulation.

2.13 Measurement of fractal dimension and stability ratio using light scattering

Fractal dimension is an index that characterizes the shape of the particle. Information on shape of aggregating particles can be obtained using light scattering at different angles. Fractal dimension is measured by plotting scattering intensity against scattering vector and fitting it by power law [Meng et al., 2013]. Structure of aggregates in different systems have been studied by several researchers using fractal dimension. Comprehensive study on soil and water humic acid structure has been done by Osterberg and Mortensen, and Rice and Lin [Osterberg and Mortensen, 1994, Rice and Lin, 1993] using fractal dimension. Bhattacharya et al., Ibaseta and Biscans, and Schaefer and Keefer studied silica gel structures using fractal dimension [Bhattacharya and Kieffer, 2005, Ibaseta and Biscans, 2010, Schaefer and Keefer, 1984].

Stability of a colloidal suspension depends on stability ratio, which is defined as the ratio of number of collision at diffusion limited regime and number of collision at reaction limited regime [Masliyeh and Bhattacharjee, 2006]. These two regimes are separated by critical coagulation concentration. Stability of a colloidal system depends on electrostatic repulsive force and van der

Waals attractive force. Presence of electrolyte or organics or change in pH of the colloidal suspension affects the magnitude of these two forces. Humic acid absorbed on the surfaces of colloidal particles decreases the inverse stability ratio [Meng et al., 2013]. Stability ratio (W) is related aggregation rate at slow and fast regime through following relation [Kobayashi et al., 2005]:

$$\frac{1}{W} = \frac{k}{k_{fast}} \quad (2.8)$$

$\frac{1}{W}$ is called inversed stability ratio. Aggregation rate at fast regime (k_{fast}) can be calculated theoretically and aggregation rate at slow regime (k) can be measured experimentally using light scattering. Increased inversed stability ratio means suppressed double layer and increased van der Waals force [Schudel et al., 1997, Kobayashi et al., 2005].

2.14 Challenges of light scattering

The major difficulty with the DLS technique is the inversion of data. Different techniques like CONTIN, cumulants, least square methods have been used to analyze auto-correlation function, each method has both advantages and disadvantages. The main problem is, autocorrelation function has low information content, specially when particles are polydispersed. To obtain more information, instead of single angle experiments, two angles can be used for bimodal colloidal suspension, one angle to derive information about size distribution and the other to gather the intensity data [Bryant and Thomas, 1995]. Non negative least square fitting is the simplest method which gives better information about single or multimodal particle size distribution. But before applying this method cumulants analysis has to be performed to determine a reasonable size range for the fitting.

Reproducibility of dynamic light scattering experiments is another challenge. One of the reasons may be difference between refractive index of particle and solvent. A bath fluid usually toluene is used to reduce stray reflection and it has different refractive index than solvent water, which may cause angular deflection. Variation or human error in sample preparation and change of particle number in a suspension with interacting particles can be other reasons for non-reproducibility of data [Harris et al., 1999]. For samples with multimodal size distribution different angle will give different result, as at a

particular angle only a particular size particle contributes significantly to the scattered intensity. If a sample give same size distribution at different angles than it can be considered as monodispersed. This can provide a way to ensure experimental reliability [Bryant and Thomas, 1995].

There is a significant time gap between the preparation of sample and beginning of measurement in the instrument [Harris et al., 1999]. Coagulation can start right from the moment when sample was being prepared. Consequently, measurement of aggregation rate using light scattering becomes complicated [Holthoff et al., 1997b] if the time of beginning of coagulation is not considered correctly. A sample with two or three closely spaced size distribution is difficult to examine using light scattering. The peak difference between two distribution should be at least 2:1. The amount of scattered light should be strong enough to be detected by the detector. If the refractive index contrast between particle and solvent is more than 0.15, light scattering from the sample will be strong [Camins and Russo, 1994]. Reliability of data can be improved by taking multiple sampling times. Accumulation time has to be optimized as it increases as gelation increases [Camins and Russo, 1994] which is indicated by expansion of the spectrum of ACF. Data at longer lag time interval is too noisy to be evaluated as correlation function. The noise characteristic can be improved by taking several short duration measurement instead of a single long measurement.

2.15 Summary

In this chapter, overall scenario of oil sands industry in Canada, technologies involved in water treatment and related problem in SAGD process are introduced. This chapter also documented a comprehensive literature review on design of experiments, Taguchi orthogonal array and analysis of variance, and silica and organics chemistry. Additionally literature survey on fundamentals of light scattering and challenges of application of this technique is presented. According to the above discussion, with DLS many experiments can be performed within short time span. So, in this research, many combination of colloids and silica at different low concentrations were studied using DLS. But, study of highly concentrated solution using light scattering is difficult because of the presence of bigger aggregates and polydispersed particle

size distribution. Therefore, use of another analytical technique, namely total organic carbon (TOC), capable of handling highly concentrated solution, UV-Vis absorbance spectroscopy and spectrofluorescence were required. As a result, characterization of silica-organics interaction, using several analytical techniques becomes expensive and time consuming compared to DLS. In order to minimize cost and time required for experiments, design of experiments was implemented. Taguchi L_18 orthogonal array and ANOVA were used to identify important parameters. Materials and methods used to study silica-organic interaction in SAGD produced water are described in the next chapter, followed by the findings of the experiments in chapter four.

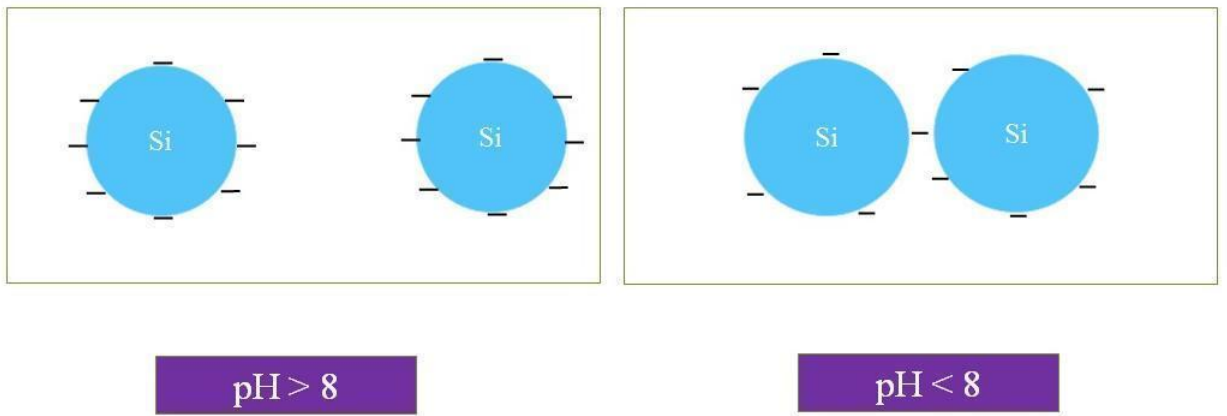


Figure 2.1 – Silica silica interaction at different pH [Iler, 1979]

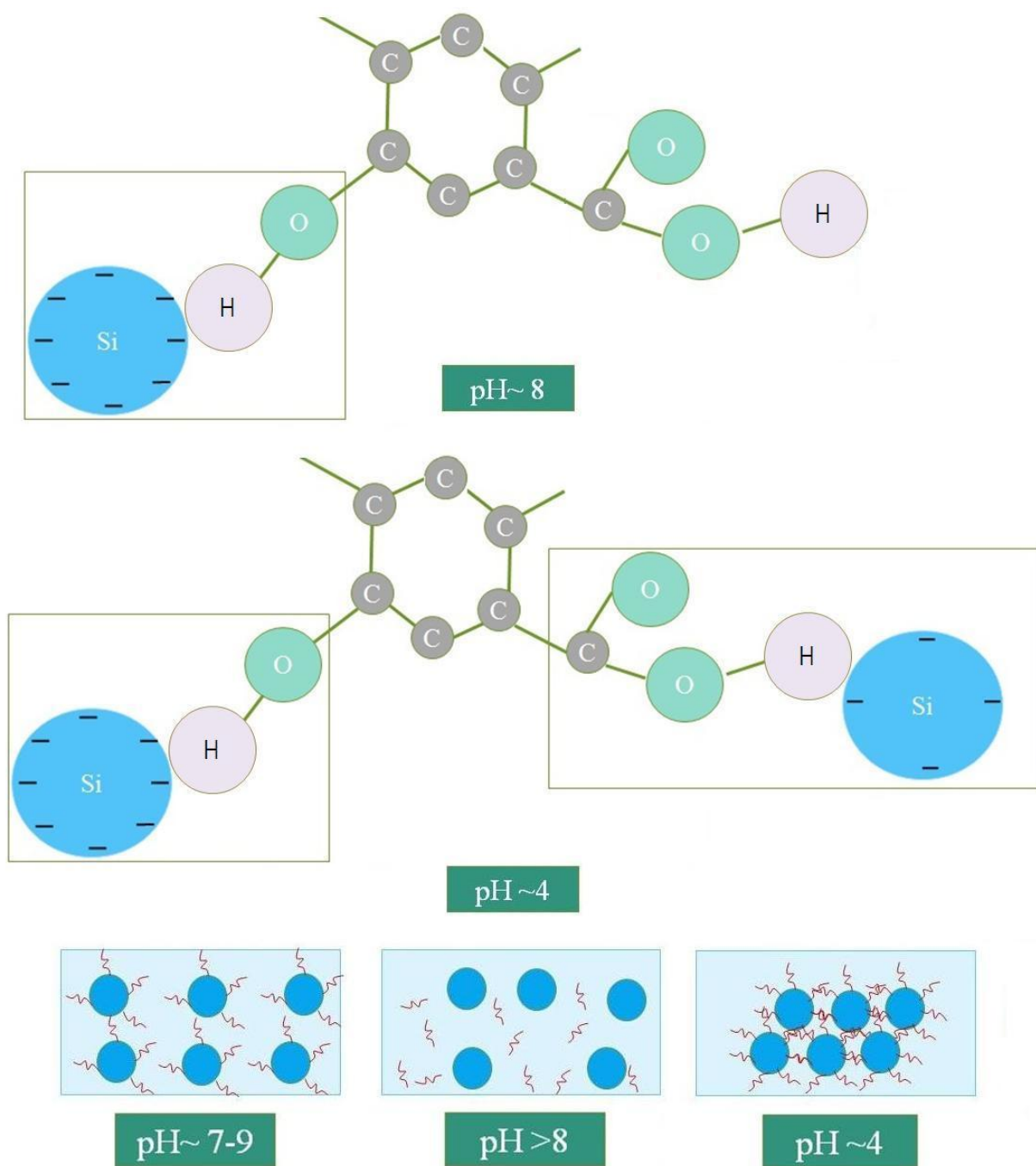


Figure 2.2 – Silica organics interaction at different pH [Iler, 1979, Taheri et al., 2013]

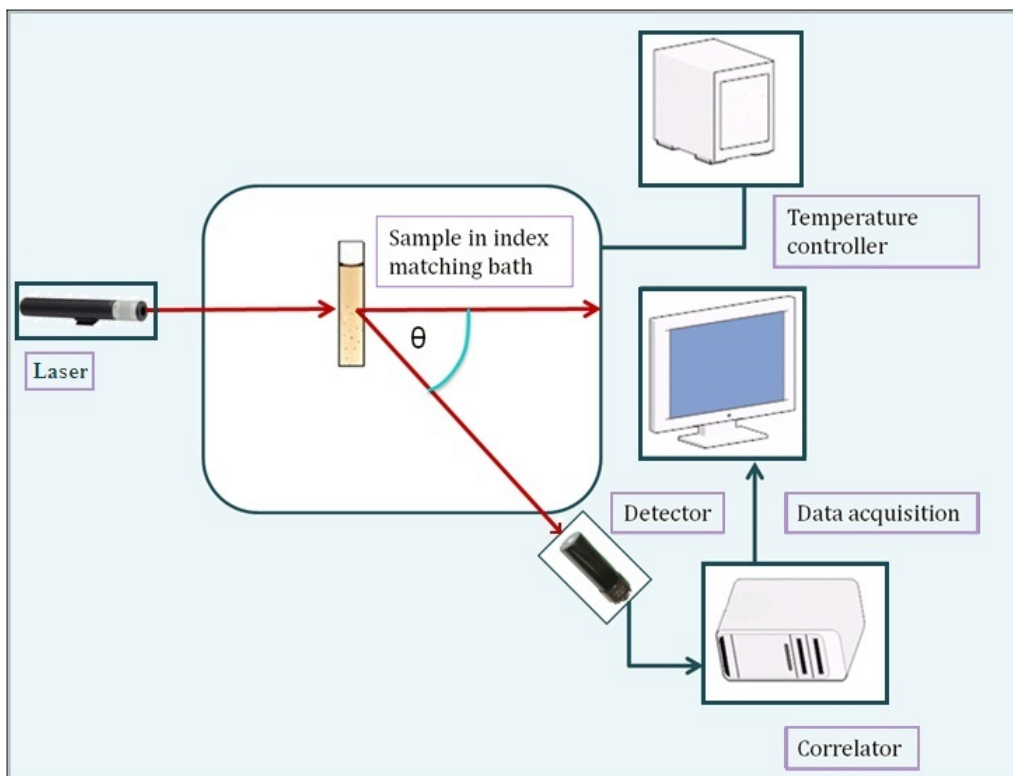


Figure 2.3 – Schematic diagram of light scattering technique

Chapter 3

Experimental Method

3.1 Introduction

In order to understand the interaction of silica and dissolved organic matter (DOM) from SAGD produced water, samples were studied using different analytical techniques. In this chapter detailed experimental procedure followed is explained along with the description of materials used and sample preparation. After reviewing literature on chemistry of silica and organics, the hypothesis for this experimental work was defined as:

- Silica aggregation is pH and concentration dependent
- At the presence of electrolytes silica will form bigger aggregates with organics through cation bridging and co-precipitate at different rate as a function of pH

For this study organic matter from boiler blow down (BBD) water from in-situ (SAGD) bitumen recovery process was selected. To understand the aggregation behavior of silica and DOM in boiler blow down water (BBD) at different pH, electroacoustic spectrometer was explored first. Since this instrument needs at least 1% solid, BBD was concentrated by distillation method. The solid content in CBD was found inadequate for size and zeta potential measurement. Based on further literature review simultaneous multi-angle static and dynamic light scattering (SMSDLS) was identified as more suitable way to study silica-organics aggregation. Dynamic light scattering technique is capable of tracking the particle growth at different time interval even at low concentrations. From static light scattering data it is possible to get an idea of the interaction between constituents (through second virial coefficient)

and also about aggregate shape through fractal dimension [Bhattacharya and Kieffer, 2005]. Fractal dimension of aggregates can be obtained by plotting scattering intensity against wave vector which gives an idea about the shape of the aggregates. So to study lower concentration of silica and organics interaction light scattering technique combined with turbidity measurement and UV-Vis absorbance was used. Finally, in order to capture influence of all the factors involved in real industrial application as high concentration of silica, organics, presence of different electrolytes etc. a systematic design of experiments was required. Taguchi L_{18} orthogonal array was selected as it is suitable for problem with several factors with three levels. Removal of DOM from the samples was selected as dependent variable for this design. This was a holistic approach combined with light scattering, specific UV absorbance at 254 nm, excitation emission matrix, X-ray photo-electron spectroscopy. This enabled to identify which factor plays main role in silica organics aggregation, which fraction of organics has precipitated following aggregation, amount of silica and organics in precipitates etc. Figure 3.1 shows the steps followed towards the goal.

In this study three different types of organics were used, these are: AHA, acid extractable organics (AEO) and raw BBD. Two types of silica, dissolved silica: Sodium meta silicate ($Na_2SiO_3 \cdot 9H_2O$) and colloidal silica (two sizes of *Snowtex*[®]), polystyrene sulfate latex were used as colloids representing silica in produced water. Samples were prepared by dissolving different concentrations of colloids into different organics at the presence of electrolytes. pH was adjusted using *HCl* and *NaOH*. Detail of all analytical methods and sample preparation procedure is described in this chapter.

3.2 Materials

Sodium meta silicate ($Na_2SiO_3 \cdot 9H_2O$) from Sigma-Aldrich was used as dissolved silica and *Snowtex*[®] ZL stock suspension (40% solids, with mean diameter 100 nm) and *Snowtex*[®] 20L (20% solids, with mean diameter 80 nm, from Nissan Chemical America Corporation was used as model colloidal silica. Polystyrene sulfate latex from interfacial dynamic Corp. (8% solids, with mean diameter 100 nm) was used as colloids. De-ionized (DI) water (*Purelab*[®] Ultra) was used for diluting samples, washing and the preparation

of blank samples. The TOC of the DI water from the purification unit was measured and found 0.95 mg/L .

Humic acid obtained from Sigma Aldrich was used as model organics. AHA was characterized using Fourier transform infrared spectroscopy (FTIR) and potentiometric titration. AEO was prepared in the laboratory from produced water samples. Solid precipitates from concentrated and acidified (at pH 2) SAGD boiler blow down water (BBD) was separated and dried at 65° to 70° C in an oven. Organic matter present in the precipitate was then separated by methanol extraction. Then the methanol extract was dried in a rotary evaporator under vacuum and dissolved in DI water. Detail AEO characteristics were obtained from the previous work of the group. Previous work from the group has confirmed that the concentration of TDS and silica are very low in AEO. BBD water samples used for this study were received from large Athabasca oilsands SAGD operation. Nitrogen blanket was used to keep the samples inert during storage. Chemistry and constituents of BBD is documented elsewhere [Maiti et al., 2012, Thakurta et al., 2013]. The raw BBD was passed through a $0.45\mu\text{m}$ syringe driven filter (Cellulose Acetate, Millipore, USA) to remove the suspended matter. Therefore, total organic carbon (TOC) content in the BBD water samples can be considered as the dissolved organic carbon (DOC) or dissolved organic matter (DOM) content.

NaOH and *NaCl* (EM Science (Merck KGaA, Germany), *CaCl₂* and *HCl* (Fisher Scientific), *AlCl₃* (Acros Organics) were used as reagents. 12N *HCl* (Fisher Scientific, USA) was diluted with DI water to obtain 1N *HCl* acid solution. Solid beads of *NaOH* was weighted and dissolved in DI water to prepare 12N *NaOH* stock solution, which later was diluted using DI water to obtain *NaOH* solution of different concentrations. *HCl* and *NaOH* solutions were used to adjust the pH as required. For Taguchi L_{18} experiments *NaCl*, *CaCl₂* and *AlCl₃* salts were weighted and dissolved directly to modify the electrolyte concentration in the samples.

3.3 Simultaneous multi-angle static and dynamic light scattering (SMSDLS)

Multi-angle dynamic and static light scattering experiments were performed

using ALV (ALV Laser Vertriebsgesellschaft m.b.H., Langden, Germany) CGS-3 light scattering instrument equipped with ALV 5000 multiple τ digital correlator (288 channels). A He-Ne laser of 22 *mW* output power and wavelength of 632.8 *nm* was used as light source. All dynamic light scattering (DLS) experiments were performed at 90° detection angle with respect to incident light. Sample was placed in a 10mm X 75mm glass cuvette in an index matching bath filled with toluene. The cuvette and other glassware were cleaned carefully using ethanol to reduce interference by dust or foreign particles. The laser beam was passed through the sample solutions and scattered light was collected for 3 runs of 30 seconds each. All measurements were performed at $25 \pm 0.3^\circ$ C. In the DLS experiments, the variation of the autocorrelation function (ACF), $g_2(\tau)$, with lag time (τ) was used to determine the amplitude autocorrelation, $g_1(\tau)$, through the Siegert relation [Lauten et al., 2001] following which, the diffusion coefficient, *D*, was estimated from the Laplace transform of $g_1(\tau)$. The hydrodynamic radius of the particle was then obtained from the diffusion coefficient using the Stokes-Einstein equation

$$r_h = \frac{k_B T}{6\pi\mu D} \quad (3.1)$$

where k_B , *T* and μ are the Boltzmann constant, absolute temperature, and solvent viscosity, respectively [Burya et al., 2001, Blanco et al., 2000].

Static light scattering (SLS) experiments were performed to collect scattered light intensity at 13 different angles ranging from 30° to 150°. Scattered intensity was obtained using Rayleigh-Gans-Debye approximation for the early stage of aggregation when doublets are assumed to be dominant. Change of scattering intensity at a certain angle is proportional to particle concentration and aggregation rate [Seinfeld and Pandis, Nemoto and Kuwahara, 1993]. Differential refractive index $\frac{dn}{dc}$ of the samples were measured by Optilab DSP differential refractometer (Wyatt Tech. Co.) with a laser of 632.8 *nm* wavelength. According to the Rayleigh theory, normalized scattering intensity obtained from DLS experiments varies with the sixth power of particle diameter and second power of concentration [Holthoff et al., 1997b,a], this interesting observation makes it a suitable parameter to understand change in size and concentration of particles in dilute suspension.

3.3.1 Calibration

Silica aggregates as function of pH and concentration. At first calibration was performed to check whether DLS can capture this phenomenon. So light scattering instrument was calibrated using both dissolved and colloidal silica.

Highly concentrated (20wt% and 40wt%) *Snowtex*[®] stock suspension at pH 10.0 was series diluted using DI water to prepare 8 different concentrations ranging from 10 to 10000 *mg/L*. Then DLS at 90° and SLS at 13 different angles (30° to 150°) were performed to obtain scattering intensity. To examine the effect of pH, 100 *mg/L* *Snowtex*[®] was acidified to different pH and scattering intensity was recorded at 90°. Prior to use, the DI water was filtered through 0.22 μ glass fiber syringe driven filter (Millipore, USA). Highly concentrated (10500 *mg/L* Si) sodium meta silicate (Na_2SiO_3) solution at pH 12.0 was prepared by dissolving appropriate amount (12gm) of Na_2SiO_3 salt in DI water. Concentration of dissolved silica was examined by Inductively coupled plasma mass spectrometry (ICPMS) analysis using EPA 200.7 analytical method at Maxxam analytics. The solution was then acidified to different pH ranging from 11 to 4 by adding 12N HCl. Then DLS at 90° was performed to obtain scattering intensity. Scattering intensity and turbidity at different pH was also examined. The next step was to check the aggregation behavior of AHA at different concentrations and pH. 0.2 grams of humic acid was dissolved in 100 *ml* DI water. DOM concentration of this solution after filtration using 0.45 μ m syringe driven filter (Cellulose Acetate, Millipore, USA) was found 920 *mg/L* using TOC analyzer. Then solution was diluted to 50 *mg/L* with 0.1M *NaCl*. pH was adjusted using 1N HCl. Particle size and scattering intensity obtained was compared at different pH and concentrations.

3.3.2 Sample preparation for humic acid and silica mixture and fractal dimension measurement

The combine effect of silica and AHA was studied. One set of experiments was done with dissolved silica and another set was with colloidal silica. For first set of experiments the stock solution of AHA was diluted using 100 *mg/L* *Snowtex*[®] 20L (80 *nm* diameter) with 0.1 M *NaCl* solution and then acidified to different pH. Normalized scattering intensity from this set was compared with 100 *mg/L* *Snowtex*[®] 20L with 0.1M *NaCl* solution without AHA at

same pH. For the second set, the stock solution of AHA was diluted using 150 mg/L Na_2SiO_3 with 0.1M $NaCl$ solution and acidified to different pH. Normalized scattering intensity from this set was compared with 150 mg/L Na_2SiO_3 with 0.1M $NaCl$ solution without AHA at same pH. Fractal dimension was also deduced from SLS data for these two sets of samples.

3.3.3 Sample preparation for particle sizes measurement with time

Next step was to study the time resolved change in particle sizes at the presence of organics and silica. 50 mg/L AHA was prepared using 150 mg/L Na_2SiO_3 with 0.1M $NaCl$ and pH was adjusted to 8.0. Then the change in particle size was recorded at every five minutes interval for one hour. Same procedure was followed for 150 mg/L Na_2SiO_3 with 0.1M $NaCl$ at pH 8.0 and 50 mg/L AHA with 0.1M $NaCl$ at pH 8.0. Following the same method, 50 mg/L AHA using 150 mg/L Na_2SiO_3 with 0.1M $NaCl$ at pH 3 was prepared and particle size was tracked for one hour. This was again compared with 150 mg/L Na_2SiO_3 and 0.1M $NaCl$ at same pH. Next step was to check Na_2SiO_3 with 0.1M $NaCl$ aggregation at the presence of AEO. Stock solution of AEO (7500 mg/L DOM concentration) was diluted to 50 mg/L using 150 mg/L Na_2SiO_3 with 0.1M $NaCl$ solution at pH 3. In order to examine the particle growth in *Snowtex*[®] 20L and organics mixture AHA stock solution was diluted to prepare 50 mg/L of AHA using 100 mg/L of *Snowtex*[®] 20L with 0.1 M $NaCl$. pH was then adjusted 3.0. Then the change in particle size was recorded at every five minutes interval for one hour. Same procedure was then followed with 100 mg/L *Snowtex*[®] 20L with 0.1M $NaCl$ at same pH.

3.4 Turbidity measurement

Turbidity is a measure of total suspended solid present in liquid. Nephelometric turbidity unit (NTU) is widely used as turbidity unit. A laser light (usually 632 nm), when passed through the sample, particulate matters present in it reflects light depending on their size, shape and reflectivity. Same samples used for light scattering instrument calibration were examined using turbid-

ity meter. Turbidity of the samples were examined using a Hach 2100AN Turbidimeter, which uses a laser of 632nm wavelength. Prior to use, the instrument was calibrated with *StablCal*[®] turbidity standard calibration kit.

3.5 UV-Vis Spectroscopy

UV-Vis Spectrophotometer was used to measure absorbance by polystyrene sulfate latex at different concentrations. A UV-Vis spectrophotometer (Varian, Cary 50, USA) equipped with Xenon flash lamp, sample cuvette holder cell and detector at 200 to 900 nm wavelength range was used. The Xenon lamp flashes and light is passed through the sample. A light beam incidents on the particle with certain energy and if that energy matches with the energy required to excite outer electron of particular molecule some portion of incident light will be absorbed. The outgoing residual light from sample is then detected by photo diode or photo-multiplier tube and converted into current. Absorbance is natural log of the ratio of incident and resultant light intensity. Since different molecules absorb light of different wavelength, absorbance spectrum will show peaks of corresponding structural group of molecules. From absorbance, concentration of the sample can also be measured using Beer-Lambert law, which states that absorbance is proportional to the product of path length and concentration.

Aggregation of polystyrene sulfate latex at different electrolyte concentrations were examined using UV-Vis spectroscopy. Different concentrations of (10, 25, 50, 100, 250 mg/L) polystyrene sulfate latex with different ionic strength (0.1M NaCl, 0.25M NaCl, 0.5M NaCl and 0.1M CaCl₂) were prepared. 0.1M NaCl solution was used as baseline. Sample was taken into cleaned quartz cuvette and scanning was performed at 200 to 900 nm wavelength range.

3.5.1 $SUVA_{254}$

Specific absorbance at 254 nm was used to examine presence of aromatic hydrophobic fraction in the samples after DOM removal. $SUVA_{254}$ of samples were calculated by dividing the corresponding absorbance at 254 nm by TOC

concentration of the sample and multiplying by 100. The sample organic concentration was kept around 20 mg/L to obtain absorbance in the range of 0 to 1.0.

3.6 Scanning electron microscope (SEM)

Surface image was obtained by a high-resolution (approximately 1.5 nm) FESEM (JEOL 6301F, Japan) equipped with conical FE electron gun and a zoom condenser lens. This instrument uses an electron gun which is focused through magnetic lens. Electron beam incident on metal coated sample and interact with the atoms of the sample. Produced X-ray, back-scattered electron, and secondary electron is collected by the detector and converted into magnified image of the surface. Chromium or gold coating is used to make the samples electron conductive.

3.6.1 Sample preparation

Four samples were studied using SEM. 150 mg/L Na_2SiO_3 solution was prepared by dissolving 0.15 grams sodium meta silicate salt in 100 ml 0.1M $NaCl$ solution. AHA Stock solution was diluted to 50 mg/L (DOM) using above mentioned 150 mg/L Na_2SiO_3 with 0.1 M $NaCl$ solution. For all cases pH was adjusted to 8.0. Silicon wafers were cleaned using 3:1 H_2SO_4 and H_2O_2 solution. Then the silicon wafer was dipped into Na_2SiO_3 sample solution for 30 minutes followed by drying in desiccators, to deposit particles onto the silicon wafer. Samples (on silicon wafer) was then coated with chromium. In order to prepare samples with *Snowtex*[®] ZL, membrane was used. 100 mg/L *Snowtex*[®] ZL was prepared by diluting the stock suspension using 0.1 M $NaCl$ solution. AHA stock solution was diluted to 50 mg/L (DOM concentration) using 100 mg/L *Snowtex*[®] ZL and 0.1M $NaCl$. 100 mg/L *Snowtex*[®] ZL with 0.1 M $NaCl$ and 50 mg/L (DOM) AHA solution was filtered through a small membrane filtration unit with a 300000 Dalton polyethersulfone membrane (Millipore, USA). The membrane was then dried inside a vacuum chamber. A small piece of it was cut and placed on stub using adhesive tape. It was then chromium coated to make electron conductive.

3.7 Atomic force microscopy (AFM)

For surface imaging of silicon wafers containing the sample deposits, a *BioscopeTM* scanning probe microscope (SPM) with Nanoscope IIIA controller (Digital instruments, Veeco Metrology Group, Santa Barbara, CA) was used in tapping mode. In tapping mode a cantilever probe made of stiff crystal silicon, oscillates to its resonant frequency (50-120 *kHz*). When silicon wafer containing the sample substrate is placed under the probe and the probe is excited with a fixed energy by the piezoelectric substance attached with it, deflection of the tip occurs according to Hooks law as it come into contact with the sample. The deflection is captured using a laser spot reflected from the tip into a photo diode array. The movement of tip reflects the laser beam of 670 *nm* wavelength and captured by photo diode array which produces the electronic signal that contains information about the surface topography.

3.7.1 Sample preparation

Four samples were examined using AFM. 100 *mg/L* *Snowtex*[®] 20L was prepared by diluting stock suspension with 0.1 M *NaCl*. AHA stock solution was diluted to 50 *mg/L* (DOM) using 100 *mg/L* *Snowtex*[®] 0.1 M *NaCl*. 150 *mg/L* *Na₂SiO₃* solution was prepared by dissolving 0.15 grams sodium meta silicate salt using 0.1M *NaCl*. AHA stock solution was diluted to 50 *mg/L* (DOM) using 150 *mg/L* *Na₂SiO₃* with 0.1M *NaCl*. For all cases pH was adjusted to 8.0. Silicon wafers were cleaned using 3:1 *H₂SO₄* and *H₂O₂* solution and dipped into sample solution for 30 minutes followed by drying in desiccators, to deposit particles onto the silicon wafer.

3.8 Design of experiments

Taguchi *L*₁₈ orthogonal array with 18 rows was selected as suitable experimental design because this standard approach is best fit for many factors with various levels problem. This method is economically efficient to find optimum condition and identify significance of each factor. Percentage of organics removal was selected as quality characteristic and larger the better *S/N* ratio

Table 3.1 – Factors and levels selected for Taguchi L_{18}

Factor	Level
Type of colloids	Two levels (<i>Snowtex</i> [®] ZL (100nm) and Latex (100nm))
Type of organics	Three levels (AHA, AEO, BBD)
Type of salt	Three levels (<i>NaCl</i> , <i>CaCl</i> ₂ , <i>AlCl</i> ₃)
Concentration of colloids	100, 250, 500 <i>mg/L</i>
Concentration of organics	100, 250, 500 <i>mg/L</i>
Concentration of salts	0.01M, 0.1M, 0.25M
pH	3, 6, 9

as desired response. Following table shows factors and levels selected for the experiments.

Snowtex[®] ZL (100 *nm*) and polystyrene latex (100 *nm*) were used as representative of colloidal particles in BBD. Concentrations of organics and silica were selected based on some preliminary screening experiments, which is described in results and discussion section. Concentration of electrolytes were selected based on their theoretical critical coagulation concentration (CCC) [Masliyah and Bhattacharjee, 2006]. pH levels were selected based on pKa values of AHA, AEO, BBD.

3.8.1 Sample preparation

Following steps were followed in sample preparation:

- 18 samples (30 *ml* each) were prepared by dissolving appropriate colloids, salts, organics (filtered through 0.45 μ m filter) and adjusting the pH.
- Then shaker was used for 24 hours to increase aggregation.
- The samples were then taken out of shaker and allowed to precipitate for 24 hours.
- Next step was to take the supernatant and filter it using 0.22 μ m filter.
- To get baseline values of DOM same samples were prepared without colloids following the same procedure. 18 samples (30 *ml* each) were prepared by dissolving appropriate colloids, salts and adjusting the pH.
- After 24 hours of settling the supernatant was filtered using same filter (0.22 μ m filter) and sent to TOC analyzer.

- Later baseline DOM value was deducted to get final DOM value.
- Experiments were repeated twice.

Detail experimental procedure is documented in Appendix B.2. Response plot was obtained using statistical software MINITAB RELEASE 16. Analysis of variance (ANOVA) was performed using Microsoft Excel.

3.9 Total organic carbon analyzer

Dissolved organic matter in AHA, AEO and BBD was measured by oxidation of samples in a catalytically-aided 680° platinum combustion TOC-VCPH analyzer (Shimadzu, Kyoto, Japan) with a detection range of 4 to 25000 *mg/L* and automatic sample acidification and sparging system. It can measure TC, IC, TOC and NPOC. The automatic dilution function enables measurements up to 25,000 *mg/L*. In this technique organic carbon is oxidized to produce CO_2 . TOC is calculated based on the volume of CO_2 produced. Total carbon is a measure of both organic and inorganic carbon content in a sample. Total organic carbon (TOC) is the amount of organic carbon present. TOC includes total suspended and dissolved organic carbon present in a water sample. TOC and dissolved organic carbon (DOC) value of the sample passed through 0.45 μ m filter can be considered as same [Thakurta, 2012]. All three types of organics were filtered using 0.45 μ m syringe driven filter (Millipore, USA) and then analyzed using TOC analyzer. TOC analyzer was calibrated using 1000 *mg/L* and 250 *mg/L* potassium hydrogen phthalate solution.

3.10 Fluorescence Spectrophotometer

A Cary eclipse fluorescence spectrophotometer (Varian, USA) was used to produce excitation emission matrix. In this technique a high intensity light is passed through sample to excite as many as molecules possible. Emission from the molecules collected at 90° with excited light. Collected data then processed to produce excitation emission matrix.

3.10.1 Sample preparation

From the Taguchi L_{18} experiments seven samples and optimum condition sample were selected based on higher removal. The supernatants from these samples were collected and diluted using DI water to obtain 20 mg/L TOC concentration. pH was adjusted to 11.0 using 12N and 0.1N $NaOH$. DOM in the samples were diluted to reduce inner filtration or quenching effect [Thakurta, 2012]. DI water was used as blank. A quartz cell (Varian, USA) was used to keep sample in the sample holder cell of fluorescence spectrophotometer. Excitation emission contour was produced by collecting the 3D emission at 200 nm to 500 nm against different excitation wavelengths (200 to 500 nm) at an interval of 5 nm . Scan speed was set as 600 nm/min . The excitation emission contour for each samples were plotted using Origin.

3.11 X-ray photoelectron spectroscopy (XPS)

From the Taguchi L_{18} experiments seven samples were selected based on higher removal of organics. Residual supernatants were separated from the precipitates carefully using micro pipette. Then the solid precipitate was dried in oven at 120° for four hours. Dried samples were then grinded and made homogeneous using mortar and pestle. Samples were labeled carefully and send for XPS analysis. XPS analysis was done using Kratos Axis 165 X-ray Photoelectron Spectrometer with ISS and AES.

3.12 Fourier transform infrared spectroscopy (FTIR)

Diffused reflectance FTIR was used to find out the functional group present in AHA. In this technique, a beam with different wavelengths filtered through a mirror incident on sample. Some of these wavelengths passed through sample, some of them are blocked by the mirror. This process is repeated many times with different combinations of wavelengths. This data is then processed to produce a spectrum. Diffused reflectance FTIR (Thermo Nicolet, Nexus 670 FTIR, USA) was used to obtain AHA spectra. At first baseline was collected

using *KBr*. *KBr* was crushed using mortar and pestle to make very fine particles and placed in sample holder to collect background. Then AHA was crushed and made homogeneous using mortar and pestle. FTIR spectrum was then collected from 600 to 4000 cm^{-1} .

3.13 pH measurement

pH of all the samples were measured using pH/ion/conductivity meter (AR50, Fisher Scientific Accumet Research, USA).

3.14 Potentiometric titration

AHA was titrated in a potentiometric titration system (PCM QC-Titrate, Mandel Scientific, Canada) with 0.1N *HCl* solution. 15 ml solution of 100 mg/L AHA at pH 11.0 was titrated to obtain pKa values and total acidity of AHA.

3.15 Summary

The goal of this study was to find out a suitable technique that can capture the colloids and organics interaction at different conditions. Different analytical techniques were employed to determine the appropriate one. Experimental methods and materials used to study colloids and organics co-precipitation were documented in this chapter. Also the working principles of the instruments and analytical techniques were explained briefly in this chapter. For this study DLS was used to observe the rate of growth of particle size. SLS data was used to obtain information about shape of aggregates. FTIR spectroscopy, UV-absorbance and Spectrofluorometer were used to obtain information about the organic functional groups, aromaticity and the organic matter concentration in the samples. SEM and AFM technique were used to obtain visual proof of silica-organic aggregates. TOC-analysis was done to find the amount of DOM removal due to colloid organic co-precipitation. XPS analysis was used to determine which elements are present in the precipitate. SUVA at 254

nm technique was utilized to identify the fractions present in treated water after DOM removal.

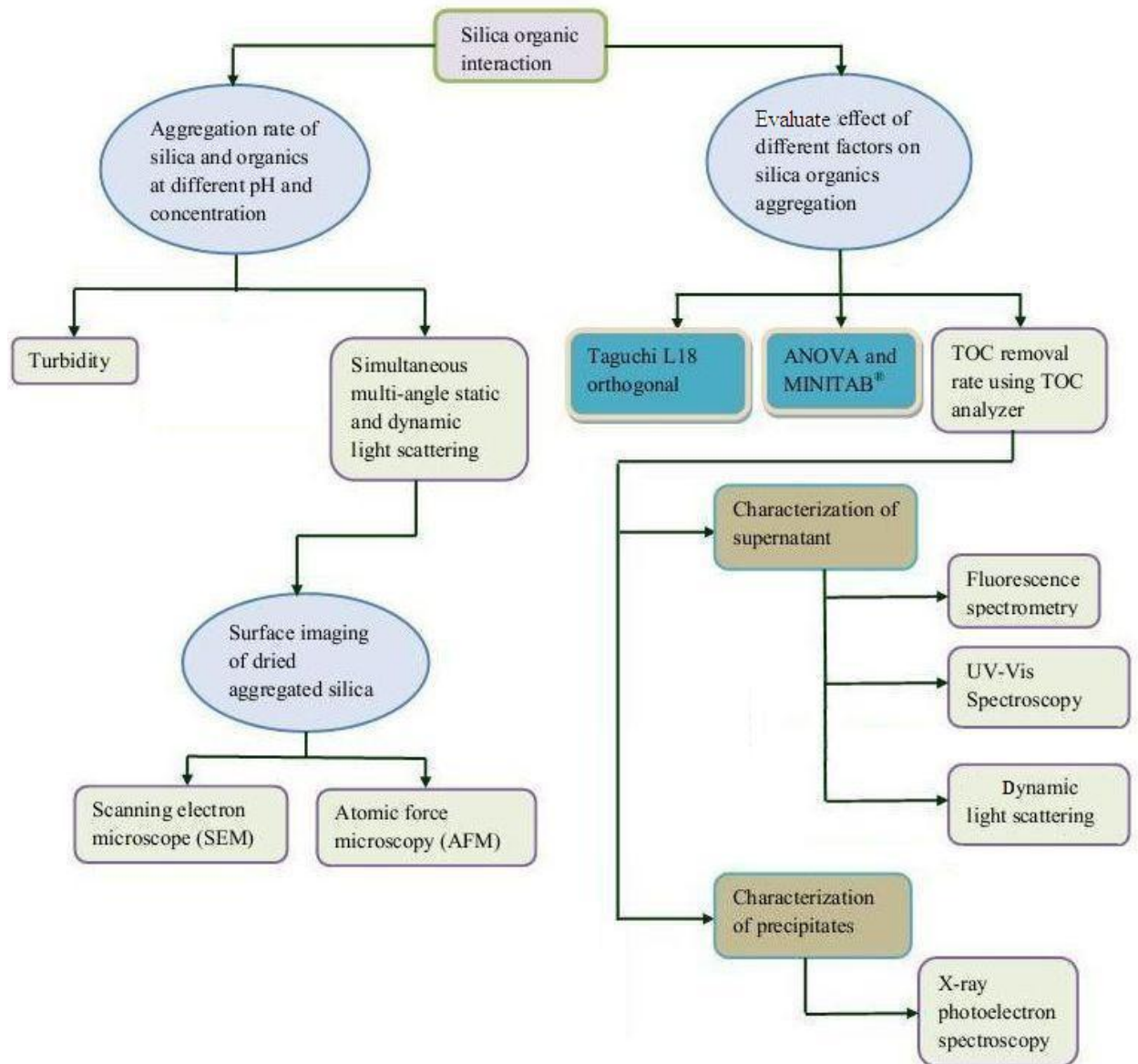


Figure 3.1 – Flow chart of sequential experimental progress

Chapter 4

Results and Discussion

4.1 Introduction

Operation of oil-sands industry in northeastern Alberta is always under scrutiny due to environmental impact caused specially by water usage and CO_2 emission. Two most popular techniques used for bitumen production, namely mining and in-situ, both use huge volume of water [Al-Bahlani and Babadagli, 2009]. In-situ oil sands extraction plants use once through steam generator (OTSG) to produce steam for bitumen recovery. After several cycles of steam generation, as contaminants concentrate due to subsequent recycling, around 20% of feed water of this type of boilers has to be replaced with same volume of fresh water. This residue water is known as boiler blow down (BBD) water. Important characteristic of this type of oil sands produced water is high content of dissolved solid (mainly sodium chloride and silica) and dissolved organic matter (DOM). Interaction of these two along with the presence of metal ions like Ca^{2+} , Mg^{2+} causes fouling of the equipments at the water treatment plants under various process conditions [Kawaguchi et al., 2012]. In addition, disposal of huge volume of boiler blow down is also a major issue. Deep well injection of this water is well practiced although it can pollute underground water aquifer. Researchers and engineers in Alberta have been working towards the target to find out a feasible economic approach to reduce fresh water intake, volume of waste water, minimize environmental impact and fouling of equipments. This study is an attempt to address this problem through application of different analytical techniques combined with statistical tool. Previous investigations were performed to understand the characteristics of oil-sands produced water, to determine types of organics present and to separate different fractions of

DOM based on chemical nature etc. The goal of this study to find out the most important parameters that causes silica-DOM co-precipitation and hence equipment surface fouling in SAGD water treatment plants. This will allow us to achieve two targets; a) identify which condition causes fouling and scaling of equipments in SAGD water plants and b) will take a step forward towards finding cost-effective ways to remove DOM.

Surface charge of silica in water depends on pH [Iler, 1979]. At favorable pH (7 to 8) silica starts to polymerize through condensation of silanol ($SiOH$) groups, which reaches highest rate at pH 6 to 3. Above pH 10 silica stays dissolved in water. Rate of polymerization also depends on concentration of silica in the solution. So silica polymerization is a function of pH and concentration. On the other hand, charge of organics surface also depends on pH and functional groups present. Characteristics of organics from different sources are different in terms of functional group, chemical composition, molecular structure, H to C ratio, molecular weight, ratio of hydrophobic and hydrophilic fraction [Khilko et al., 2011]. The fraction of organics that passes through $0.45\mu m$ filter is called dissolved organic matter (DOM). In natural water more than half of the dissolved organic matter are in the form of negatively charged, hydrophobic humic acids [Thurman and Malcolm, 1981, Kretzschmar et al., 1998]. The rest consists of hydrophilic aliphatic carbon and nitrogenous compounds, such as carbohydrates, proteins, sugars and amino acids [Matilainen et al., 2011]. Adsorption of organics on silica surface occurs through hydrogen bonding, hydrophobic or van der Waals interaction [Parida et al., 2006].

In real SAGD plant environment, water goes through several cycles of change of - pH, concentration of silica, concentration of different fractions of organics and different cations. To understand the aggregation behavior of silica and organics the role of all these parameters has to be considered. Light scattering is a easily applicable and faster technique to study aggregation rate and shape in a dilute solution within short time. In this research, first step was to study the aggregation kinetics and aggregate shape at different low concentrations of silica and organics by varying pH and using light scattering technique. But for concentrated samples light scattering is not suitable technique. In order to capture silica-organics co-precipitation in high silica and organics containing solution, a combination of Taguchi design of experiments method and TOC analysis was employed in this study. To accommodate all

the parameters at different levels, fractional factorial design of experiments was required. Use of Taguchi L_{18} orthogonal array for design of experiments allowed us to find out the importance of different parameters [Elizalde-Gonzalez and Garca-Daz, 2010, Ghani et al., 2004, Gopalsamy et al., 2009, Ramkumar and Ragupathy, 2013] affecting aggregation, in a cost and time effective manner with a minimum number of experiments. The initial and final supernatant solutions were characterized using different analytical techniques namely, TOC analyzer, spectrofluorescence, dynamic light scattering, UV-Vis absorbance and X-ray photoelectron spectroscopy. TOC analyzer was used to know the residual organic concentration for samples with high initial organic concentration.

From literature study we already know that pH and concentration plays important role on silica aggregation [Iler, 1979, Alexander et al., 1954, Nordström et al., 2011]. The most interesting finding from this work was to identify humic fraction of DOM as the most important factor that promotes aggregation in SAGD plant environment. By a systematic approach and minimum number of experiments incorporating all the factors it was possible to identify the main factors that causes silica organic co-precipitation. Another finding of this work was, by varying different parameters selective fractions of DOM can be removed from BBD. This chapter documented the detail mechanism of these findings.

4.2 Examining aggregate size and shape

4.2.1 Surface imaging

In order to understand role of humic acids on silica aggregation Aldrich humic acid (AHA) was used as model organic acid. Aggregation behavior of Na_2SiO_3 and *Snowtex*[®] ZL (100 nm) were investigated with AHA at pH 8. Fig 4.1(a) and (b) shows SEM image of 150 mg/L Na_2SiO_3 in 0.1M *NaCl* without and with AHA at pH 8. From the image it is evident that at the presence of organics silica formed dense layer. Also 100 mg/L *Snowtex*[®] ZL in 0.1M *NaCl* without and with AHA (Figure 4.1(c), (d)) at pH 8 shows same characteristics. Silica organics interaction is pH dependent. At pH 8 silica

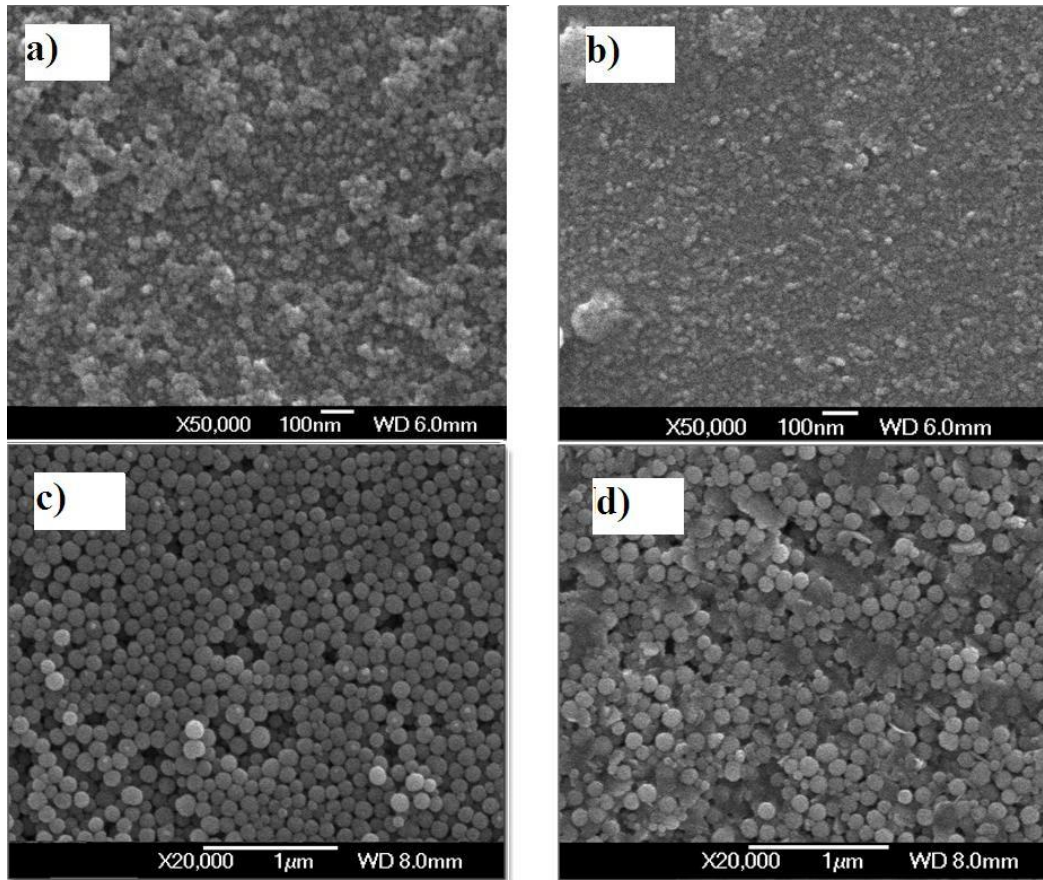


Figure 4.1 – SEM image of 150 mg/L Na_2SiO_3 and 0.1M $NaCl$ at pH 8 (a) without and (b) with 50 mg/L AHA and 100 mg/L *Snowtex*[®] ZL and 0.1M $NaCl$ at pH 8 (c) without and (d) with 50 mg/L AHA

starts to form polysilicic acid and becomes more hydrophobic [Iler, 1979]. So hydrophobic AHA will start to form aggregates with silica. However, these images were taken at dried state which is not true representation of colloidal suspension state in oil-sands produced water. Same conclusion can be drawn for AFM images (Figure 4.2(a),(b),(c),(d)).

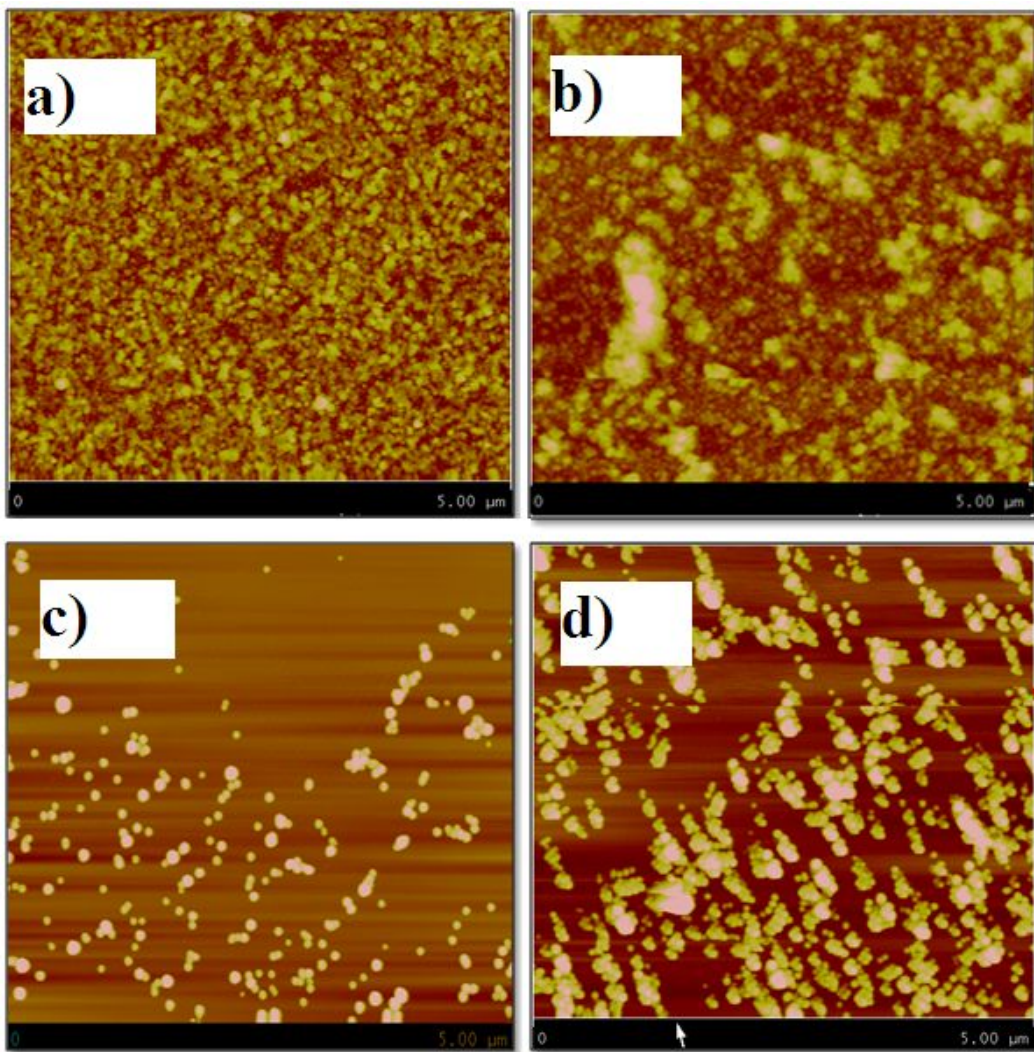


Figure 4.2 – AFM image of 150 mg/L Na_2SiO_3 and 0.1 M $NaCl$ at pH 8 a) without and b) with 50 mg/L AHA and 100 mg/L *Snowtex*[®] 20L and 0.1M $NaCl$ at pH 8 c) without and d) with 50 mg/L AHA

Necessity of further investigations was felt from the above experience, which led to preparation of a detail plan using light scattering technique for low concentration and application of Taguchi method combining with TOC analysis for higher concentration of silica and organics.

4.2.2 Light scattering

To study silica organic interaction in low concentration solution dynamic light scattering (DLS) and static light scattering (SLS) technique was applied.

In a suspension, particles go through random Brownian motion, as a result they collide with each other. If the surface charge of particles are same and high, they repel each other, but when surface charge is opposite or reduced due to increase in H^+ or cation adsorption on surface, they collide and form aggregates. Also reduction in double layer thickness at the presence of electrolyte leads to aggregation. Aggregation reduces total number of particles, i.e concentration of particles in suspension [Masliyah and Bhattacharjee, 2006]. Use of light scattering to understand silica organics behavior at low concentration was started based on the hypothesis that dynamic light scattering can capture change in concentration of particles due to aggregation.

Calibration

At first calibration were performed using both Na_2SiO_3 as dissolved silica and *Snowtex*[®] 20L as colloidal silica. AHA was also examined at different concentration and pH using static light scattering technique. DLS was calibrated using both colloidal and dissolved silica at different concentration and pH. Results of calibration are documented in Appendix A.1. Figure 1 and 2 in Appendix shows that *Snowtex*[®] scattering intensity increases linearly with concentration. Figure 3 in Appendix shows that the trend of DLS intensity matches with turbidity result. For different pH scattering intensity and turbidity increases from higher to lower pH (Figure 4 and 5). Since silica starts to polymerize [Iler, 1979, Gorrepati et al., 2010] by condensation of monosilicic acid to cyclic oligomer from pH around 8, there was gradual increase in scattering intensity from higher to lower pH. For Na_2SiO_3 scattering intensity increases linearly with concentration. Na_2SiO_3 was also examined by changing pH of very highly concentrated solution (Fig 7, 8, 9, 10 in Appendix). At higher concentration aggregation and gelation is visible so it was possible to compare visible changes with DLS results. Again scattering intensity and turbidity increased from higher to lower pH. Comparison of scattering intensity of dissolved silica and colloidal silica (Figure 6, Appendix A.1) reveals that colloidal silica has higher intensity, as they are already polymerized spherical particles, where as dissolved Na_2SiO_3 is in the process of forming monomer, dimer and so on as pH and concentration changes.

4.2.3 Light scattering by humic acid

Aldrich humic acid (AHA) was prepared by dissolving in DI water. AHA was used as model organic acid and examined at different pH and concentrations using DLS at 90° and SLS at different angles varying from 30° to 150° (Figure 11, Appendix A.1). Particle size obtained through DLS at lower pH is around 50 nm and higher pH varied upto 80 nm. At higher pH humic acid molecules are large, flexible and linear shape. At this condition DLS considers this as larger particle. At low pH or high ionic strength or high humic concentration they become rigid sphere either due to neutralization of COOH and OH groups or due to complexation of humic acids with cation [Wang and Kasperski, 2010]. As a result DLS particle size obtained at lower pH is smaller than at higher pH. Size obtained at different pH is quite larger than HA size reported in literature [Wagoner et al., 1997, Thurman et al., 1982]. This is because HA stays as aggregates in water [Abe et al., 2011]. At pH 11 scattering intensity is lower than pH 7 to 9. There is no significant difference between scattering intensity at pH 7 to 9, because at this pH range there is no significant reduction of humic acid surface charge. Reason behind reduced scattering intensity at pH 3 is that, at this pH humic acid surface charge is less negative [Tipping, 2002], as a result they formed aggregate and precipitated quickly. But due to the limitation of DLS this rapid phenomena cannot be captured.

4.2.4 Static light scattering (SLS) of humic silica mixture

SLS study of humic silica mixture was performed at different pH to examine the pH effect on silica organic aggregation. Scattering intensities at 150 mg/L Na_2SiO_3 with 0.1 NaCl and 50 mg/L AHA at pH 11.0, 9.0, 8.0, 3.0 is compared with 150 mg/L Na_2SiO_3 with 0.1 NaCl at similar pH (Figure 4.3). For all pH scattering intensity varies with angle which confirms the presence of aggregates [Folta-Stogniew and Williams, 1999]. At the presence of organics scattering intensity is high for all pH. Scattering intensity increases with decreasing pH. Similar trend was found for *Snowtex*[®] 20L (Figure 4.4). Surface charge of humic acid decreases from pH 9 to 2. At acidic pH silica surface adsorbs proton which in turn screens the surface charge and reduces

the repulsion between colloidal silica that leads to tighter aggregates [Singh and Song, 2007b, Illes and Tombacz, 2006]. At alkali pH adsorption of hydroxide ions increases negative charge on the colloidal particles, these reduces aggregation rate.

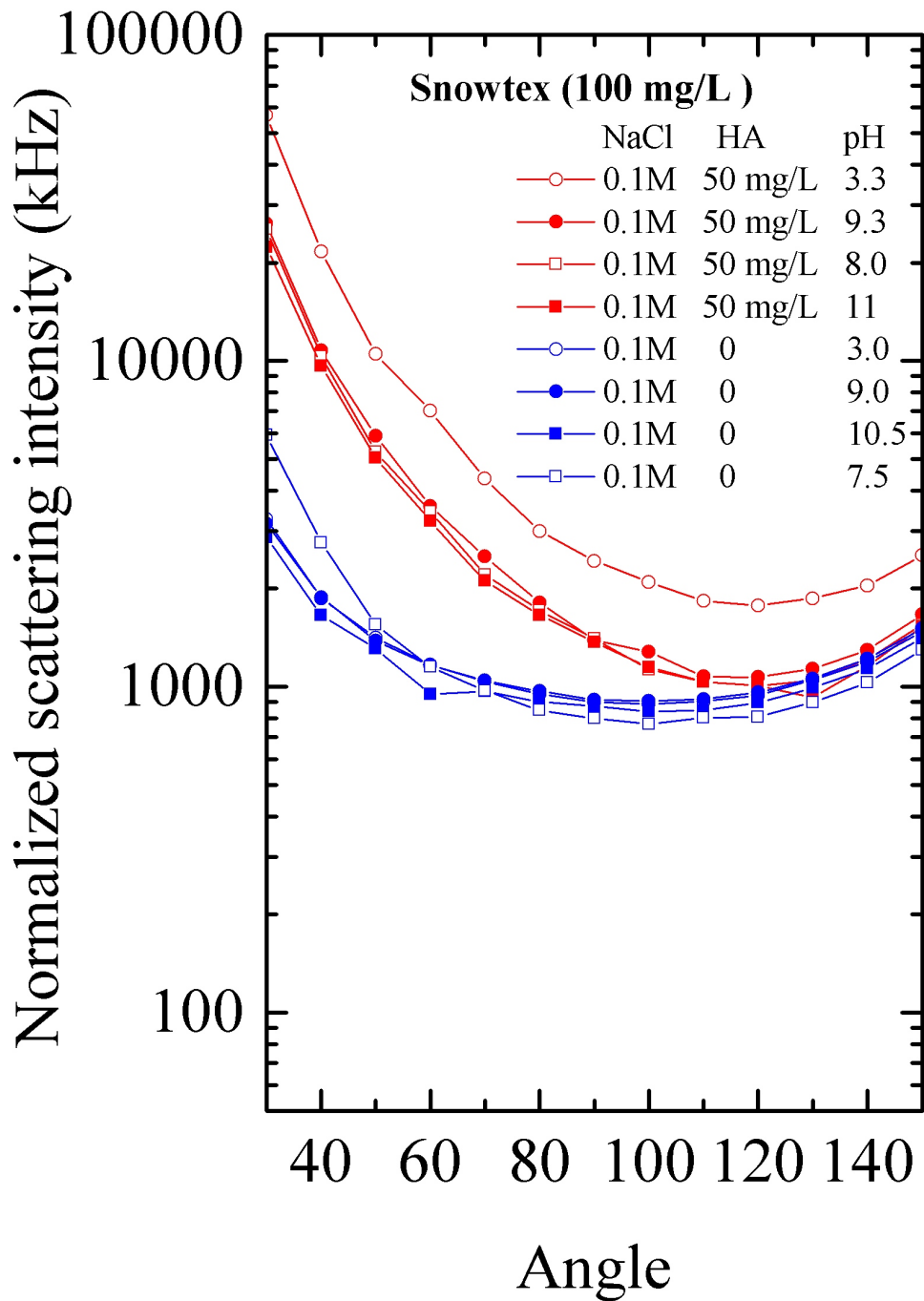


Figure 4.3 – 100 mg/L Snowtex[®] 20L and 0.1 M NaCl with and without 50 mg/L AHA

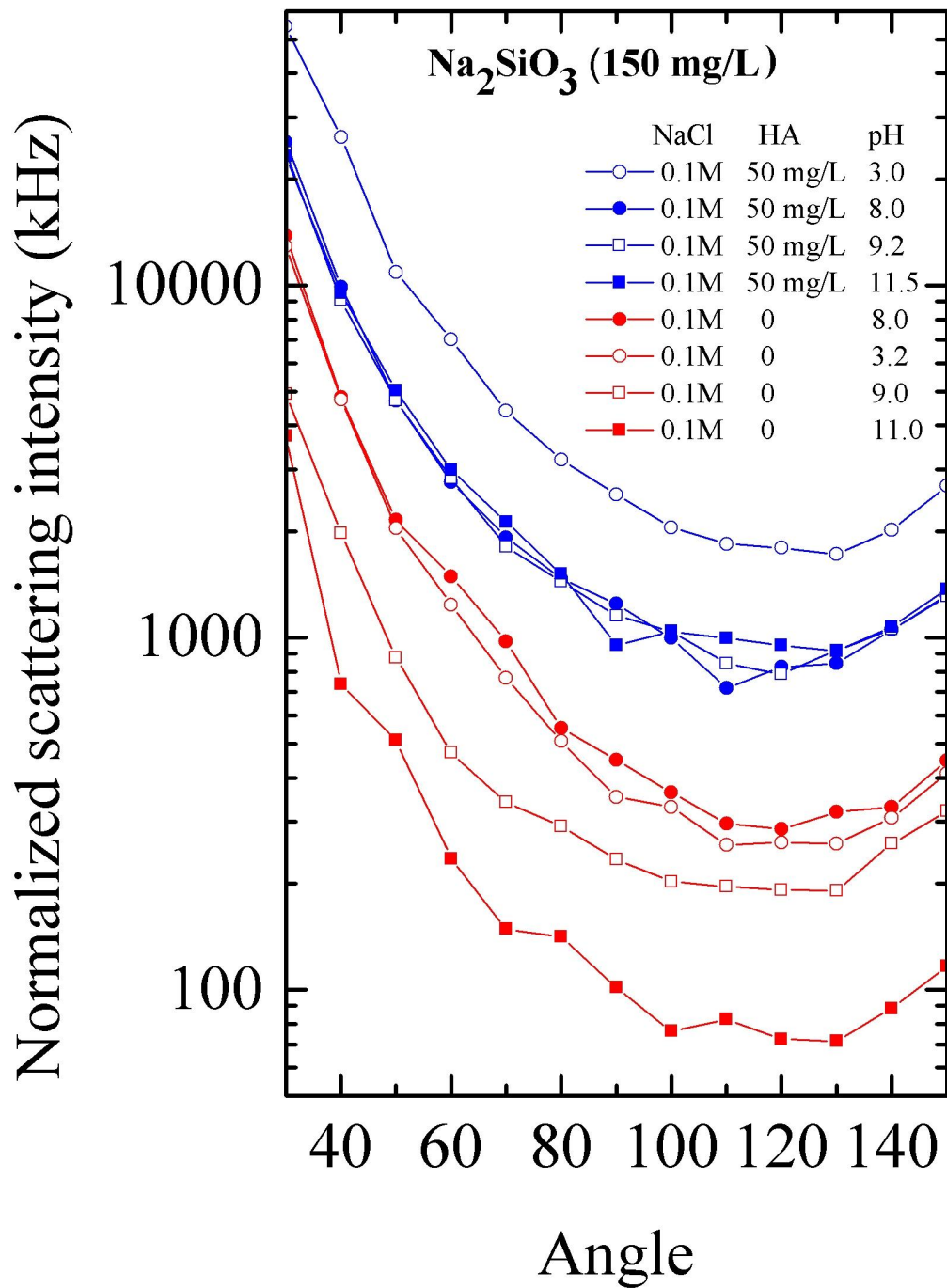


Figure 4.4 – 150 mg/L Na₂SiO₃ and 0.1 M NaCl with and without 50 mg/L AHA

4.2.5 Aggregation rate

Rate of increase in particle size was studied with dynamic light scattering. 150 mg/L Na_2SiO_3 was prepared with 0.1M $NaCl$ at pH 8, with and without 50 mg/L humic acid. DLS radius was recorded at every 5 minute for 1 hour (Figure 4.5). Also aggregation rate of 50 mg/L AHA at pH 8.0 was tracked for the same time range. For all three cases particle radius does not change with time. At alkaline pH both humic acid and silica is still negatively charged. So formation of Si-Si, Si-HA, HA-HA aggregate is unlikely [Gill, 1993]. Also Na_2SiO_3 particle size was found larger than humic acid and silica mixture particle size.

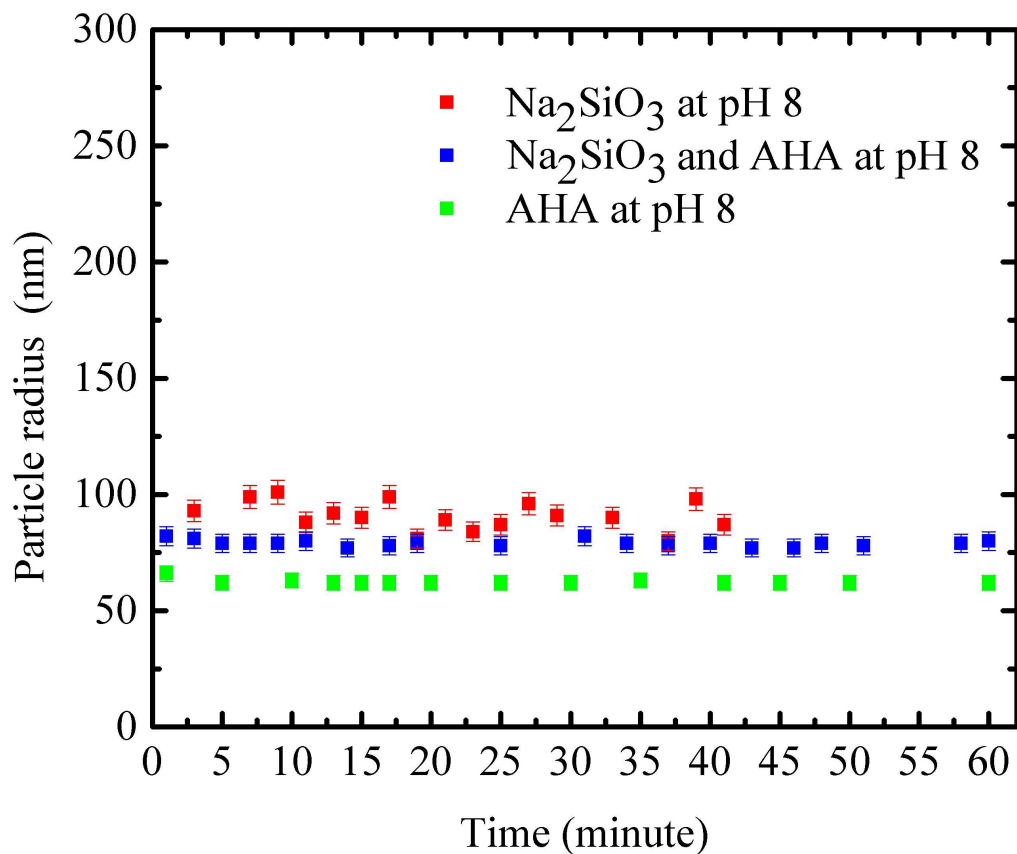


Figure 4.5 – Aggregation rate of 150 mg/L Na_2SiO_3 and 0.1 M $NaCl$ at pH 8 with and without 50 mg/L AHA

The reason behind this is, at this pH, silica forms the gel network structure consists of large number of small nano-particles, instead of ideal spherical particle [Iler, 1979], this causes increased scattering of light. As a result DLS calculates bigger hydrodynamic radius of silica particle alone. At pH 3 (Figure 4.6) we can see that particle size is increasing with time for all three cases and rate of increase is higher at the presence of AHA. Also from figure 4.5 and 4.6 all hydrodynamic radii (Na_2SiO_3 , AHA, and Na_2SiO_3 -AHA mixture) are higher at pH 3 compared to at pH 8.

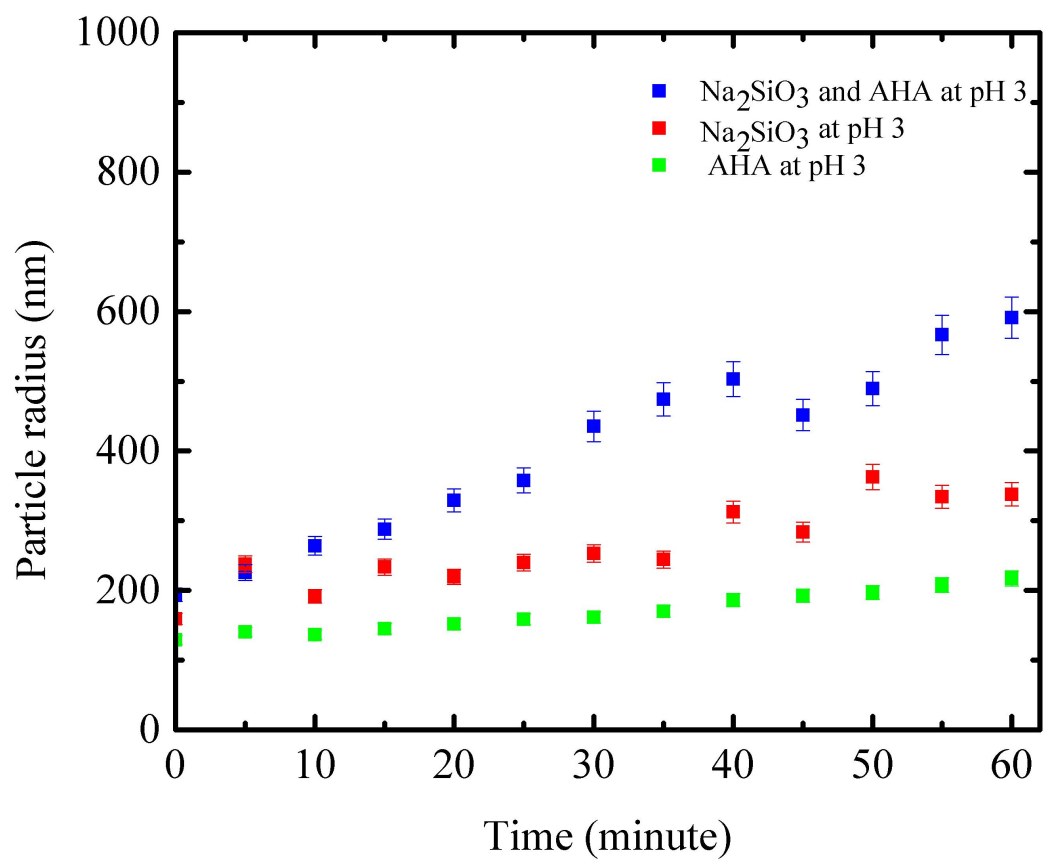


Figure 4.6 – Aggregation rate of 150 mg/L Na₂SiO₃ and 0.1 M NaCl at pH 3 with and without 50 mg/L AHA

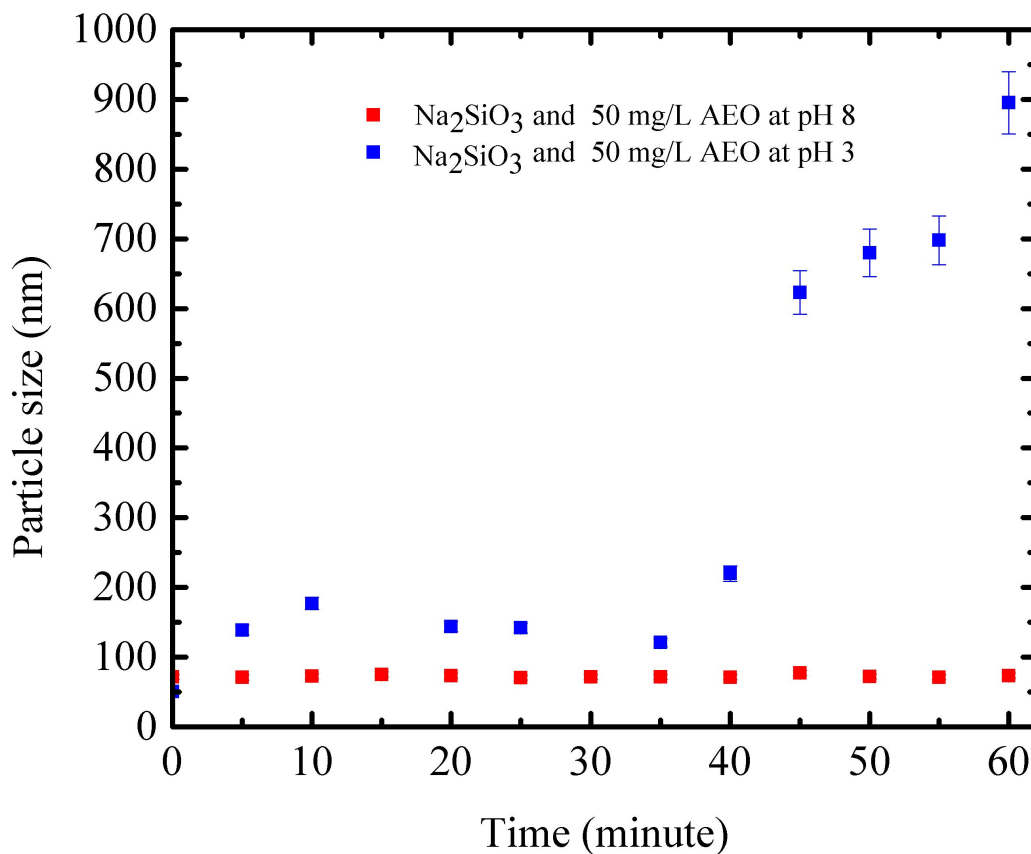


Figure 4.7 – Aggregation rate of 150 *mg/L* Na_2SiO_3 with 0.1 M $NaCl$ and 50 *mg/L* AEO at pH 8 and 3

Aggregate size with acid extractable organics (AEO) was also compared at pH 3 and 8. At the presence of 50 *mg/L* AEO aggregation rate of Na_2SiO_3 also increases at pH 3 (Figure 4.7). Because at low pH reduced surface charge of silica and organics causes aggregates as they collide.

Particle size in 50 *mg/L* AHA solution has increased in size at pH 3 at the absence of silica. But with *Snowtex*[®] 20L even at pH 3 increase in aggregation rate with AHA is not observed (Figure 4.8). This may be due to three reasons. Firstly, concentration of cation (Na^+ from 0.1M $NaCl$) is not enough to neutralize the negative surface charge of organics and silica to increase aggregation. Another reason may be, aggregation of *Snowtex*[®] with AHA at pH 8 is a slower process compared to Na_2SiO_3 . As a result DLS has not been able to capture silica organics interaction within the same period

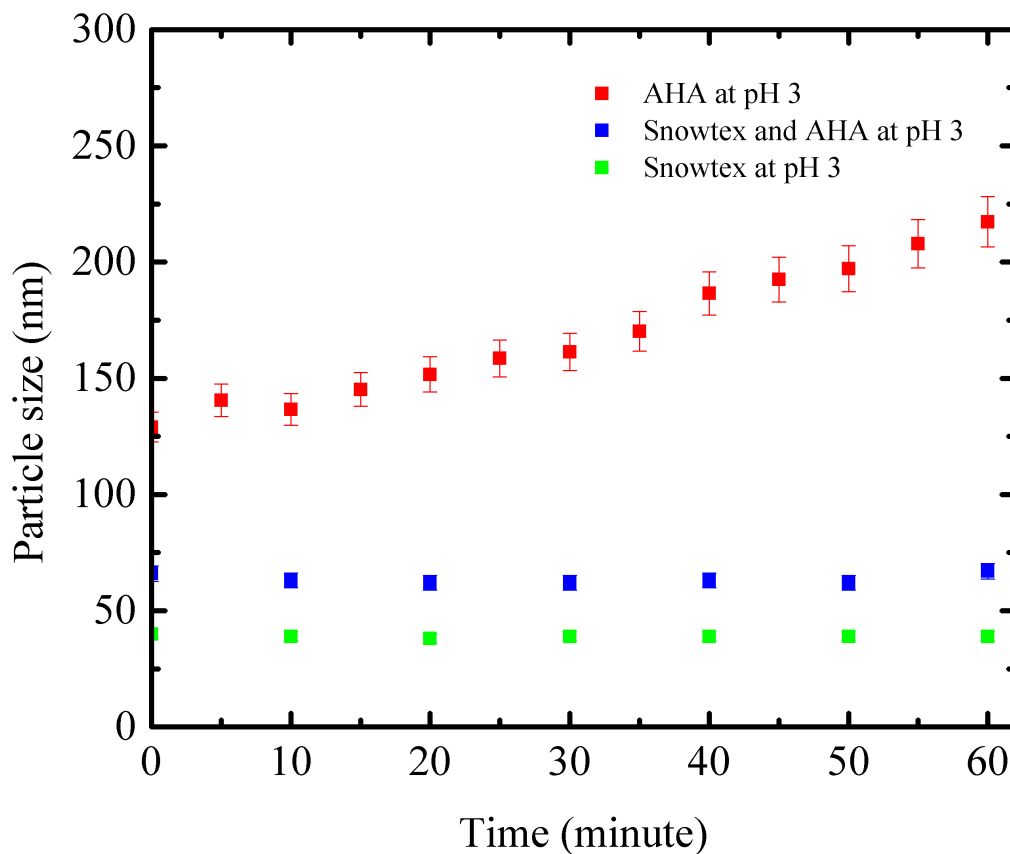


Figure 4.8 – Aggregation rate of 100 mg/L *Snowtex*[®] 20L and 0.1 M NaCl at pH 3 with and without 50 mg/L AHA

of time. Moreover, DOM adsorption on metal oxide occurs through complex formation between functional group of organics and the charged site of oxides surface [Illes and Tombacz, 2006]. So the third reason may be there were not enough silica surface sites for organics to be adsorbed. In order to find out if there is any interaction fractal dimension obtained from scattering intensity can be utilized.

In order to study shape of the aggregates fractal dimension obtained using light scattering technique was used. Detail analysis is given in Appendix B.

According to Rayleigh theory of light scattering, scattering intensity is proportional to the sixth power of diameter and second power of concentration [Holthoff et al., 1997b, Georgalis et al., 2012]. Scattering intensity increases due to increase in both particle size and concentration. So from above discussion, it can not be concluded undoubtedly that increase in scattering intensity

at the presence of humic acid is due to formation of bigger aggregates or due to increase in particle number. In order to obtain more information about silica organics interaction under industrial process conditions further analysis were performed with higher concentration of silica and organics.

4.3 Application of Taguchi method

In order to test a hypothesis, experiments are performed systematically under controlled environment at laboratory or at industrial scale for product design. Instead of one factor at a time (OFAT) or best guess approach, use of design of experiments (DOE) provides a cost effective way to understand a large problem with different factors and the probable response without doing large number of actual experiments [Montgomery, 2013]. According to [Montgomery, 2013] basic stages of DOE are shown in Figure 4.10.

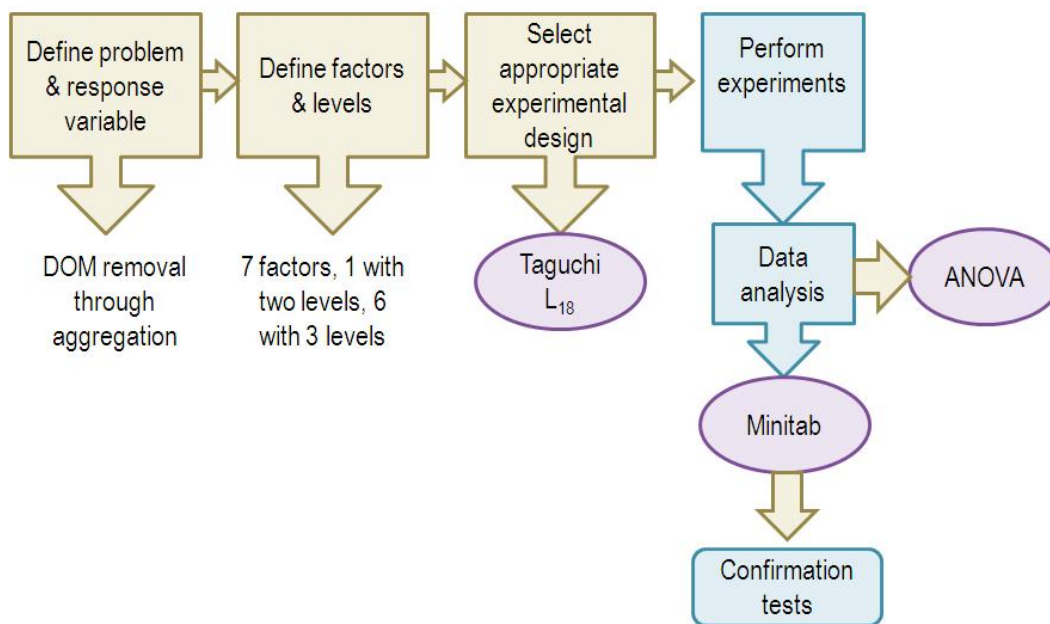


Figure 4.9 – Steps followed for design of experiments

4.3.1 Selection of appropriate experimental matrix

Problem with several factors at different levels requires factorial design in order to reduce cost and improve efficiency. Fractional factorial design can be an option which runs a subset of full factorial design. There are different orthogonal arrays with different number of rows designed by Taguchi to study larger problems with small number of experiments. By selecting appropriate OA for specific problem and with the help of software it is possible to predict the response for all possible combinations. Taguchi orthogonal arrays (OA) are widely used as a tool for factorial design. OAs are standard tables designed based on number of factors and levels. L_{18} is one type of OA which can be used for mixed level problems. It can accommodate one factor with two levels and seven factors with three levels [Pourjavadi et al., 2008, Elizalde-Gonzlez and Garca-Daz, 2010]. Standard L_{18} OA is shown in Appendix C.1. Three objectives can be achieved by Taguchi: optimize design parameters, estimate the contribution of each parameter, and predict optimal quality characteristic [Mohammadi et al., 2004a]. With the help of Taguchi OAs it is possible to find the influential factors and levels for optimum condition, minimize effects of noise factors within the allowable limit with minimum cost and higher process reliability [Montgomery, 2013]. ANOVA was used as statistical tool for data analysis. ANOVA is widely used as post experimental data analysis tool, to find out the significance of different process parameter. Percentage contribution of each factors can be determined using variance from ANOVA table [Gopalsamy et al., 2009].

Number of rows in an OA means the required number of experiments. Based on the factors and their levels, degrees of freedom is calculated and number of experiments should be at least equal to the degree of freedom [Bagci and Imrek, 2013]. This study considered seven parameters to understand silica organics co-precipitation. These are: types of colloids, types of organics, types of electrolytes or salt, pH, concentration of colloids, concentration of salt, and concentration of organics. Three levels for all the factors except for colloid type, were selected. Two types of colloids *Snoutex*[®] and polystyrene latex were selected based on their surface charge characteristics. So one factor with two levels and 6 factors with 3 levels were considered for this study. As a result, the degree of freedom (DOF) becomes, $1 \times (2 - 1) + 6 \times (3 -$

1) = 13. Based on these information Taguchi L_{18} OA with 18 rows was selected so that enough number of experiments (18) can be done. L_{18} has 8 column for 8 factors. The problem under consideration has 7 factors, so one column was left empty. Orthogonality will prevail even if one column is left empty [Rao et al., 2008]. In Taguchi method S/N ratio measure the deviation of quality characteristic from desired value. S/N ratio shows the variations among replicates [Ng and Ng, 2006]. Uncontrollable factors such as noise factors cause deviation and therefore loss. Elimination of noise factor is often impossible. So Taguchi seeks to minimize the effect of noise and determine the optimum level of important controllable factors. It tries to find out the best set of controllable factors irrespective of the variation of magnitude of uncontrollable factors. Taguchi utilizes three types of S/N ratios, larger the better, smaller the better and nominal the better. Since our response variable is removal of DOM, we considered larger the better scenario, which was calculated using following equation [Rao et al., 2008]:

$$\frac{S}{N} = -10 \log\left(\frac{1}{n} \sum \frac{1}{y^2}\right) \quad (4.1)$$

4.3.2 Preliminary screening and selection of levels

Since the target of these phase was to take higher concentrations of silica and organic into account, some preliminary screening experiments were performed to find out the range of concentrations to work with. Results of the screening experiments are shown in table 4.2:

Table 4.1 – Screening experiments (all concentrations are in mg/L)

Colloid type	Colloid conc.	AHA conc.	pH	%removal
<i>Snowtex</i> [®] ZL	200	500	3	77
<i>Snowtex</i> [®] ZL	500	500	4	77
<i>Snowtex</i> [®] ZL	500	100	3	83
<i>Snowtex</i> [®] ZL	1000	500	4	71
<i>Snowtex</i> [®] ZL	1000	100	6	32

From the results it can be marked that, for *Snowtex*[®] ZL both concentrations (500 and 1000 mg/L) results in higher removal i.e. aggregation, at AHA concentration of 500 mg/L . Again 500 mg/L *Snowtex*[®] ZL with 100 mg/L AHA resulted in higher removal. So the concentrations for both colloid and organics were selected as 100 mg/L , 500 mg/L , and 250 mg/L was selected as mid level of concentration. Effect of valence of cation is also important on coagulation rate [Masliyah and Xu, 2011]. *NaCl*, *CaCl*₂, *AlCl*₃ were selected as monvalent, divalent and trivalent ions. The concentrations of salts were selected as 0.01M, 0.1 M, and 0.25M so that all of them were above theoretical critical coagulation concentration (CCC). In order to compare effectiveness of different types of organics on coagulation we considered three types of organics in this study, a) model humic acid (AHA), b) raw boiler blow down (BBD) from SAGD plant, and c) acid extractable organics from BBD. Three pH were selected based on the pKa values of organics, colloid surface charge, and SAGD operating conditions. Detail operating procedure is described in Appendix C.2. Samples were prepared by combining all the factors, then shaker was used for 24 hours to enhance aggregation. After letting the sample precipitate for 24 hours, the supernatant was taken carefully and analyzed using TOC analyzer. Image of all the samples are attached in Appendix C.3.

4.3.3 Experimental matrix and results

The experimental matrix and results from L_{18} experiments are shown in the following tables:

Table 4.2 – Experimental matrix (all concentrations are in *mg/L*)

Exp. no.	Coll. type	Org. type	Salt type	Coll.conc.	Org. conc.	Salt conc.	pH
1	<i>Snowtex</i> [®] ZL	AHA	<i>NaCl</i>	100	100	0.01	3
2	<i>Snowtex</i> [®] ZL	AHA	<i>CaCl₂</i>	250	250	0.1	6
3	<i>Snowtex</i> [®] ZL	AHA	<i>AlCl₃</i>	500	500	0.25	9
4	<i>Snowtex</i> [®] ZL	AEO	<i>NaCl</i>	100	250	0.1	9
5	<i>Snowtex</i> [®] ZL	AEO	<i>CaCl₂</i>	250	500	0.25	3
6	<i>Snowtex</i> [®] ZL	AEO	<i>AlCl₃</i>	500	100	0.01	6
7	<i>Snowtex</i> [®] ZL	BBD	<i>NaCl</i>	250	100	0.25	6
8	<i>Snowtex</i> [®] ZL	BBD	<i>CaCl₂</i>	500	250	0.01	9
9	<i>Snowtex</i> [®] ZL	BBD	<i>AlCl₃</i>	100	500	0.1	3
10	Latex	AHA	<i>NaCl</i>	500	500	0.1	6
11	Latex	AHA	<i>CaCl₂</i>	100	100	0.25	9
12	Latex	AHA	<i>AlCl₃</i>	250	250	0.01	3
13	Latex	AEO	<i>NaCl</i>	250	500	0.01	9
14	Latex	AEO	<i>CaCl₂</i>	500	100	0.1	3
15	Latex	AEO	<i>AlCl₃</i>	100	250	0.25	6
16	Latex	BBD	<i>NaCl</i>	500	250	0.25	3
17	Latex	BBD	<i>CaCl₂</i>	100	500	0.01	6
18	Latex	BBD	<i>AlCl₃</i>	250	100	0.1	9

Average percentage removal was calculated based on initial organics concentration and by deducting the final organics concentration from initial value. These results were analyzed using statistical software MINITAB RELEASE 16. The response mean found was 48% DOM removal and average *S/N* ratio was 30. Optimum condition with two log removal (>99%) of organics was found at following levels of all the factors:

Table 4.3 – DOM removal

Exp. no.	Average percentage removal	<i>S/N</i> ratio
1	73	39.8
2	91.7	37.3
3	81.4	38.2
4	14.1	22.8
5	66.5	36.5
6	85.9	38.7
7	11.8	21.4
8	2.7	8.6
9	41.2	32.3
10	14.0	22.7
11	86.4	38.7
12	85.3	38.6
13	23.9	27.5
14	49.7	33.7
15	65.1	36.3
16	23.3	27.2
17	1.5	2.1
18	51.5	34.3

Table 4.4 – Optimum condition

Factor	Level
Type of colloid	<i>Snowtex</i> [®]
Type of organics	AHA
Type of salt	<i>AlCl</i> ₃
Conc. of colloid	250 <i>mg/L</i>
Conc. of organics	100 <i>mg/L</i>
Conc. of salt	0.25M
pH	3

Confirmation test was performed using MINITAB predicted optimum condition (table 4.5). DOM removal obtained was 90%, which can be considered as significant removal. From tables 4.4 and 4.5 it is evident that this result is also comparable with number 2 condition, with $CaCl_2$ and 250 mg/L AHA.

4.3.4 Predicted response obtained using MINITAB

From the MINITAB prediction recorded in Appendix C.4 it is evident that, with silica concentration 100 mg/L and all other conditions being same as optimum condition still two log removal is possible. Moreover, DOM removal of AEO samples are comparable with AHA samples at same conditions. At optimum condition, if BBD is taken into consideration the removal will be reduced to 72%. If, initial DOM value of BBD is changed to 500 mg/L removal will reduce dramatically to 48% (at the presence of 100 mg/L silica) and 52% (250 mg/L silica). Instead of $AlCl_3$, if 0.25 M $CaCl_2$ is considered with 100 mg/L BBD and 100 mg/L silica at pH 3, removal will be 38% and 42% with 250 mg/L silica. With the increase in DOM concentration in BBD the removal percentage will be reduced to 22%. With $NaCl$ all the conditions shows lower removal. Only significant removal percentage is 20% with 0.25 M $NaCl$, 100 mg/L BBD, 250 mg/L silica at pH 3. 0.01M and 0.1M $NaCl$ are very low concentrations to affect the colloidal stability [Furman et al., 2013]. All these predictions suggests that with BBD removal is very low at low salt concentration specially with monovalent cation.

pH is a very important parameter in SAGD plant condition as the water goes through pH changes during the process. Change of pH also has significant affect on silica-organics co-precipitation. Analysis of the results using MINITAB prediction tool without considering salt type and salt concentrations parameters shows that, at low pH (pH 3) DOM removal is 69% even at higher concentration of AHA and silica (500 mg/L). Without any salt optimum condition is predicted at pH 3 with 250 mg/L *Snowtex*[®] and 100 mg/L AHA. Around pH 6 and at extreme concentrations of silica and AHA (500 mg/L) removal is still around 57%, which reduces to 54% at pH 9. For AEO (100 mg/L) highest removal (82%) without salt is predicted at pH 3, and with 250 mg/L *Snowtex*[®]. Whereas with BBD highest removal is predicted as

53% with all other conditions being same. Lowest removal at extreme condition (500 mg/L *Snowtex*[®] and BBD at pH 9) is predicted to be around 5% which is higher than the predicted removal at extreme condition with salt. These predicted results corroborates with the results of previous works by the group members, which identified that at low concentration of multivalent cations or coagulants pH is the most effective parameter that causes silica-DOM aggregation.

4.3.5 Effects of parameters at different levels

The main effects plot (Figure 4.11) shows effect of different factors at different levels. It is apparent from the figure that aggregation of *Snowtex*[®] is higher compared to sulfate latex. This can be explained by zeta potential as a function of pH plot. *Snowtex*[®] is less negatively charged compared to latex. Latex is more stable at different pH range [Herman and Walz, 2013, Mamun, 2012]. Silica aggregation rate is higher with AHA i.e humic acid compared to AEO and BBD. AHA has more acidic functional group (carboxylic and phenolic) which increases aggregation rate.

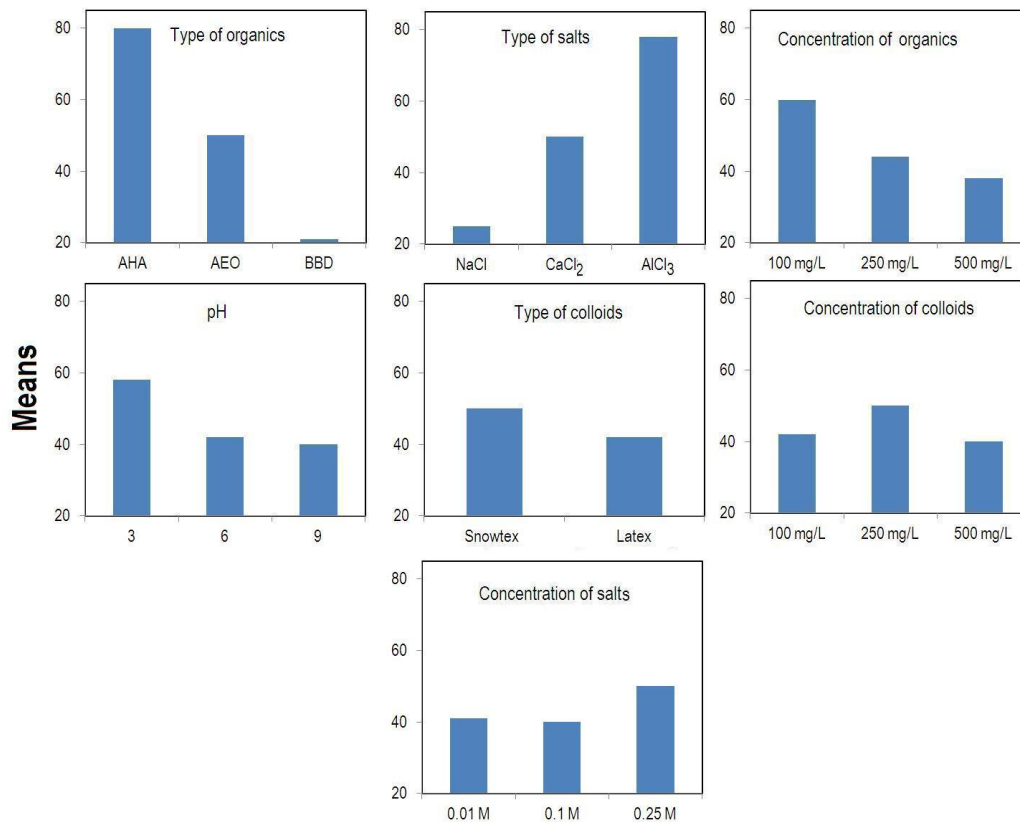


Figure 4.10 – Main effects plot for means

Total acidity of AHA, AEO and BBD is 75.5, 44.1 and 33.8 *meq/g* of organic carbon. $SUVA_{254}$ value of these three organics measured are 10, 5.0 and 3.1, which indicates the presence of hydrophobic, aromatic compounds in AHA and AEO [Thurman et al., 1982]. FTIR spectrum of AHA (Figure 4.12) shows presence of COOH group (peak at 1580 cm^{-1}). FTIR analysis of BBD showed peaks due to Si-OH (968.7 cm^{-1}), Si-O-Si (1017 and 1098 cm^{-1}) bond stretching, presence of COOH (1412 cm^{-1}), N-H (1548 cm^{-1}), aliphatic and aromatic C=C (1660 cm^{-1}), and C-H (2870 and 2931 cm^{-1}) bond [Thakurta et al., 2013]. AEO was obtained from BBD by precipitating the hydrophobic fraction at pH 2 and major fraction of AEO is also humic like substances. All the information mentioned above indicates that humic fraction consists of mainly carboxylic group increases aggregation rate.

All levels of electrolyte concentrations were well above critical coagulation concentration (CCC) of three types salts [Masliyah and Bhattacharjee, 2006].

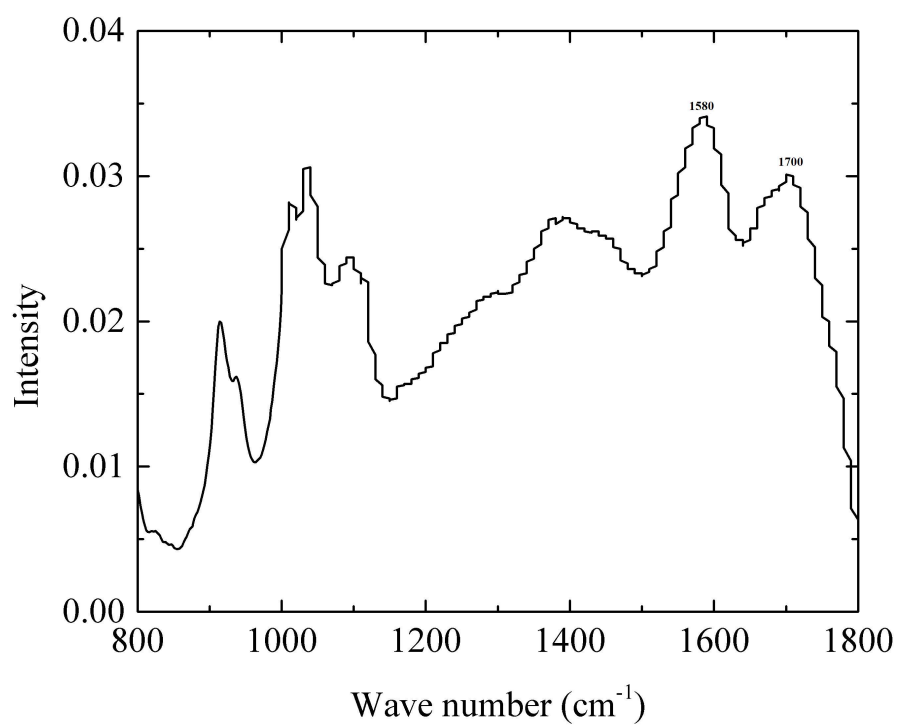


Figure 4.11 – FTIR spectrum of AHA

For polystyrene latex CCC is around 0.3M and it is stable below 0.25M monovalent salt [Seebergh and Berg, 1995]. This was confirmed by series of UV-Vis absorbance experiments at different salt concentration (Figure 4.13). With the increase in salt concentration from 0.1M to 0.25M *NaCl* UV-Vis absorbance increased. Then above 0.25 M concentration of *NaCl* and also with 0.1M *CaCl₂* absorbance decreased. For *NaCl* 0.5M is above CCC and divalent Ca^{2+} is more effective even in lower concentration according to Schulze-Hardy rule [Masliyah and Bhattacharjee, 2006]. At these conditions colloidal stability is reduced which leads to formation of bigger aggregates.

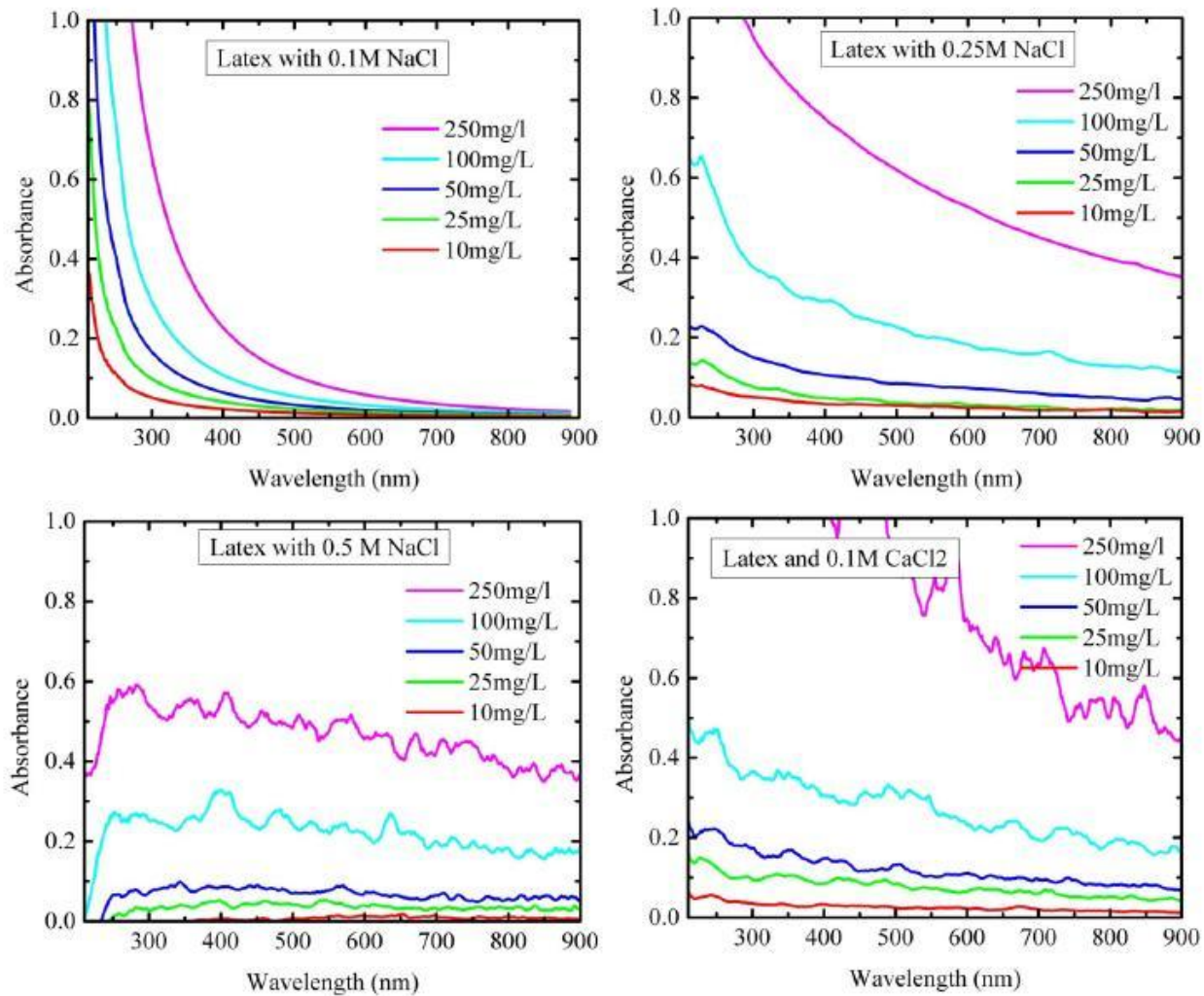


Figure 4.12 – UV-Vis spectroscopy of Polystyrene sulfate latex

Percentage removal of DOM increases with the increase in salt (electrolyte) concentration due to the compression of double layer thickness and surface charge reversal. At CCC of salt, energy barrier is zero and the stability ratio becomes 1 which means aggregation rate is same as fast coagulation region [Masliyah and Bhattacharjee, 2006]. Site binding of cations with a particular functional group of organics through electrostatic interaction leads to charge reversal [Majzik and Tombacz, 2007, Manning et al., 2000]. As a result organics form aggregates with metal oxides. Increase in salt concentration also decrease the net negative surface charge [Maiti et al., 2012] which in turn increases aggregation. CCC value changes as the amount of organics added increases [Illes and Tombacz, 2006].

Potentiometric titration (Figure 4.14) of AHA identified two pKa values, 9.8 and 6.3. Singh and Song, 2007 found that with humic acid and *Snowtex*[®] 20L and ZL [Singh and Song, 2007b] membrane fouling potential increases at pH around 10, this also indicates that the presence of pKa value at pH around 10 increase the aggregation. AEO has pKa at 3, 5.5. pKa values of BBD are 3.3, 7.3, and 10.2 [Maiti et al., 2012]. pKa values are a measure of dissociation of proton or functional groups [Li et al., 2005]. For carboxylic group pKa range is within 2.5 to 5 and phenolic pKa value is around 9 to 10 [Metsmuuronen et al., 2014]. So bridging with silica through cation will be produced by carboxylic group of organics at pH range 2.5 to 5 and by phenolic group at pH range 9 to 10.

Silica and organics interact through hydrogen bonding and van der Waals attraction [Maiti et al., 2012]. Hydrogen bonding could occur between the hydrogen of Si-OH and oxygen and nitrogen of different functional groups of organic matter. They may exchange legands or at the presence of cation form silica-cation-organic bridge [Tipping, 2002]. Hydrophobic interaction also has effect on aggregation. Above pH 8 silica is negatively charged species and will remain dissolved, but at pH below 8 it becomes less negative charged species and interact with organics to form aggregates [Iler, 1979]. Diffusivity of humic acid also increases with decreasing pH and increasing calcium concentration. Higher diffusivity means higher collision and higher aggregation rate [Masliyah and Xu, 2011]. So at low pH and high ionic strength humic acid molecules form compact aggregates.

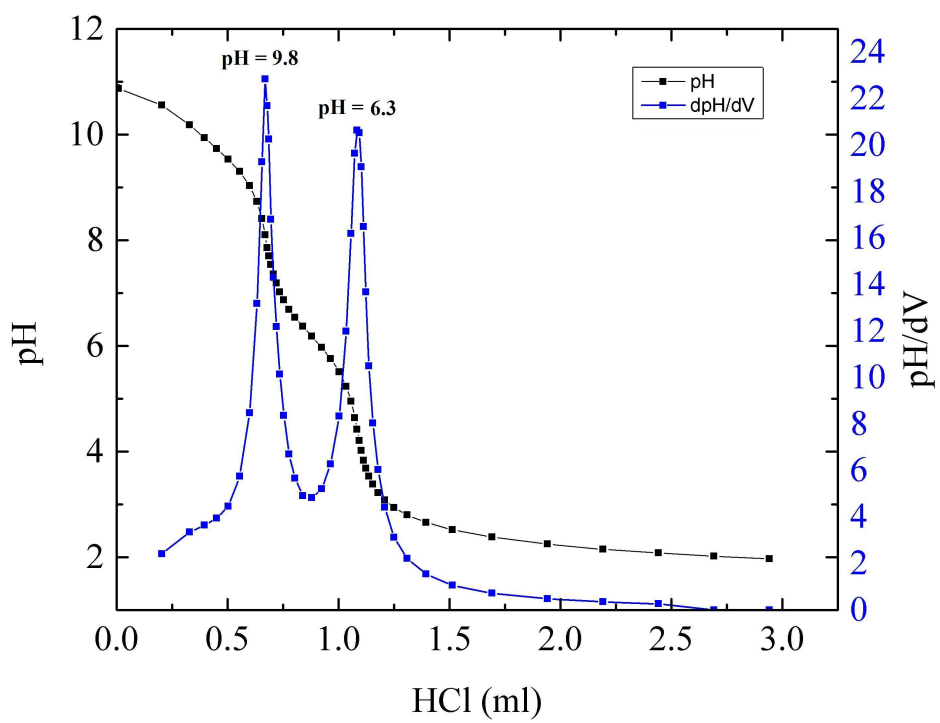


Figure 4.13 – Potentiometric titration of AHA

Valence of cations has dominant effect on colloidal stability [Masliyah and Xu, 2011]. Percentage removal increases with the increase of valence of salt (electrolyte) following Schulze-Hardy rule [Masliyah and Bhattacharjee, 2006]. Besides Ca^{2+} has affinity for COOH group of humic acid and forms aggregates. Al^{+3} also enhance aggregation through double layer compression, inter-particle bridging or charge neutralization by adsorption on surface [Metsmuuronen et al., 2014]. Adsorption of cation is maximum at the pKa values of organics [Tipping, 2002, Majzik and Tombcz, 2007]. So at all pH (3.0, 6.0, 9.0) adsorption of counter ion on silica surface reduces electric repulsion and particles can come closer to form aggregates. Reduction of surface charge due to cation adsorption has more impact than electric double layer thickness reduction by increasing electrolyte concentration [Masliyah and Xu, 2011]. pKa values or degree of dissociation also depends on ionic strength [Marinsky and Ephraim, 1986]. It is also evident from the figure 4.15, which shows type of salt has higher percentage contribution than salt concentration.

Effect of multivalent cation and pH on organic precipitation

Charge of humic acid is mainly due to presence of carboxylic group and phenolic group. At high pH only phenolic group is protonated but at low pH both carboxylic and phenolic groups are protonated. At higher pH (9 to 10) organic molecules are more negatively charged [Wang and Kasperski, 2010]. At higher pH (greater than pH 8) cation binding becomes more significant [Furman et al., 2013] in the organic precipitation process. Surface charge of colloids also depends on pH. At lower pH (below 5) surface charge of silica is reduced due to availability of H^+ ions. As a result aggregation between protonated organic acid and less negatively charged silica is enhanced due to hydrogen bonding [Tipping, 2002]. For these above mentioned reasons DOM removal is higher at low pH (3) and less at higher pH, as shown in the main effects plot. There is no significant difference between mean response at pH 6 and 9. At pH 6 all negatively charged organic molecules are not yet neutralized. A large fraction of organic molecules is still negatively charged. Thus, aggregation is not as high at pH 6 as observed for pH 3. Here, the relative effectiveness of multivalent cations and pH is worth to notice. DOM removal is high even at pH 6 (for sample 2 with 0.1M $CaCl_2$: 91.7% and sample 6 with 0.01M $AlCl_3$: 85.7%). But at the presence of monovalent $NaCl$, even

at higher concentration (0.25M) the DOM removal is low (sample 7: 11.8%). At pH 9 with 0.25M $AlCl_3$ DOM removal is 81.4% (sample 3), with 0.25M $CaCl_2$ DOM removal is 86.4% (sample 11). DOM removal decreases again at the presence of $NaCl$ at pH 9 (sample 4: 14.1%). From these results it can be concluded that multivalent cations are more effective in neutralizing the negative surface charge of organics and silica even at higher pH.

4.3.6 ANOVA

Analysis of variance (ANOVA) is useful statistical tool and a type of regression analysis that compares the group mean with a grand mean. In this study ANOVA was employed to find out whether the variance is due to different levels of a factor or just experimental error [Sadrzadeh and Mohammadi, 2008]. There are three different types of ANOVA, one way independent, two way independent and three way repeated measure. In one way ANOVA, one factor has different levels and each observation is independent [Allen, 2005]. In our study one way ANOVA was used to calculate sum of Squares, degree of freedom, variance, F value and p value.

Table 4.5 – ANOVA table

Parameters	Sum Sq.	DOF	Variance	F measured	F_{table} at 95%	p value
Type of org.	14559	2	7279	55.87	3.44	0.000
Type of salt	10732	2	5366	41.18	3.44	0.000
Conc. of org.	2454	2	1227	9.42	3.44	0.001
pH	1478	2	739	5.67	3.44	0.010
Type of coll.	687	1	687	5.27	4.30	0.032
Conc. of coll.	1115	2	557	4.28	3.44	0.027
Conc. of salt	688	2	344	2.64	3.44	0.094

Sum square for each factor was calculated using following equation in Excel:

$$SS_F = \sum_{i=1}^L \left(\frac{Z^2}{n_Z} \right) - \frac{T^2}{N} \quad (4.2)$$

L is the number of levels for the factor, n_Z is the number of total observation at same level of that factor, Z is sum of all observation at the same level. T is sum of all observation and N is number of total observation. Sum of error was calculated using following equation:

$$SST = \sum (T - T_{(mean)})^2 \quad (4.3)$$

Here $T_{(mean)}$ is the grand mean of all observations. Sum of error, SSE = SST-(Summation of sum squares for all factors).

Variation between the groups for a factor is calculated by dividing the sum square for a factor by its degree of freedom.

$$\text{Variation between group} = \frac{SS_F}{DOF} \quad (4.4)$$

Variation within group is calculated as follows

$$\text{Variation within group} = \frac{SSE}{\text{error } DOF} \quad (4.5)$$

Degree of freedom (DOF) represents data points or sample size. DOF is the independent pieces of information that can go in to the estimation of a parameter. If a data set contains n number of observations it means, it has n individual pieces of information. This leaves n-1 degrees of freedom for estimating variability. F value is the ratio of variation between group and variation within group. So large variance between groups will cause higher

F value and large variance due to error will cause small F value. As a result, from F values it is possible to identify significant factors which affects the performance. F value is ratio so it cannot be zero. If it is less than one that means error is higher than the effect variance [Allen, 2005]. p value gives the probability of occurrence of a particular F value. Percentage contribution is calculated by dividing the variance by sum of all variances and then by multiplying with 100. Percentage contribution gives quantitative information regarding influence of each factor. F extracted values were found from statistical table of 95% confidence level using degree of freedom. From ANOVA table it is obvious that, F measured values for factors: type of organics and type of salt exceeds F extracted values for 95% confidence level. Therefore, it can be said with 95% confidence that these factors have significant impact on DOM removal. Chance of type I error is 0.05% if we conclude that, type of organics and type of salt is most significant for higher DOM removal. p values are less than significance level (0.05) for factors type of organics and type of salt. So we can reject the null hypothesis and conclude that there is significant difference among means due of these factors. So these are influential factors which cause higher DOM removal (higher aggregation).

Percentage contribution for each factor is calculated using following equation:

$$P = \frac{\text{Variance}}{\text{Sum of variance}} \times 100 \quad (4.6)$$

Pareto chart (Figure 4.15) shows the percentage contribution by each parameter (causes) [Card, 1998]. Change in the type of organics governs the degree of aggregation mostly, followed by type of salt, concentration of organics, pH, type of colloids, concentration of colloids, and finally, concentration of salt.

Important observation from the ANOVA table is that the type of organics is the most critical factor affecting aggregation. And the optimum condition shows that humic acid contributes most on silica-organic co-precipitation. According to Tipping, 2002, Matilainen et al., 2011, and Manning et al., 2000 [Tipping, 2002, Matilainen et al., 2011, Manning et al., 2000] humic-like fraction of DOM is mostly hydrophobic, negatively charged and it consists of aliphatic, aromatic as well as carboxylic acid, amine, carbonyl, and alcohol functional group. Based on elemental analysis of purified Aldrich humic acid,

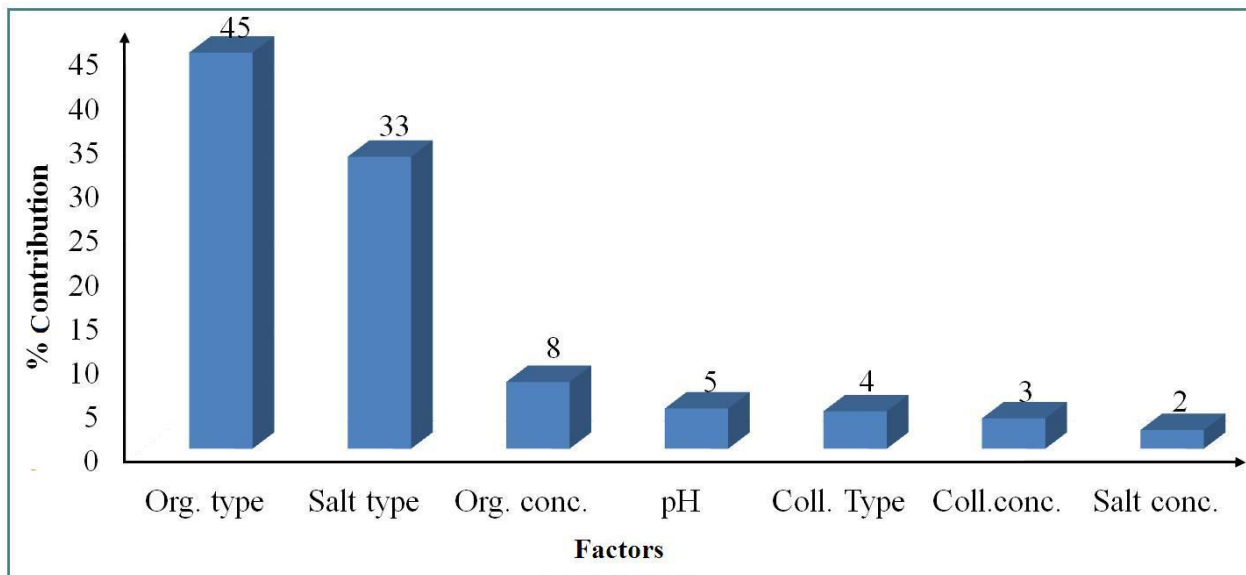


Figure 4.14 – Pareto chart

it has 55.08% Carbon, 4.25% Hydrogen and 0.71% Nitrogen [Koopal et al., 1998]. If molar ratio of H to C is less than 1 it means majority of aromatic structure, if the ratio is within 1 to 1.4 there is majority of aliphatic structure [Khilko et al., 2011]. Aromatic fractions with more acidic functional group are more effective to increase aggregation. Humic acids are negatively charged poly-electrolytes [Metsmuuronen et al., 2014]. They adsorb on silica surface by electrostatic attraction, legand-exchange with protonated surface hydroxyl group, cation bridging, water bridging at the presence of hydrated cations on the surface, hydrophobic interaction of uncharged macromolecules of humic acid. At acidic condition adsorbed humic acid on silica surface may cause charge reversal [Kretzschmar et al., 1998]. Besides, hydrophobic humic-like fraction has higher charge density and lower zeta potential compared to hydrophilic fraction [Metsmuuronen et al., 2014].

BBD also has 36.8% HPoA (mostly humic acid) 27% HPiN (aliphatic amines, amides) [Thakurta et al., 2013]. SUVA values at 254 *nm* of BBD fractions are: HPoA 4.24, HPoN 3.95, HPiA 2.02, HPiA 1.11, HPoB 0.61, HPiN 0.7. FTIR of BBD showed precipitation of aromatic carboxylic acid, OH group, CO group at pH 2 [Thakurta et al., 2013]. At lower pH due to protonation of humic acids hydrophobic interaction becomes more dominant and precipitates as they become less water soluble [Metsmuuronen et al., 2014]. Moreover, AEO is also mainly the hydrophobic fraction of BBD that has precipitated at pH 2. Since humic acid is the major fraction of BBD [Thakurta

et al., 2013] it can be concluded that in SAGD water treatment plant humic-like fraction of BBD is mainly responsible for silica and organic aggregation.

4.3.7 Interaction between parameters

Taguchi L_18 is designed to examine interaction between only column 1 and 2. So from the above experimental matrix and results it is not possible to identify interaction between other factors [Maghsoodloo et al., 2004]. So separate experiments were performed to see the interaction between pH and type of organics (Figure 4.16). Four samples were studied, two with AHA and two with BBD at pH 3 and 9. Same colloid ($250 \text{ mg/L Snowtex}^{\text{®}}$) and salt concentration (0.1 M CaCl_2) were maintained. From the figure, it is noticeable that AHA at pH 3 and 9 are not interacting with BBD at pH 3 and 9. So, it can be concluded that there is no interaction between pH and types of organics. This means change of pH will not affect the results due to change in the organics type.

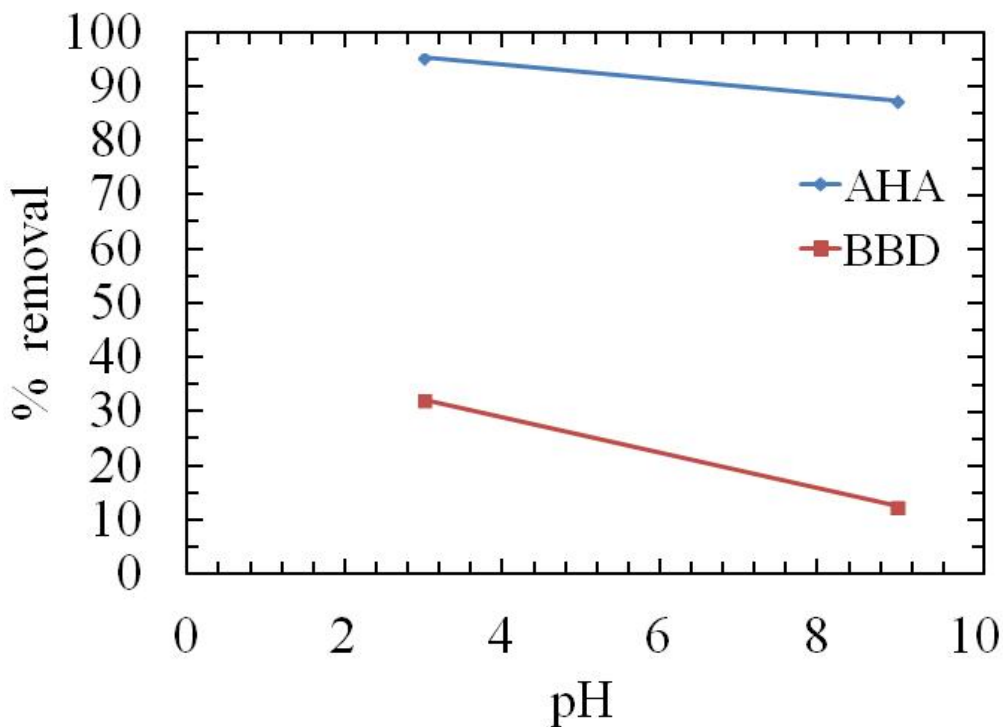


Figure 4.15 – Interaction between organics type and pH

4.3.8 Analysis of supernatant using $SUVA_{254}$

$SUVA_{254}$ is another way of characterizing DOM. Different molecules absorb light strongly at different wavelength. For organic molecules 220 nm to 280 nm is appropriate range to identify different chromophore [Matilainen et al., 2011]. Aromatic groups absorb light at 254 nm. So from the specific UV-absorbance at 254 presence of aromatic group can be identified.

At lower pH, aromatic and humic-like organics are less negative and since they are hydrophobic, they precipitate. But aliphatic fulvic acid fraction is hydrophilic so they remain soluble in water [Tipping, 2002]. From table 4.7 it is obvious that aromatic humic-like fraction is not present in the supernatant for most of the samples. So removal of humic-like fraction was possible through varying pH, salt type and concentrations. Fluorescence analysis also confirmed this finding. Only in sample 1, 10 and 13 there is trace of aromatic groups. This due to the fact that these samples had $NaCl$ (0.01 and 0.1M concentration) which is not as effective as $CaCl_2$ and $AlCl_3$ to increase aggregation.

Table 4.6 – $SUVA_{254}$ values (in $Lmg^{-1}m^{-1}$) of the samples

Sample	$SUVA_{254}$
1	4.6
2	3
3	2.9
4	2.7
5	3.7
6	0.89
7	3.1
8	3.8
9	3.4
10	6.5
11	2.2
12	0.47
13	8.1
14	2.5
15	0.25
16	2.3
17	2.9
18	1.2

4.3.9 Analysis of supernatant using fluorescence spectroscopy

Fluorescence excitation emission matrix were generated for samples of 1, 2, 3, 6, 9, 12, 15, 18, and optimum condition (Figure 4.17, 4.18, and 4.19). For AHA no fluorophore excitation was observed. According to Matilainen et al. 2011, [Matilainen et al., 2011] although conjugated double bonds, aromatic rings, NH_2 enhance fluorescence, but carboxylic group (COOH) reduces it. Since humic acid is consists of mostly COOH group, it can explained that fluorophore were weakened by this group. Ex/Em peaks of Aldrich humic acid was found at 350/450 nm and 390/485 nm at a concentration of 10 mg/L and peaks at 480/540 nm at 100 mg/L concentration [Matthews et al., 1996]. Optimum sample (Figure 4.18) shows a peak at Ex/Em wavelength 250-270 nm and 425-427 nm . Sample 1 containing AHA has two peaks. One occurred at Ex/Em wavelength 250-350 nm and 400-500 nm and another at 200-250 nm and 400-500 nm . Sample 2,3, and 12 with AHA shows removal of all types of DOM fraction. Sample 6 which has AEO has peaks at Ex/Em wavelength 220-275/ 325-450 nm for Tyrosin and protein like compounds and at 275-300/350-

375 *nm* is due to tryptophan like compounds [Matilainen et al., 2011]. Sample 9 with BBD has peaks at Ex/Em wavelength 300-350/400-450 *nm* and 225-250/400-420 *nm* due to fulvic acid. Sample 15 with AEO has peak at Ex/Em wavelength 225-250/350-425 *nm*. Sample 18 with BBD has peaks at Ex/Em wavelength 300-325/375-425 *nm* and 225-250/375-450 *nm* due to humic-like fractions. From the analysis it is evident that different fractions of organics were removed at different treatment conditions.

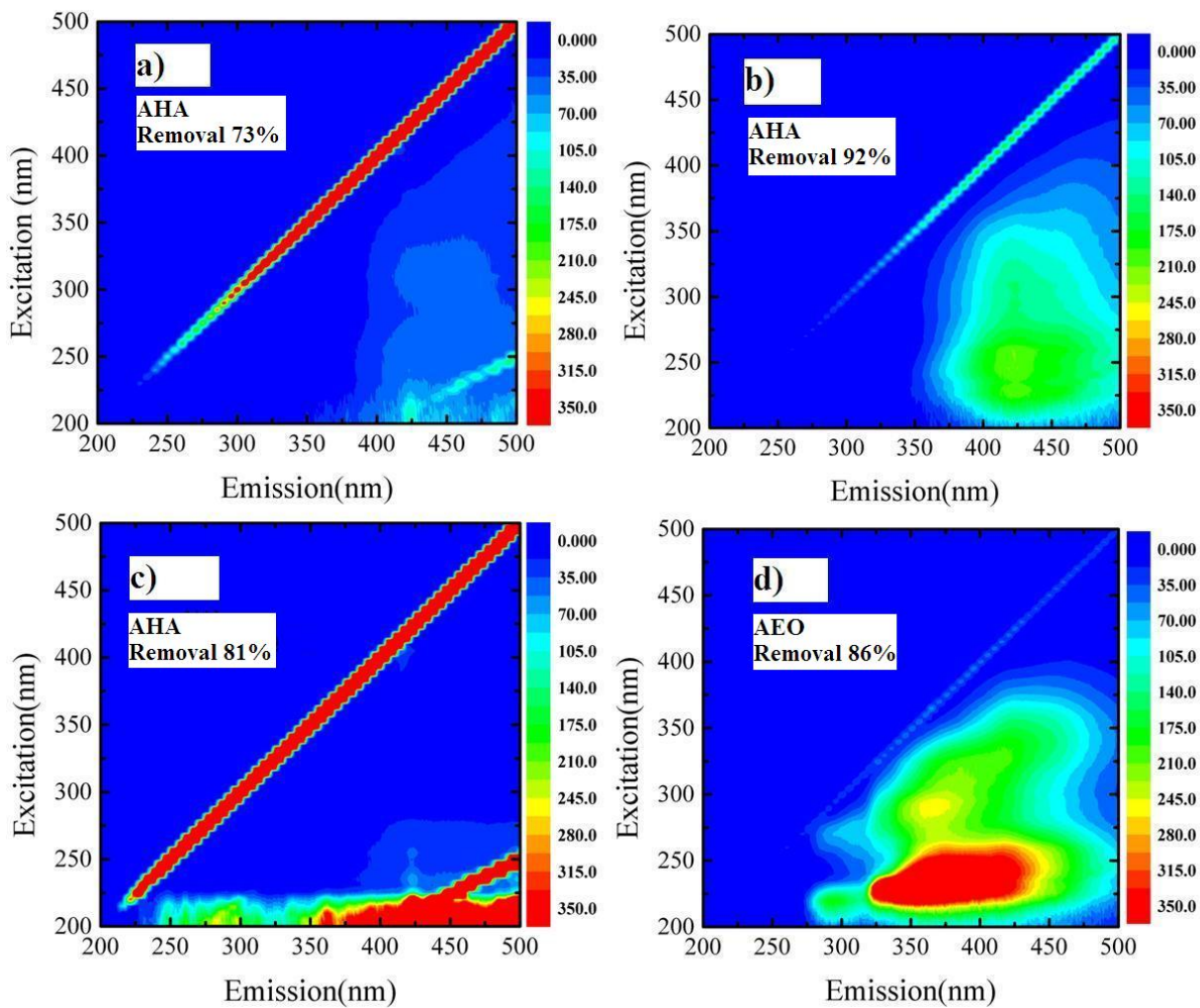


Figure 4.16 – Fluorescence image of a) sample 1 (100 mg/L *Snowtex*[®], 100 mg/L AHA, 0.01M *NaCl* at pH 3), b) 2 (250 mg/L *Snowtex*[®], 250 mg/L AHA, 0.10M *CaCl*₂ at pH 6), c) 3 (500 mg/L *Snowtex*[®], 500 mg/L AHA, 0.25M *AlCl*₃ at pH 9), d) 6 (500 mg/L *Snowtex*[®], 100 mg/L AEO, 0.01M *AlCl*₃ at pH 6)

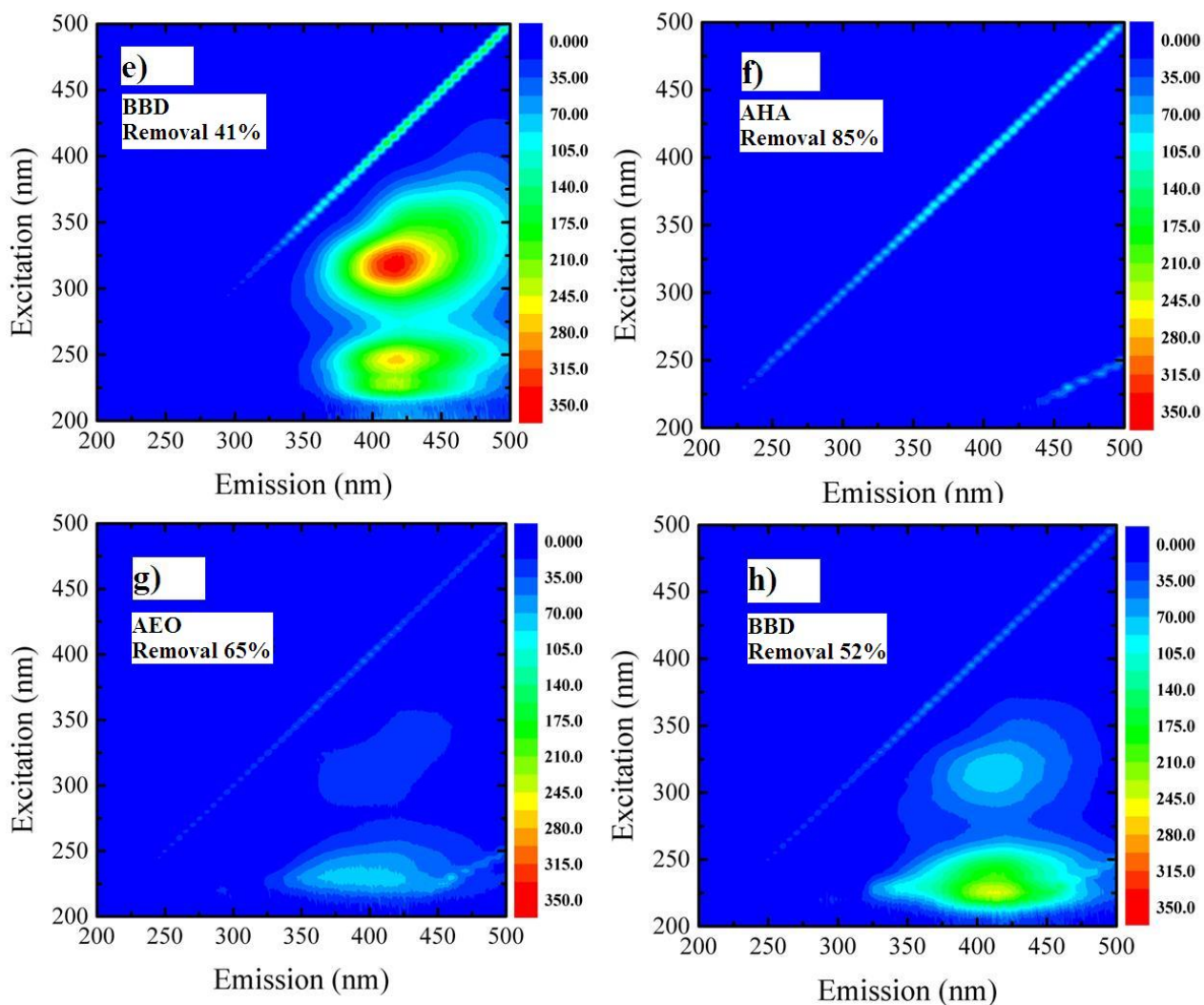


Figure 4.17 – Fluorescence image of e) sample 9(100 mg/L *Snowtex*[®], 500 mg/L BBD, 0.10M $AlCl_3$ at pH 3), f) 12 (250 mg/L latex, 250 mg/L AHA, 0.01M $AlCl_3$ at pH 3), g) 15 (100 mg/L latex, 250 mg/L AEO, 0.25M $AlCl_3$ at pH 6), h) 18 (250 mg/L latex, 100 mg/L BBD, 0.10M $AlCl_3$ at pH 9)

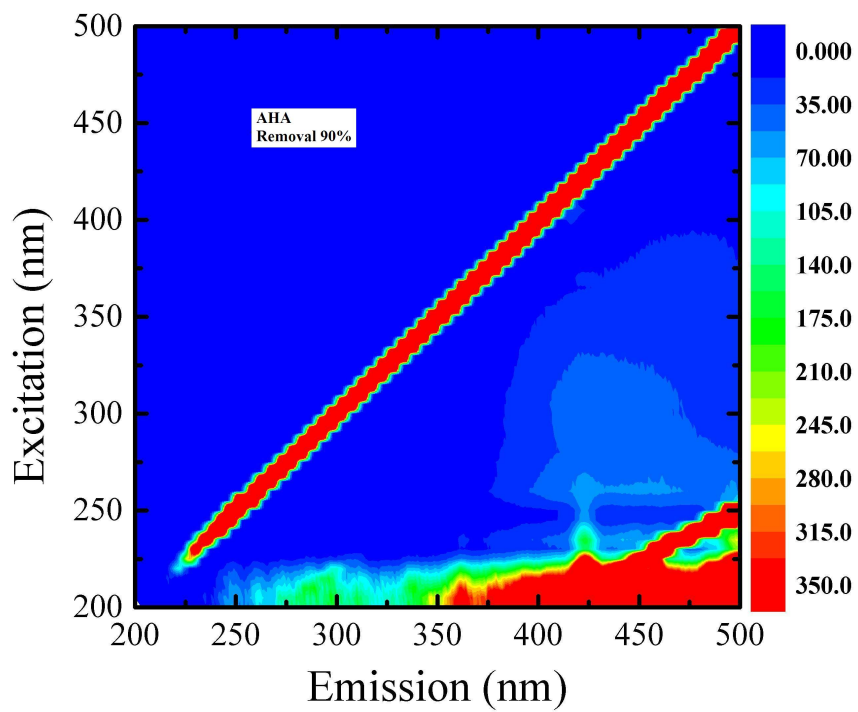


Figure 4.18 – Fluorescence image of optimum condition (250 *mg/L* *Snowtex*[®], 100 *mg/L* AHA, 0.25M *AlCl*₃ at pH 3)

4.3.10 Analysis of supernatant using dynamic light scattering

Scattering intensities from DLS analysis of all unfiltered supernatant was found too low. Comparison of autocorrelation function can be helpful to understand this [Cao, 2003]. For example, sample 1 originally had 100 *mg/L* silica. In Figure B.5 in Appendix, comparison with the shape of autocorrelation function of original 100 *mg/L* colloidal suspension and the shape of sample 1 reveals that there are very small number of particles remained in sample 1. Also scattering intensities of 100, 250 and 500 *mg/L* silica and latex solutions are much higher than scattering intensities of all the 18 samples after aggregation and precipitation. This means maximum colloidal particles have precipitated.

Table 4.7 – Comparison of scattering intensity

Sample	Normalized scattering intensity (kHz)
100 <i>mg/L</i> Snowtex	46368
250 <i>mg/L</i> Snowtex	57904
500 <i>mg/L</i> Snowtex	103014
100 <i>mg/L</i> Latex	189080
250 <i>mg/L</i> Latex	266392
500 <i>mg/L</i> Latex	371780
Unfiltered supernatant from samples 1 - 18	less than 20 kHz

4.3.11 Analysis of precipitates using X-ray photon spectroscopy (XPS)

For XPS analysis samples were selected based on higher DOM removal from AHA, AEO, and BBD containing samples. Precipitates from the samples were collected and dried to perform XPS analysis. Result is attached in Appendix D. Elemental analysis of samples 2, 3, 6, 9, 12, 15, 18 shows presence of C and O. This again indicates the precipitation of organics.

4.4 Summary

Widely used DLVO theory explains particle particle interaction in suspension based on double layer repulsive force and van der Waals attractive forces. DLVO can predict the critical coagulation concentration of electrolytes that separate slow coagulation regime from fast coagulation regime [Masliyah and Bhattacharjee, 2006]. According to Schulz-Hardy rule valence of electrolyte also affects the rate of coagulation [Masliyah and Xu, 2011, Sano et al., 2001]. Depending on the type of organics [Tipping, 2002, Wagoner et al., 1997] rate of coagulation can also be different. Degree of coagulation of organics also depends on pH. All above mentioned factors are present in oil-sands water treatment facilities. These factors play roles in silica organics co-precipitation and fouling of equipments. Pre-treatment of water to remove organics and silica can reduce fouling problems. In order to identify key factors that influence silica organics coagulation within limited cost and effort, design of experiments (DOE) was employed. Taguchi L_{18} was selected as suitable method. Due to orthogonality it can provide information about the effect of certain level of a

factor compared to the other level of the same factor, while the other factors are balanced. ANOVA was used to identify the most influential factors that affect silica and organics co-precipitation. This study identified that humic acid fraction causes the highest co-precipitation at lower pH at the presence of cations. This study also provides an idea about variation of degree of coagulation depending on the concentration of organics, pH of solution, valence of cations in the salt, and most importantly nature of organics. Based on above discussion, it can be concluded that coagulation and sedimentation can be an option to separate silica and organics to some extent from SAGD produced water.

Chapter 5

Conclusions and Future Work

5.1 Concluding remarks

Performance of both in-situ and mining operation for bitumen recovery from oil-sands largely depends on water treatment and recycling efficiency. As a vital natural resource proper management of water is very important. Dissolved solids, ionic species and organics are present in oil-sands produced water, specially in SAGD disposal water, which accumulate on equipment surfaces and increase energy consumption, operational and maintenance expenses and reduce life time [Kim et al., 2011]. Higher ionic strength and change of pH causes reduction of repulsive force between silica and DOM, in particular humic fraction of DOM and enhances aggregation. Aggregates become compact and increase in the size from dissolved phase to particulate phase [Baalousha et al., 2006]. Further knowledge about aggregation process and parameters will be useful to improve process reliability of water treatment plant and to reduce make up and disposal water. This research work was undertaken to assess the statistical significance of each parameter on enhanced aggregation of silica and organics. This chapter provides the conclusions related to the objectives of the present study. The objectives of the present study were:

1. Study aggregation rate in the presence of organics using dynamic light scattering (DLS): DLS is an established and swift technique to study aggregation rate of particles in suspension. In this study DLS was calibrated to study silica-DOM aggregation. A systematic approach to study silica-DOM aggregation at low concentrations of silica (both dissolved and colloidal) and organics was developed. Na_2SiO_3 was used as dissolved silica and *Snowtex*[®] was used as colloidal silica.

2. Examine the silica-organic aggregate size and shape: DLS technique was used to study the aggregate size at different low concentrations of silica (100 and 150 *mg/L*) and DOM (20 and 50 *mg/L*) and pH. Fractal dimension obtained from light scattering, SEM and AFM images were used to study the shape of silica-DOM aggregates.
3. Combine statistical tool with analytical techniques to characterize organics and silica interaction by incorporating all the parameters involved in water treatment plant environment: The effects of dissolved organic matter from AHA, AEO, and BBD, two types of colloids, *Snowtex*[®] ZL and Latex (both have diameter around 100 *nm*) at three concentrations- 100, 250, and 500 *mg/L*, three salts with different valence (monovalent- *NaCl*, di-valent- *CaCl₂*, tri-valent- *AlCl₃*), at different concentrations (0.01M, 0.1M, and 0.25M), and at three pH (3, 6, and 9) on silica-DOM aggregation were studied using Taguchi experimental design. Total 18 samples were prepared based on the Taguchi OA table. Same procedure was repeated twice to analyze the variance.
4. Identify the key factors which cause enhanced silica organics co-precipitation: One way ANOVA and Minitab were used to analyze data and evaluate the effect of different factors on silica-DOM aggregation.
5. Determine the optimum condition that causes maximum aggregation: Minitab was used to identify optimum condition.
6. Characterize the treated water after silica-DOM aggregation: Fluorescence Ex/Em matrix and *SUVA₂₅₄* were used to identify which fractions of DOM were removed through precipitation. DLS was used to examine the precipitation of colloids through aggregation. Also XPS analysis was used to confirm the presence of organics in the precipitates.

The key information obtained in pursuing the above objectives are presented below:

1. Taguchi method was successfully used to model this problem taking seven factors into account.
2. Contribution of all the seven factors were quantified. ANOVA has shown that type of organics, type of salt, concentration of organics, and pH are the most important variables.

3. Most significant parameter that affects silica organics aggregation highly is the type of organics (with 45% contribution).
4. Presence of humic-like substances causes highest aggregation.
5. Optimum condition for silica organics aggregation is 250 *mg/L* silica in the presence of 100 *mg/L* humic acid and 0.25M *AlCl₃* at pH 3. At this condition at least 90% of organics will be removed from solution through aggregation and precipitation.
6. Different fractions of organics can be removed by varying different parameters. For example, Fluorescence Ex/Em matrix of different samples has shown that, HPoA and HPoN fractions were removed at the presence of 0.1 M *AlCl₃* at pH 3 (with 500 mg/L BBD and 100 mg/L Snowtex). All the HPo fractions have been removed at pH 9 with 0.1 M *AlCl₃* (with 250 mg/L BBD and 100 mg/L Latex).
7. In the presence of organics and cations, silica and organics form aggregate through cation bridging. Also comparison of scattering intensities of unfiltered treated water (after aggregation) with scattering intensities of original samples has shown that most of the colloids have been precipitated through silica-DOM aggregation.
8. Valence of cation of salt plays major role on enhanced silica-DOM aggregation. Analysis of data obtained using Taguchi experimental method has shown that, surface charge reduction due to cation adsorption is more influential than electric double layer thickness reduction by increasing salt concentration.
9. An important observation from *SUVA₂₅₄* values of the samples is that hydrophobic, humic-like fractions have been removed through aggregation from 15 samples out of total 18. Only three samples with *NaCl* at low concentrations have higher *SUVA₂₅₄* values, which indicates that monovalent cation is not as effective as di-valent or tri-valent cations on neutralizing negative surface charge of organics and increase aggregation to remove humic-like fractions.
10. Light scattering can be used to examine silica and organics aggregation at low concentrations.

DLS technique was effectively used to study aggregation rate of dissolved silica and AHA at low concentrations. An observation from the DLS study is that, at the absence of di-valent or tri-valent cation colloidal silica (*Snowtex*[®]) are more stable compared to dissolved silica. With colloidal silica, duration of DLS experiments, and concentrations of silica and AHA may not be enough to see any significant increase in aggregation rate. In addition, study of silica-DOM aggregation at higher concentrations of silica and organics is difficult due to the absorbance of light by increased organics concentration and reduced Brownian motion due to higher concentration of silica. Types of organics, types of organics, concentration of organics, and pH are the four major contributors on increased silica-DOM co-precipitation. DOM in humic acid (AHA) has more acidic functional group compared to acid extractable organics (AEO) and boiler blow down water (BBD) which increases aggregation rate. Adsorption of di-valent and tri-valent cations neutralizes the negative surface charge of organics and at lower pH (pH 3), availability of H^+ also reduces silica surface charge. At this condition different functional groups of organics and silica form aggregates through hydrogen bond and van der Waals interaction. For higher pH, there were no significant difference in DOM removal through aggregation at pH 6 and 9 conditions. This is because at these pH, negative surface charge of organics are not fully neutralized to form aggregates.

From the above findings important conclusion can be drawn that, Taguchi orthogonal arrays can be used as a cost effective and efficient way to address SAGD related water characterization problems. Also removal of organics and silica through coagulation can be effective as an inexpensive pre-treatment option for oil sands produced water.

5.2 Future work

A framework to understand the effect of pH, type of organics, ions, and colloids, concentration of ions, organics, and silica on silica-organics enhanced aggregation in SAGD BBD water was presented in this research. Few recommendation for future development in this area are listed bellow:

1. In order to make the process more robust more levels of each parameters can be studied using other Taguchi OAs. For example, L_{25} OA can be used to study the effect of seven parameters with five levels of the effects.

2. In this study seven parameters were used. In the presence of monovalent, di-valent, tri-valent salts, or coagulant, aggregation of humic-like fraction and silica will govern the silica-DOM co-precipitation process. Since SAGD BBD water has negligible amount of salt, another L_{18} experimental matrix with five factors excluding salt type and concentration can be studied to identify which parameter is most influential for equipment surface fouling and deep well injection jamming under oil sands produced water treatment conditions.
3. Other design of experiment methods can be applied for the same problem to compare the results with Taguchi method.
4. Other SAGD produced water can be studied using same procedure.
5. Use of humic-like substances as a coagulant to remove DOM and silica can be tested. Also efficiency of other coagulants can be compared with humic-like substances.
6. Removal of all fractions of DOM may not be required to prevent scaling [Thakurta et al., 2013]. Further investigation can be done to examine if the removal of hydrophobic fraction is effective enough to reduce scaling.

Bibliography

- Abe, T., Kobayashi, S., and Kobayashi, M. (2011). Aggregation of colloidal silica particles in the presence of fulvic acid, humic acid, or alginate: Effects of ionic composition. *Colloids and Surfaces A: Physicochemical and Engineering Aspects*, 379(1-3):21–26.
- Al-Bahlani, A. M. and Babadagli, T. (2009). Sagd laboratory experimental and numerical simulation studies: A review of current status and future issues. *Journal of Petroleum Science and Engineering*, 68(3-4):135–150.
- Alexander, G. B., Heston, W. M., and Iler, R. K. (1954). The solubility of amorphous silica in water. *Journal of Physical Chemistry*, 58(6):453–455.
- Allen, T. T. (2005). *Introduction to engineering statistics and six sigma: statistical quality control and design of experiments and systems*. Springer.
- Annunziata, O., Buzatu, D., and Albright, J. G. (2005). Protein diffusion coefficients determined by macroscopic-gradient rayleigh interferometry and dynamic light scattering. *Langmuir*, 21(26):12085–12089.
- Baalousha, M., Heino, M. M., and Coustumer, P. L. (2006). Conformation and size of humic substances: Effects of major cation concentration and type, ph, salinity, and residence time. *Colloids and Surfaces A: Physicochemical and Engineering Aspects*, 272(12):48–55.
- Bagci, M. and Imrek, H. (2013). Application of taguchi method on optimization of testing parameters for erosion of glass fiber reinforced epoxy composite materials. *Materials and Design*, 46:706–712.
- Baldyga, J., Jasinska, M., Jodko, K., and Petelski, P. (2012). Precipitation of amorphous colloidal silica from aqueous solutions-aggregation problem. *Chemical Engineering Science*, 77:207–216.

- Beyer, H. G. and Sendhoff, B. (2007). Robust optimization - a comprehensive survey. *Computer Methods in Applied Mechanics and Engineering*, 196(33-34):3190–3218.
- Bhattacharya, A., Das, S., Majumder, P., and Batish, A. (2009). Estimating the effect of cutting parameters on surface finish and power consumption during high speed machining of aisi 1045 steel using taguchi design and anova. *Production Engineering*, 3(1):31–40.
- Bhattacharya, S. and Kieffer, J. (2005). Fractal dimensions of silica gels generated using reactive molecular dynamics simulations. *Journal of Chemical Physics*, 122(9).
- Blanco, M. C., Leisner, D., Vazquez, C., and Lopez-Quintela, M. A. (2000). Dynamic light scattering in transient reversible gels. *Langmuir*, 16(23):8585–8594.
- Bottero, J. Y., Tchoubar, D., Arnaud, M., and Quienne, P. (1991). Partial hydrolysis of ferric nitrate salt. structural investigation by dynamic light scattering and small-angle x-ray scattering. *Langmuir*, 7(7):1365–1369.
- Bryant, G. and Thomas, J. C. (1995). Improved particle size distribution measurements using multiangle dynamic light scattering. *Langmuir*, 11(7):2480–2485.
- Burya, Y. G., Yudin, I. K., Dechabo, V. A., and Anisimov, M. A. (2001). Colloidal properties of crude oils studied by dynamic light-scattering. *International Journal of Thermophysics*, 22:1397–1410.
- Bushell, G. C., Yan, Y. D., Woodfield, D., Raper, J., and Amal, R. (2002). On techniques for the measurement of the mass fractal dimension of aggregates. *Advances in Colloid and Interface Science*, 95:1–50.
- Butler, R. (1998). Sagd comes of age! *Journal of Canadian Petroleum Technology*, 37(7):9–12.
- Butler, R. (2001). Some recent developments in sagd. *Journal of Canadian Petroleum Technology*, 40(1):18–22.
- Camins, B. and Russo, P. S. (1994). Following polymer gelation by depolarized dynamic light scattering from optically and geometrically anisotropic latex particles. *Langmuir*, 10(11):4053–4059.

- Cao, A. (2003). Light scattering. recent applications. *Analytical Letters*, 36(15):3185–3225.
- Card, D. N. (1998). Learning from our mistakes with defect causal analysis. *Software, IEEE*, 15(1):56–63.
- Chang, N. J. and Kaler, E. W. (1986). Quasi-elastic light scattering study of five-component microemulsions. *Langmuir*, 2(2):184–190.
- Chen, W., Allen, J. K., Tsui, K. L., and Mistree, F. (1996). A procedure for robust design: Minimizing variations caused by noise factors and control factors. *Journal of Mechanical Design, Transactions Of the ASME*, 118(4):478–485.
- Cobb, B. D. and Clarkson, J. M. (1994). A simple procedure for optimising the polymerase chain reaction (pcr) using modified taguchi methods. *Nucleic acids research*, 22(18):3801–3805.
- Czarnecki, J., Radoev, B., Schramm, L. L., and Slavchev, R. (2005). On the nature of athabasca oil sands. *Advances in Colloid and Interface Science*, 114-115:53–60.
- de Lange, R. S. A., Hekkink, J. H. A., Keizer, K., and Burggraaf, A. J. (1995). Polymeric-silica-based sols for membrane modification applications: sol-gel synthesis and characterization with saxs. *Journal of Non-Crystalline Solids*, 191(12):1–16.
- Deng, X. (2005). Recovery performance and economics of steam/propane hybrid process. In *SPE/PS-CIM/CHOA International Thermal Operations and Heavy Oil Symposium Proceedings*, volume 2005, pages A407–A414.
- Edmunds, N. and Chhina, H. (2001). Economic optimum operating pressure for sagd projects in alberta. *Journal of Canadian Petroleum Technology*, 40(12):13–17.
- Edmunds, N. R., Kovalsky, J. A., Gittins, S. D., and Pennacchioli, E. D. (1994). Review of phase a steam-assisted gravity-drainage test. *SPE Reservoir Engineering (Society of Petroleum Engineers)*, 9(2):119–124.
- Elhamzaoui, H., Toupance, T., Maugey, M., Zakri, C., and Jousseau, B. (2007). Particle growth of hybrid materials followed by dynamic light scattering. *Langmuir*, 23(2):785–789.

- Elizalde-Gonzalez, M. P. and Garca-Daz, L. E. (2010). Application of a taguchi 116 orthogonal array for optimizing the removal of acid orange 8 using carbon with a low specific surface area. *Chemical Engineering Journal*, 163(12):55–61.
- Eshuis, A., Harbers, G., Doornink, D. J., and Mijnlief, P. (1985). Experimental determination of particle size distributions in colloidal systems by dynamic light scattering. application to polystyrene latex spheres and to nonionic microemulsions. *Langmuir*, 1(3):289–293.
- Folta-Stogniew, E. and Williams, K. (1999). Determination of molecular masses of proteins in solution: Implementation of an hplc size exclusion chromatography and laser light scattering service in a core laboratory. *Journal of Biomolecular Techniques*, 10(2):51–63. cited By (since 1996)127.
- Furman, O., Usenko, S., and Lau, B. L. T. (2013). Relative Importance of the Humic and Fulvic Fractions of Natural Organic Matter in the Aggregation and Deposition of Silver Nanoparticles. *ENVIRONMENTAL SCIENCE & TECHNOLOGY*, 47(3):1349–1356.
- Gates, I. D. and Chakrabarty, N. (2006). Optimization of steam assisted gravity drainage in mcmurray reservoir. *Journal of Canadian Petroleum Technology*, 45(9):54–62.
- Georgalis, Y., Philipp, M., Aleksandrova, R., and Kr??ger, J. K. (2012). Light scattering studies on ficoll pm70 solutions reveal two distinct diffusive modes. *Journal of colloid and interface science*, 386(1):141–147.
- Ghani, J. A., Choudhury, A., and Hassan, H. H. (2004). Application of taguchi method in the optimization of end milling parameters. *Journal of Materials Processing Technology*, 145(1):84–92.
- Gill, J. S. (1993). Inhibition of silicasilicate deposit in industrial waters. *Colloids and Surfaces A: Physicochemical and Engineering Aspects*, 74(1):101–106.
- Gopalsamy, B. M., Mondal, B., and Ghosh, S. (2009). Taguchi method and anova: An approach for process parameters optimization of hard machining while machining hardened steel. *Journal of Scientific and Industrial Research*, 68(8):686–695.

- Gorrepati, E. A., Wongthahan, P., Raha, S., and Fogler, H. S. (2010). Silica precipitation in acidic solutions: Mechanism, ph effect, and salt effect. *Langmuir*, 26(13):10467–10474.
- Harris, D. R., Keir, R. I., Prestidge, C. A., and Thomas, J. C. (1999). A dynamic light scattering investigation of nucleation and growth in supersaturated alkaline sodium aluminate solutions (synthetic bayer liquors). *Colloids and Surfaces A: Physicochemical and Engineering Aspects*, 154(3):343–352.
- Heins, W. and Schooley, K. (2004). Achieving zero liquid discharge in sagd heavy oil recovery. *Journal of Canadian Petroleum Technology*, 43(8):37–42.
- Heins, W. F. (2010). Is a paradigm shift in produced water treatment technology occurring at sagd facilities? *Journal of Canadian Petroleum Technology*, 49(1):10–15.
- Herman, D. and Walz, J. Y. (2013). Stabilization of weakly charged microparticles using highly charged nanoparticles. *Langmuir*, 29(20):5982–5994.
- Holthoff, H., Borkovec, M., and Schurtenberger, P. (1997a). Determination of light-scattering form factors of latex particle dimers with simultaneous static and dynamic light scattering in an aggregating suspension. *Physical Review E - Statistical Physics, Plasmas, Fluids, and Related Interdisciplinary Topics*, 56(6):6945–6953.
- Holthoff, H., Egelhaaf, S. U., Borkovec, M., Schurtenberger, P., and Sticher, H. (1996). Coagulation rate measurements of colloidal particles by simultaneous static and dynamic light scattering. *Langmuir*, 12(23):5541–5549.
- Holthoff, H., Schmitt, A., Fernandez-Barbero, A., Borkovec, M., Cabrerzo-Vlchez, M. A., Schurtenberger, P., and Hidalgo-Ivarez, R. (1997b). Measurement of absolute coagulation rate constants for colloidal particles: Comparison of single and multiparticle light scattering techniques. *Journal of colloid and interface science*, 192(2):463–470.
- Huang, M. C. and Tai, C. C. (2001). Effective factors in the warpage problem of an injection-molded part with a thin shell feature. *Journal of Materials Processing Technology*, 110(1):1–9.
- Ibaseta, N. and Biscans, B. (2010). Fractal dimension of fumed silica: Comparison of light scattering and electron microscope methods. *Powder Technology*, 203(2):206–210.

- Iler, R. K. (1979). *The chemistry of silica*. John Wiley and Sons, New York.
- Illes, E. and Tombacz, E. (2006). The effect of humic acid adsorption on pH-dependent surface charging and aggregation of magnetite nanoparticles. *Journal of colloid and interface science*, 295(1):115–123.
- Jacques, S., Alter, C., and Prael, S. (1987). Angular dependence of hene laser light scattering by human dermis. *Lasers Life Sci*, 1(4):309–333.
- Jennings, D. W. and Shaikh, A. (2007). Heat-exchanger deposition in an inverted steam-assisted gravity drainage operation. part 1. inorganic and organic analyses of deposit samples. *Energy Fuels*, 21(1):176–184.
- Kawaguchi, H., Li, Z., Masuda, Y., Sato, K., and Nakagawa, H. (2012). Dissolved organic compounds in reused process water for steam-assisted gravity drainage oil sands extraction. *Water research*.
- Keuren, E. R. V., Wiese, H., and Horn, D. (1993). Fiber-optic quasielastic light scattering in concentrated latex dispersions: Angular dependent measurements of singly scattered light. *Langmuir*, 9(11):2883–2887.
- Khilko, S. L., Kovtun, A. I., and Rybachenko, V. I. (2011). Potentiometric titration of humic acids. *Solid Fuel Chemistry*, 45(5):337–348.
- Kim, E.-S., Liu, Y., and Gamal El-Din, M. (2011). The effects of pretreatment on nanofiltration and reverse osmosis membrane filtration for desalination of oil sands process-affected water. *Separation and Purification Technology*, 81(3):418–428.
- Kim, K. J. and Shahinpoor, M. (2003). Ionic polymer-metal composites: II. manufacturing techniques. *Smart Materials and Structures*, 12(1):65–79.
- Kobayashi, M., Juillerat, F., Galletto, P., Bowen, P., and Borkovec, M. (2005). Aggregation and charging of colloidal silica particles: Effect of particle size. *Langmuir*, 21(13):5761–5769.
- Koopal, L., Yang, Y., Minnaard, A. J., Theunissen, P., and Riemsdijk, W. V. (1998). Chemical immobilisation of humic acid on silica. *Colloids and Surfaces A: Physicochemical and Engineering Aspects*, 141(3):385 – 395.
- Kretzschmar, R., Holthoff, H., and Sticher, H. (1998). Influence of pH and humic acid on coagulation kinetics of kaolinite: A dynamic light scattering study. *Journal of colloid and interface science*, 202(1):95–103.

- Lauten, R. A., Kjnicksen, A. L., and Nyström, B. (2001). Colloid polymer interactions and aggregation in aqueous mixtures of polystyrene latex, sodium dodecyl sulfate, and a hydrophobically modified polymer: A dynamic light scattering study. *Langmuir*, 17(3):924–930.
- Li, Y. C. and Chen, C., Chang, Y., Chuang, P., Chen, J., Chen, H., Hsu, C., Ivanov, V. A., Khalatur, P. G., and Chen, S. (2009). Scattering study of the conformational structure and aggregation behavior of a conjugated polymer solution. *Langmuir*, 25(8):4668–4677.
- Li, H., Robertson, A. D., and Jensen, J. H. (2005). Very fast empirical prediction and rationalization of protein pka values. *Proteins: Structure, Function, and Bioinformatics*, 61(4):704–721.
- Luo, F., Dong, B., Xie, J., and Jiang, S. (2012). Scaling tendency of boiler feedwater without desiliconization treatment. *Desalination*, 302(0):50–54.
- Maghsoodloo, S., Ozdemir, G., Jordan, V., and Huang, C. (2004). Strengths and limitations of taguchi’s contributions to quality, manufacturing, and process engineering. *Journal of Manufacturing Systems*, 23(2):73–126.
- Maiti, A., Sadrezadeh, M., Guha Thakurta, S., Pernitsky, D. J., and Bhattacharjee, S. (2012). Characterization of boiler blowdown water from steam-assisted gravity drainage and silicaorganic coprecipitation during acidification and ultrafiltration. *Energy & Fuels*, 26(9):5604–5612.
- Majzik, A. and Tombcz, E. (2007). Interaction between humic acid and montmorillonite in the presence of calcium ions ii. colloidal interactions: Charge state, dispersing and/or aggregation of particles in suspension. *Organic Geochemistry*, 38(8):1330–1340.
- Mamun, M. A.-A. (2012). Colloidal fouling of salt rejecting nanofiltration membranes: Transient electrokinetic model and experimental study.
- Manning, T. J., Bennett, T., and Milton, D. (2000). Aggregation studies of humic acid using multiangle laser light scattering. *Science of the Total Environment*, 257(2-3):171–176.
- Marinsky, J. A. and Ephraim, J. (1986). A unified physicochemical description of the protonation and metal ion complexation equilibria of natural organic acids (humic and fulvic acids). 1. analysis of the influence of polyelectrolyte

- properties on protonation equilibria in ionic media: Fundamental concepts. *Environmental science & technology*, 20(4):349–354.
- Masliyah, J. H., C. J. and Xu, Z. (2011). *Handbook on Theory and Practice of Bitumen Recovery from Athabasca Oil Sands*.
- Masliyah, J. H. and Bhattacharjee, S. (2006). *Electrokinetic and Colloid Transport Phenomena*. Wiley-Interscience.
- Matilainen, A., Gjessing, E. T., Lahtinen, T., Hed, L., Bhatnagar, A., and Sillanp, M. (2011). An overview of the methods used in the characterisation of natural organic matter (nom) in relation to drinking water treatment. *Chemosphere*, 83(11):1431–1442.
- Matthews, B. J. H., Jones, A. C., Theodorou, N. K., and Tudhope, A. W. (1996). Excitation-emission-matrix fluorescence spectroscopy applied to humic acid bands in coral reefs. *Marine Chemistry*, 55(3-4):317–332.
- Medebach, M., Moitzi, C., Freiberger, N., and Glatter, O. (2007). Dynamic light scattering in turbid colloidal dispersions: A comparison between the modified flat-cell light-scattering instrument and 3d dynamic light-scattering instrument. *Journal of colloid and interface science*, 305(1):88–93.
- Meng, Z., Hashmi, S. M., and Elimelech, M. (2013). Aggregation rate and fractal dimension of fullerene nanoparticles via simultaneous multiangle static and dynamic light scattering measurement. *Journal of colloid and interface science*, 392(1):27–33.
- Metsmuuronen, S., Sillanp, M., Bhatnagar, A., and Manttari, M. (2014). Natural organic matter removal from drinking water by membrane technology. *Separation and Purification Reviews*, 43:1–61.
- Mikula, R., Munoz, V., and Omotoso, O. (2008). Water use in bitumen production: Tailings management in surface mined oil sands. In *Canadian International Petroleum Conference*.
- Mohammadi, T., Moheb, A., Sadrzadeh, M., and Razmi, A. (2004a). Separation of copper ions by electrodialysis using taguchi experimental design. *Desalination*, 169(1):21–31.

- Mohammadi, T., Razmi, A., and Sadrzadeh, M. (2004b). Effect of operating parameters on pb2+ separation from wastewater using electro dialysis. *Desalination*, 167(1-3):379–385.
- Montgomery, D. C. (2013). Design and analysis of experiments.
- Nasr, T. N. and Ayodele, O. R. (2005). Thermal techniques for the recovery of heavy oil and bitumen. In *IIORC 05 - 2005 SPE International Improved Oil Recovery Conference in Asia Pacific, Proceedings*, pages 87–101.
- Nemoto, N. and Kuwahara, M. (1993). Dynamic light scattering of ctab/-nasal long threadlike micelles in the semidilute regime: Applicability of the dynamic scaling law. *Langmuir*, 9(2):419–423.
- Ng, E. Y. K. and Ng, W. K. (2006). Parametric study of the biopotential equation for breast tumour identification using anova and taguchi method. *Medical and Biological Engineering and Computing*, 44(1-2):131–139.
- Nordstrm, J., Nilsson, E., Jarvol, P., Nayeri, M., Palmqvist, A., Bergenholtz, J., and Matic, A. (2011). Concentration- and ph-dependence of highly alkaline sodium silicate solutions. *Journal of colloid and interface science*, 356(1):37–45.
- Osterberg, R. and Mortensen, K. (1994). The growth of fractal humic acids: Cluster correlation and gel formation. 33(3):269–276–.
- Parida, S. K., Dash, S., Patel, S., and Mishra, B. K. (2006). Adsorption of organic molecules on silica surface. *Advances in Colloid and Interface Science*, 121(13):77–110.
- Park, G. J., Lee, T. H., Lee, K. H., and Hwang, K. H. (2006). Robust design: An overview. *AIAA Journal*, 44(1):181–191.
- Pedenaud, P., Goulay, C., Pottier, F., Garnier, O., and Gauthier, B. (2006). Silica-scale inhibition for steam generation in otsg boilers. *SPE Production and Operations*, 21(1):26–32.
- Petersen, M. A. and Grade, H. (2011). Analysis of steam assisted gravity drainage produced water using two-dimensional gas chromatography with time-of-flight mass spectrometry. *Industrial & Engineering Chemistry Research*, 50(21):12217–12224.

- Pourjavadi, A., Amini-Fazl, M. S., and Barzegar, S. (2008). Optimization of synthesis conditions of a novel carrageenan-based superabsorbent hydrogel by taguchi method and investigation of its metal ions adsorption. *Journal of Applied Polymer Science*, 107(5):2970–2976.
- Prada, J. W. V. and Cunha, L. B. (2008). Assessment of optimal operating conditions in a sagd project by design of experiments and response surface methodology. *Petroleum Science and Technology*, 26(17):2095–2107.
- Provdar, T. (1997). Challenges in particle size distribution measurement past, present and for the 21st century. *Progress in Organic Coatings*, 32(1?4):143–153.
- Ramkumar, R. and Ragupathy, A. (2013). Optimization of cooling tower performance analysis using taguchi method. *Thermal Science*, 17(2):457–470.
- Rao, R. S., Kumar, C. G., Prakasham, R. S., and Hobbs, P. J. (2008). The taguchi methodology as a statistical tool for biotechnological applications: A critical appraisal. *Biotechnology Journal*, 3(4):510–523.
- Reyhani, A., Rajaei, F., Shahmoradi, M., and Kahkesh, A. (2013). A study of a polymeric membrane performance in an ultrafiltration system to use in industrial application. *Desalination and Water Treatment*. Article in Press.
- Rice, J. A. and Lin, J. S. (1993). Fractal nature of humic materials. *Environmental Science & Technology*, 27(2):413–414.
- Ricka, J. (1993). Dynamic light scattering with single-mode and multimode receivers. *Applied Optics*, 32(15):2860–2875.
- Rojanski, D., Huppert, D., Bale, H. D., Dacai, X., Schmidt, P. W., Farin, D., Seri-Levy, A., and Avnir, D. (1986). Integrated fractal analysis of silica: Adsorption, electronic energy transfer, and small-angle x-ray scattering. *Phys. Rev. Lett.*, 56:2505–2508.
- Sadeghi, S. H., Moosavi, V., Karami, A., and Behnia, N. (2012). Soil erosion assessment and prioritization of affecting factors at plot scale using the taguchi method. *Journal of Hydrology*, 448449(0):174–180.
- Sadrzadeh, M. and Mohammadi, T. (2008). Sea water desalination using electro dialysis. *Desalination*, 221(1-3):440–447.

- Sadrzadeh, M., Razmi, A., and Mohammadi, T. (2007). Separation of monovalent, divalent and trivalent ions from wastewater at various operating conditions using electrodialysis. *Desalination*, 205(1-3):53–61.
- Sano, M., Okamura, J., and Shinkai, S. (2001). Colloidal nature of single-walled carbon nanotubes in electrolyte solution: The schulze-hardy rule. *Langmuir*, 17(22):7172–7173.
- Schaefer, D. and Keefer, K. (1984). Fractal geometry of silica condensation polymers. *Journal Name: Phys. Rev. Lett.*, 53.
- Schaefer, D., Martin, J., Wiltzius, P., and Cannell, D. (1984). Fractal geometry of colloidal aggregates. *Physical Review Letters*, 52(26):2371–2374.
- Schudel, M., Behrens, S. H., Holthoff, H., Kretzschmar, R., and Borkovec, M. (1997). Absolute aggregation rate constants of hematite particles in aqueous suspensions: A comparison of two different surface morphologies. *Journal of colloid and interface science*, 196(2):241–253.
- Seebergh, J. E. and Berg, J. C. (1995). Evidence of a hairy layer at the surface of polystyrene latex particles. *Colloids and Surfaces A: Physicochemical and Engineering Aspects*, 100(0):139 – 153.
- Seinfeld, J. H. and Pandis, S. N. Atmospheric chemistry and physics - from air pollution to climate change (2nd edition).
- Sheikholeslami, R., Al-Mutaz, I. S., Tan, S., and Tan, S. D. (2002). Some aspects of silica polymerization and fouling and its pretreatment by sodium aluminate, lime and soda ash. *Desalination*, 150(1):85–92.
- Shin, H. and Polikar, M. (2005). New economic indicator to evaluate sagd performance. In *SPE Western Regional Meeting, Proceedings*, pages 627–633.
- Shojaeefard, M. H., Khalkhali, A., Akbari, M., and Tahani, M. (2013). Application of taguchi optimization technique in determining aluminum to brass friction stir welding parameters. *Materials and Design*, 52:587–592.
- Singh, G. and Song, L. (2007a). Experimental correlations of ph and ionic strength effects on the colloidal fouling potential of silica nanoparticles in crossflow ultrafiltration. *Journal of Membrane Science*, 303(1-2):112–118.

- Singh, G. and Song, L. (2007b). Experimental correlations of pH and ionic strength effects on the colloidal fouling potential of silica nanoparticles in crossflow ultrafiltration. *Journal of Membrane Science*, 303(12):112–118.
- Souza, G. and Miller, J. (2001). Oligonucleotide detection using angle-dependent light scattering and fractal dimension analysis of gold-dna aggregates [3]. *Journal of the American Chemical Society*, 123(27):6734–6735.
- Sutton, R. and Sposito, G. (2005). Molecular structure in soil humic substances: The new view. *Environmental Science and Technology*, 39(23):9009–9015.
- Taheri, A. H., Sim, L. N., Haur, C. T., Akhondi, E., and Fane, A. G. (2013). The fouling potential of colloidal silica and humic acid and their mixtures. *Journal of Membrane Science*, 433(0):112–120.
- Tang, P., Colflesh, D. E., and Chu, B. (1988). Temperature effect on fractal structure of silica aggregates. *Journal of Colloid and Interface Science*, 126(1):304 – 313.
- Teklebrhan, R. B., Ge, L., Bhattacharjee, S., Xu, Z., and Sjöblom, J. (2012). Probing structure-nanoaggregation relations of polyaromatic surfactants: A molecular dynamics simulation and dynamic light scattering study. *Journal of Physical Chemistry B*, 116(20):5907–5918.
- Thakurta, S. G. (2012). Characterization of the dissolved organic matter in steam assisted gravity drainage boiler blow-down water.
- Thakurta, S. G., Maiti, A., Pernitsky, D. J., and Bhattacharjee, S. (2013). Dissolved organic matter in steam assisted gravity drainage boiler blow-down water. *Energy and Fuels*, 27(7):3883–3890.
- Thurman, E. M. and Malcolm, R. L. (1981). Preparative isolation of aquatic humic substances. *Environmental Science & Technology*, 15(4):463–466.
- Thurman, E. M., Wershaw, R. L., Malcolm, R. L., and Pinckney, D. J. (1982). Molecular size of aquatic humic substances. *Organic Geochemistry*, 4(1):27–35.
- Tipping, E. (2002). *Cation Binding by Humic Substances*. Cambridge University Press.

- Tseng, K. H., Shiao, Y. F., Chang, R. F., and Yeh, Y. T. (2013). Optimization of microwave-based heating of cellulosic biomass using taguchi method. *Materials*, 6(8):3404–3419.
- Urban, C., Romer, S., Scheffold, F., and Schurtenberger, P. (2000). *Structure, dynamics and interactions in concentrated colloidal suspensions and gels*, volume 115 of *Progress in Colloid and Polymer Science*.
- Wagoner, D. B., Christman, R. F., Cauchon, G., and Paulson, R. (1997). Molar mass and size of suwannee river natural organic matter using multi-angle laser light scattering. *Environmental Science and Technology*, 31(3):937–941.
- Wang, X. and Kasperski, K. L. (2010). Analysis of naphthenic acids in aqueous solution using hplc-ms/ms. *Anal. Methods*, 2(11):1715–1722.
- Wang, Y., Combe, C., and Clark, M. M. (2001). The effects of ph and calcium on the diffusion coefficient of humic acid. *Journal of Membrane Science*, 183(1):49–60.
- Woignier, T., Phalippou, J., Vacher, R., Pelous, J., and Courtens, E. (1990). Different kinds of fractal structures in silica aerogels. *Journal of Non-Crystalline Solids*, 121(13):198–201.
- Yang, W. and Tarng, Y. (1998). Design optimization of cutting parameters for turning operations based on the taguchi method. *Journal of Materials Processing Technology*, 84(1-3):122–129.
- Yu, W. L. and Borkovec, M. (2002). Distinguishing heteroaggregation from homoaggregation in mixed binary particle suspensions by multiangle static and dynamic light scattering. *Journal of Physical Chemistry B*, 106(51):13106–13110.

Appendix A

Calibration of light scattering instrument

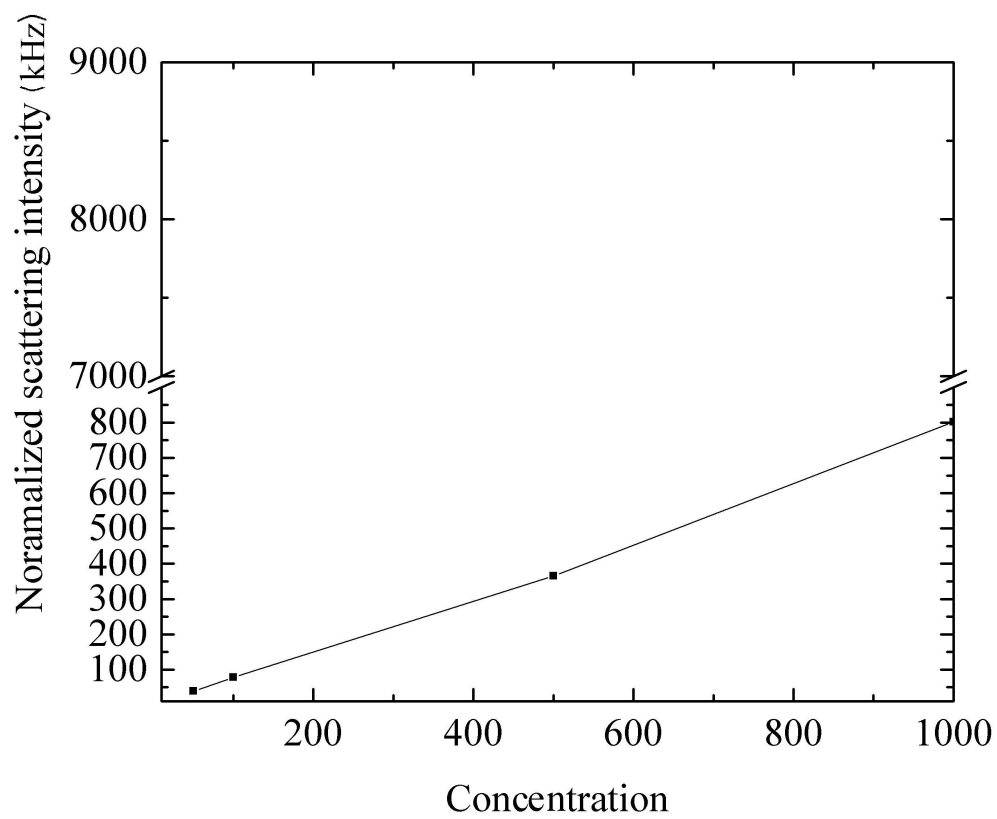


Figure A.1 – Scattering intensity from dynamic light scattering at 90° of *Snowtex*[®] 20L at different concentrations

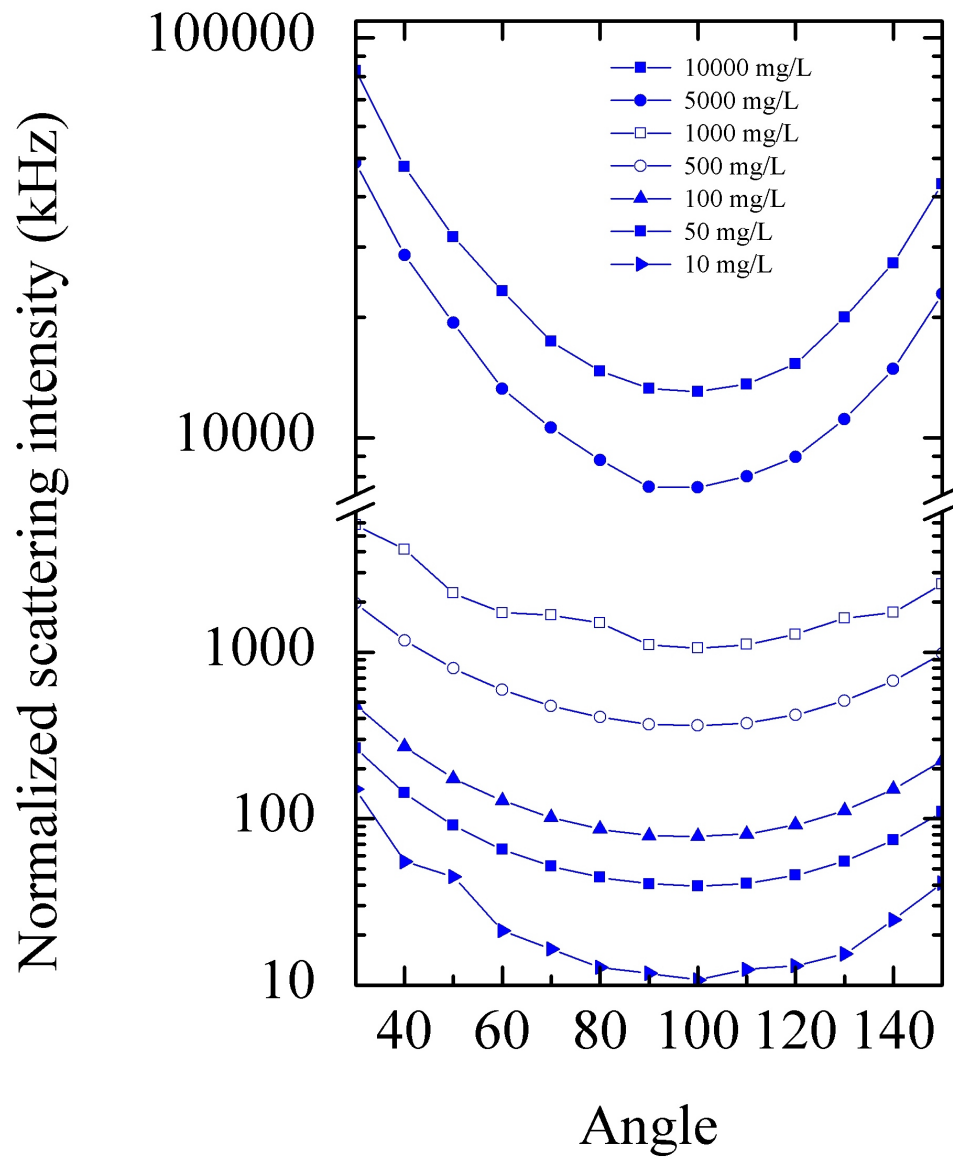


Figure A.2 – Scattering intensity from static light scattering of *Snowtex*® 20L at different concentrations

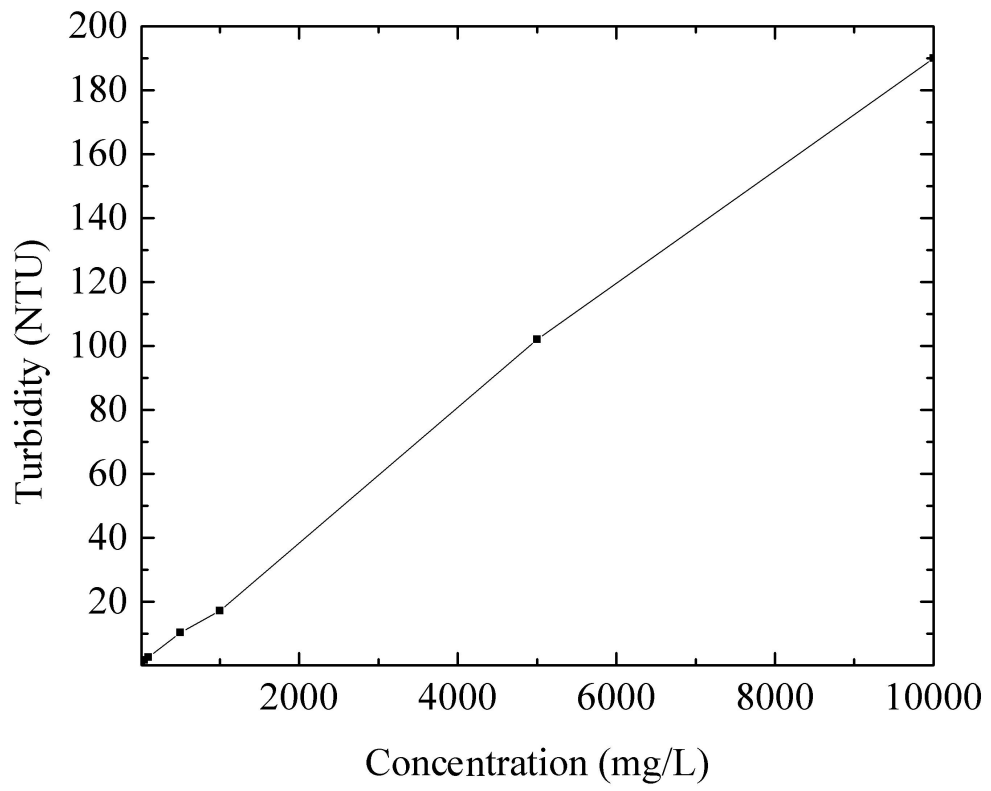


Figure A.3 – Turbidity of *Snowtex*[®] 20L at different concentrations

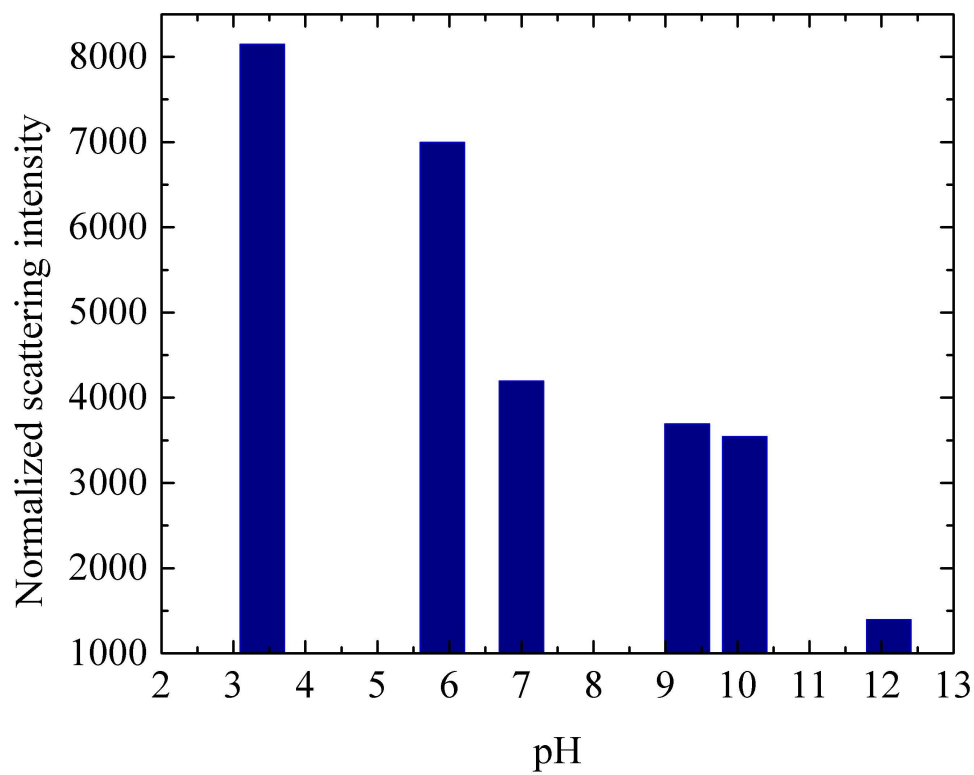


Figure A.4 – Scattering intensity from dynamic light scattering at 90° of 100 mg/L *Snowtex*[®] 20L at different pH

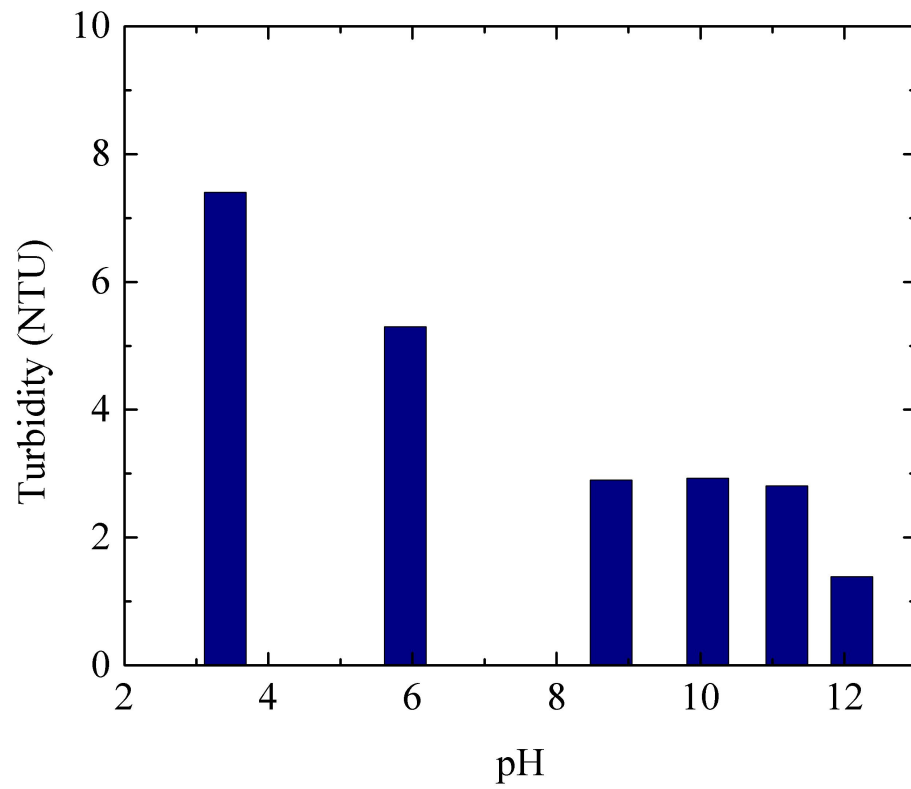


Figure A.5 – Turbidity of 100 mg/L Snowtex[®] 20L at different pH

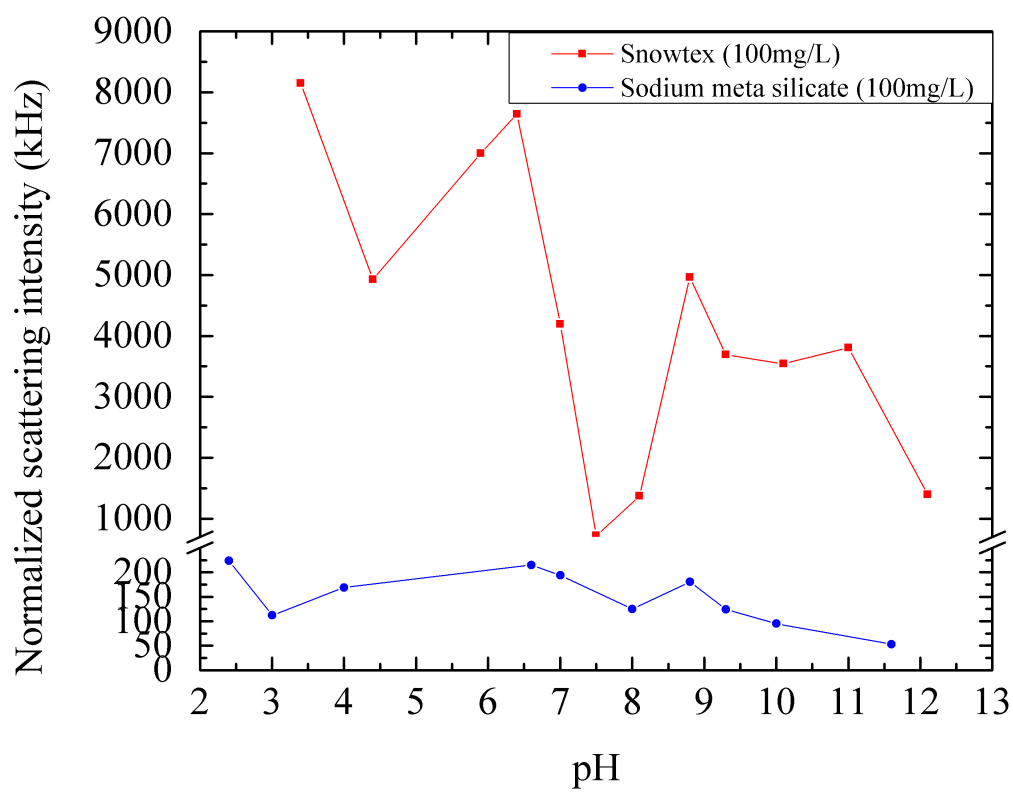


Figure A.6 – Comparison of normalized scattering intensity of *Snowtex*[®] 20L and Na_2SiO_3

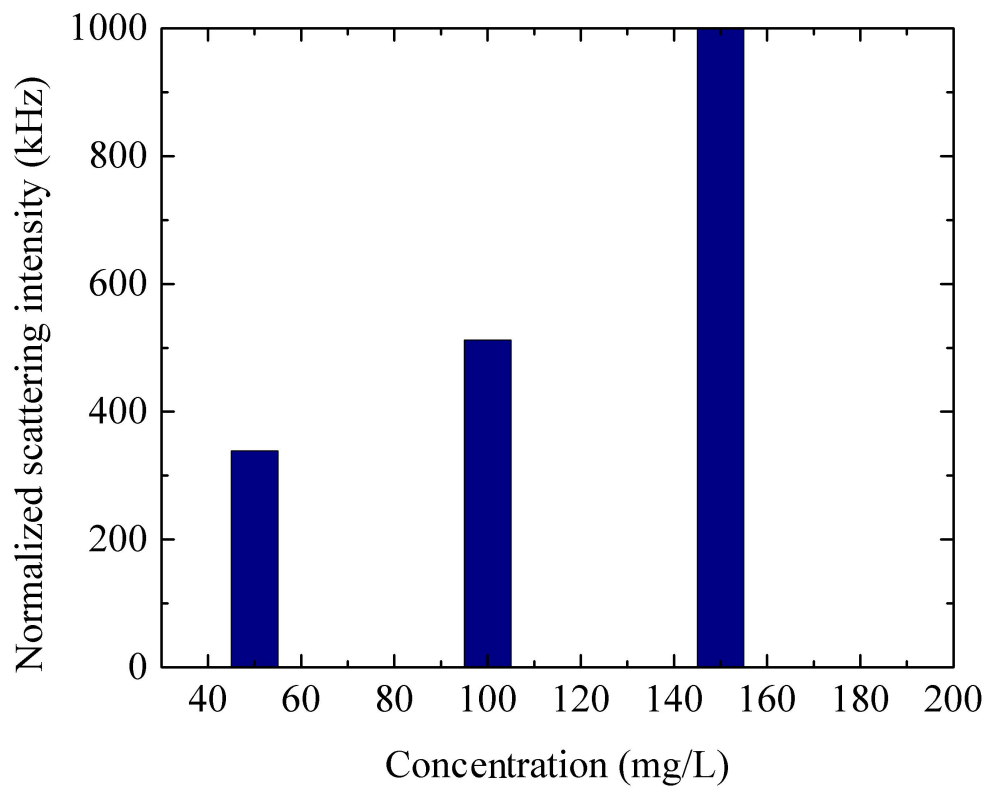


Figure A.7 – Scattering intensity from dynamic light scattering at 90° of Na_2SiO_3 at different concentrations

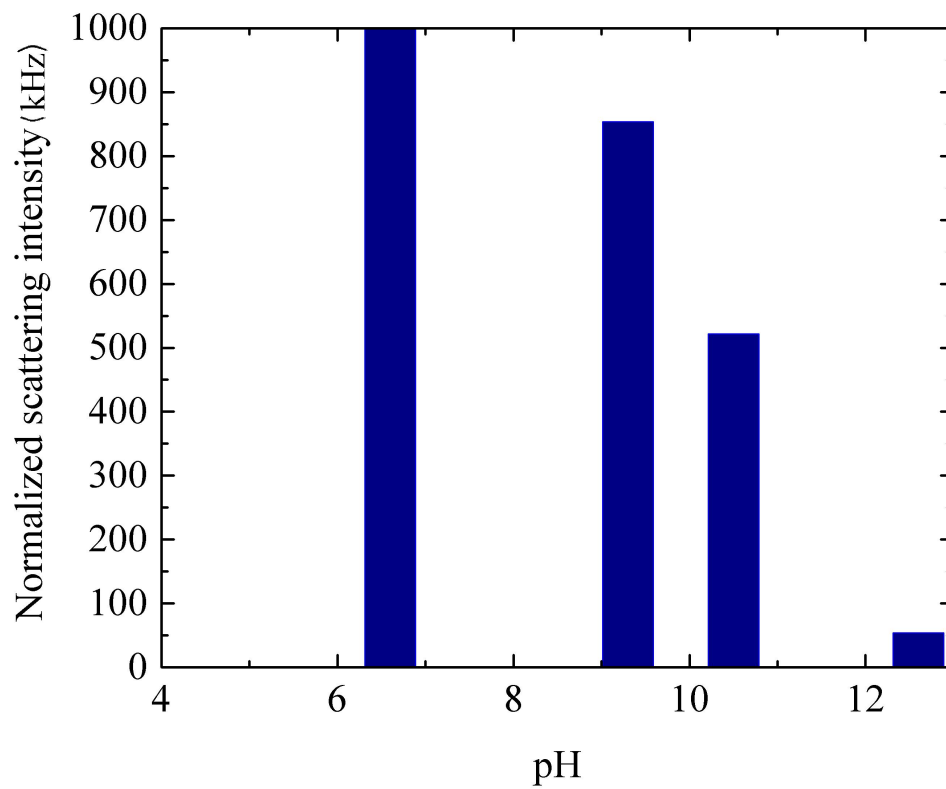


Figure A.8 – Scattering intensity from dynamic light scattering at 90° of Na_2SiO_3 (12200 mg/L) at different pH

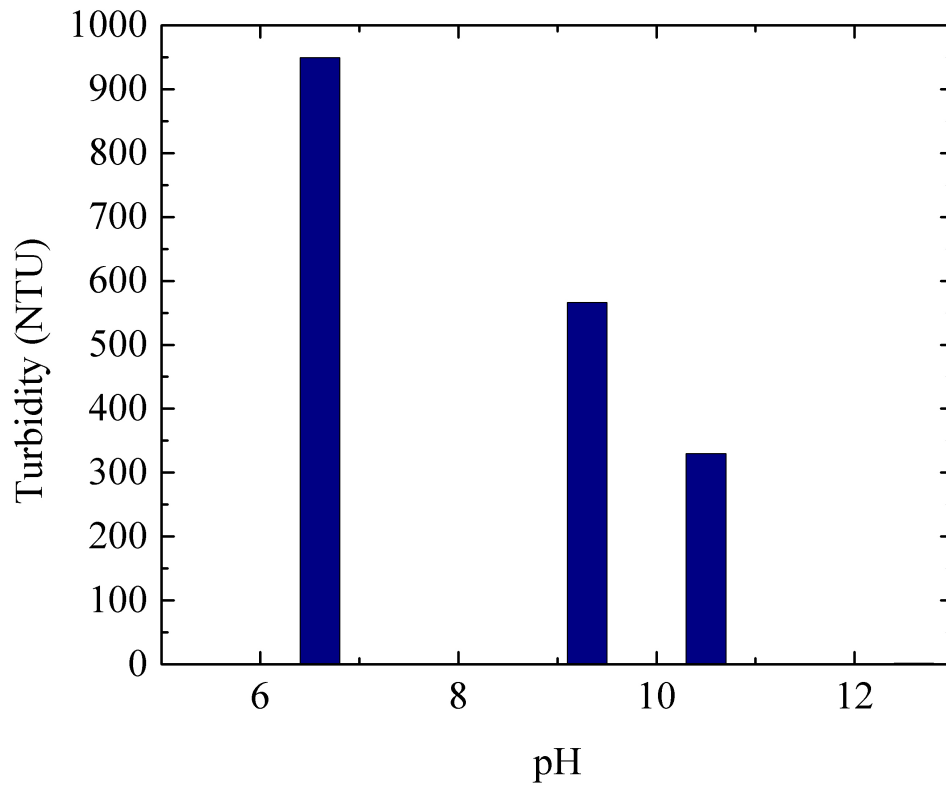


Figure A.9 – Turbidity of Na_2SiO_3 (12200 mg/L) at different pH

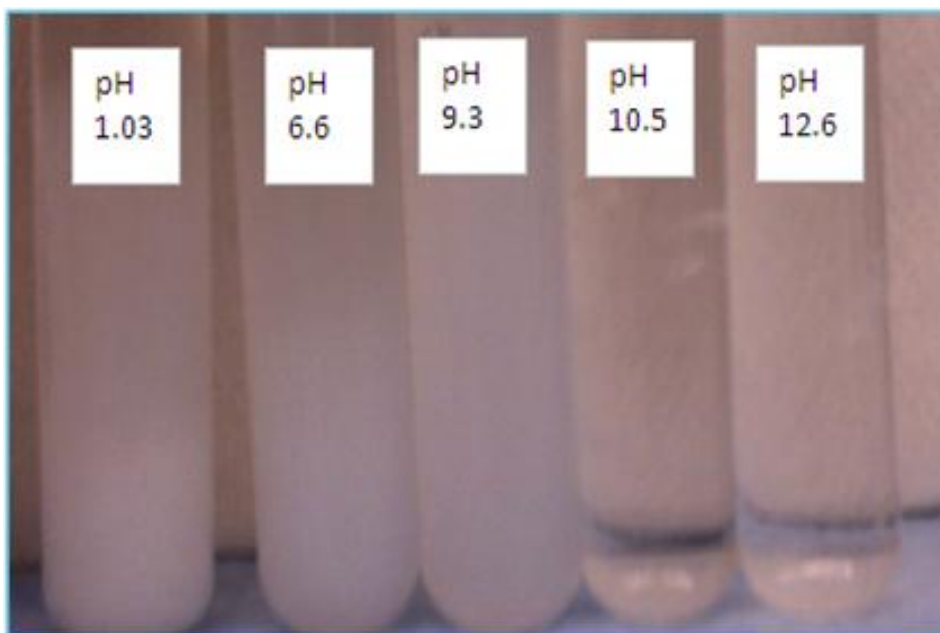


Figure A.10 – Na_2SiO_3 (12200 mg/L) at different pH

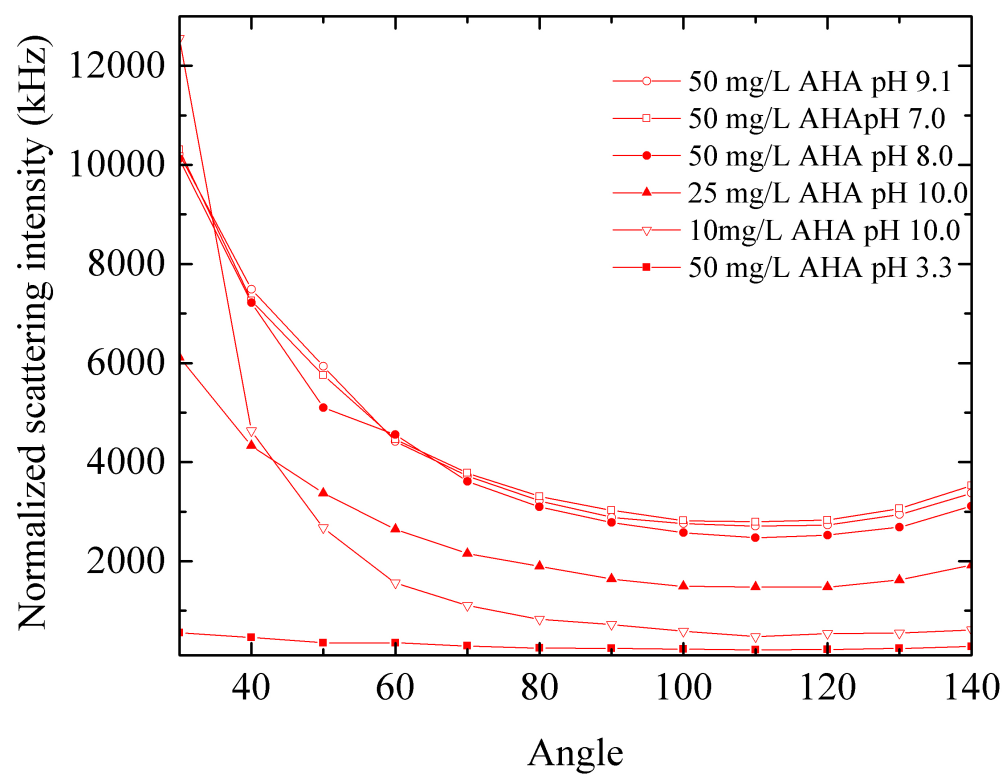


Figure A.11 – Static light scattering at different angles by AHA at different pH and concentrations

Appendix B

Fractal dimension

For a fractal object mass varies with its radius by D_f th power. D_f is called fractal dimension. So every object with a mass has fractal dimension (D_f) [Woignier et al., 1990]. Fractal dimension can be obtained by plotting scattering intensity against scattering vector (q) from static light scattering [Souza and Miller, 2001, Schaefer et al., 1984](Figure 4.9). Power law decay of static structure factor obtained from this type of plot is fractal dimension [Schaefer and Keefer, 1984].

Following table shows fractal dimension for AHA, mixture of Na_2SiO_3 and AHA at different pH and mixture of *Snowtex*[®] 20L and AHA at different pH. This data was obtained by collecting scattering intensity at different angles for all samples and calculating scattering vector q for each angle.

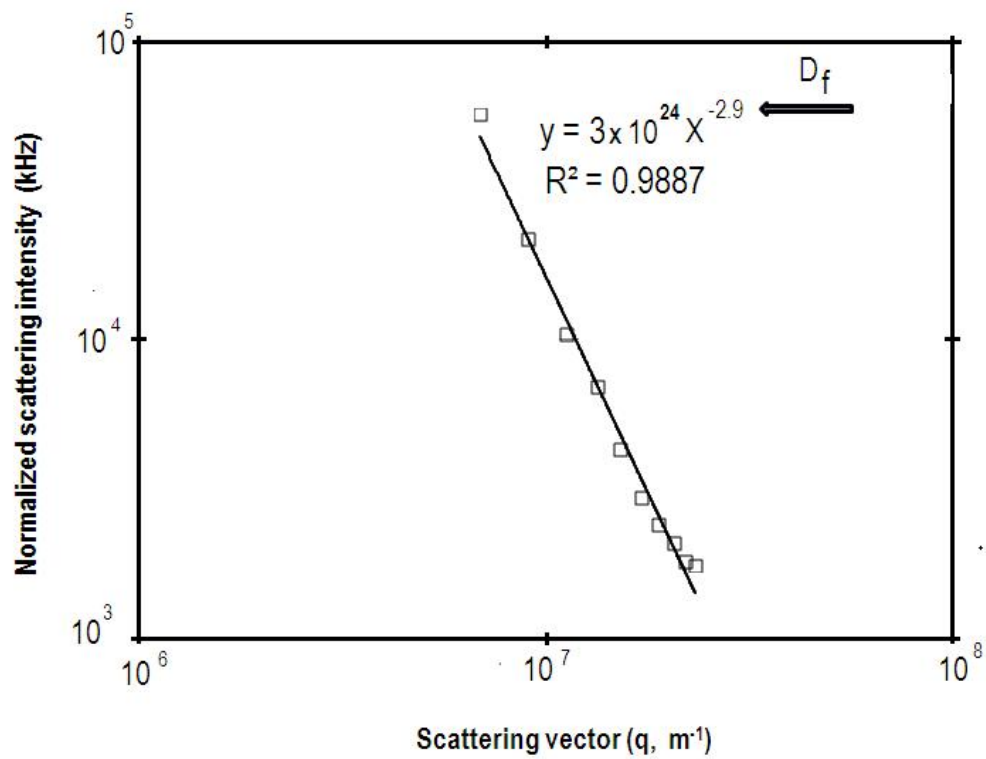


Figure B.1 – Fractal dimension measurement of 100 mg/L *Snowtex*[®] 20L and 0.1 M *NaCl* with 50 mg/L AHA at pH 3

Table B.1 – Fractal dimension

Sample	Fractal dimension
50 <i>mg/L</i> AHA with 0.1M <i>NaCl</i>	
pH 11.0	1.3
pH 9.0	1.3
pH 8	1.3
pH 7	1.2
pH 3.2	0.9
150 <i>mg/L</i> Na_2SiO_3 + 0.1M <i>NaCl</i>	
pH 11.0	3.4
pH 9.0	3.0
pH 8	3.3
pH 3.3	3.5
150 <i>mg/L</i> Na_2SiO_3 +50 <i>mg/L</i> AHA 0.1M <i>NaCl</i>	
pH 11.0	3.0
pH 9.0	3.0
pH 8	3.0
pH 3.3	3.1
100 <i>mg/L</i> <i>Snowtex</i> [®] + 0.1M <i>NaCl</i>	
pH 11.0	1.1
pH 9.0	1.1
pH 8	0.9
pH 3.3	1.7
100 <i>mg/L</i> <i>Snowtex</i> [®] +50 <i>mg/L</i> AHA with 0.1M <i>NaCl</i>	
pH 11.0	2.6
pH 9.0	2.7
pH 8.0	2.7
pH 3.0	2.9

Low fractal dimension means loose and open structure [Bushell et al., 2002]. For samples with only AHA or only *Snowtex*[®], fractal dimension varied from 1 to 1.7, which indicates presence of very weak branch polymer or sol [de Lange et al., 1995]. *Snowtex*[®] fractal dimension increases with the addition of humic acid (from 1.3 to 2.9) which indicates system in transition structure or in formation of compact structure [Ibaseta and Biscans, 2010]. Porous silica gel fractal dimension is normally vary from 2.0 to 3.0 [Bhattacharya and Kieffer, 2005]. For Na_2SiO_3 fractal dimension was found varying from 3.0 o 3.5. Since 3.0 is highest value possible for a fractal structure of any object [Rojanski et al., 1986, Bushell et al., 2002], it can be considered as error occured from multiple scattering from branched silica network [Urban et al., 2000]. But fractal dimension reduced to around 3.0 with addition of humic acid, which may be due to formation of compact structure which reduces multiple scattering. Experimental values from the above table showed that fractal dimension varied widely from 0.9 to 3.5. An object can have either 1 or 2 or 3 dimensions so fractal dimension less than 1 or greater than 3 is not possible physically. Lower than 1 or higher than 3 fractal dimension obtained from light scattering experiments can be due to experimental error or interference by dust. In addition, light scattering may not be an effective technique for studying fractal dimension of organics, and silica-organics mixture.

Appendix C

Taguchi method

C.1 Standard Taguchi L_{18} orthogonal array

L18 Orthogonal array

	Control Factors							
Expt. No.	A	B	C	D	E	F	G	H
1	1	1	1	1	1	1	1	1
2	1	1	2	2	2	2	2	2
3	1	1	3	3	3	3	3	3
4	1	2	1	1	2	2	3	3
5	1	2	2	2	3	3	1	1
6	1	2	3	3	1	1	2	2
7	1	3	1	2	1	3	2	3
8	1	3	2	3	2	1	3	1
9	1	3	3	1	3	2	1	2
10	2	1	1	3	3	2	2	1
11	2	1	2	1	1	3	3	2
12	2	1	3	2	2	1	1	3
13	2	2	1	2	3	1	3	2
14	2	2	2	3	1	2	1	3
15	2	2	3	1	2	3	2	1
16	2	3	1	3	2	3	1	2
17	2	3	2	1	3	1	2	3
18	2	3	3	2	1	2	3	1

C.2 Standard operating procedure

The objective of this project is to develop a standard and scientific operating procedure to measure organic carbon removal and identify most important factor that cause highest removal using Taguchi L_{18} experiments. This SOP describes the methods followed to measure the DOM removal rates due to colloid organic co-precipitation from the experiments designed using Taguchi L_{18} orthogonal array (OA).

Background and Project Goals

The objective of this study is to find out the most influential factors those responsible for aggregation i.e highest DOM removal in high concentration organic-colloids system. The project goal is outlined as follows:

- Find out suitable experimental design
- Prepare experimental matrix
- Prepare samples
- Analyze samples using TOC, DLS, UV-Vis spectroscopy, turbidimeter, photographs
- Analyze results using different tools (S/N ratio, ANOVA)

Health, safety and environment

- Handling: Gloves, eye protection as well as a lab coat should be used while handling the samples.
- Sample disposal: Used samples should be transferred into a closed glass container for organic waste storage.
- Cleaning: Glassware should be cleaned first with water, then with soap water and acetone and finally with DI water.
- Emergency procedure for handling Aluminium chloride
- Should be prepared in fume hood.
- Use eye protector, gloves and lab coat
- Chemicals, if used, must be disposed according to CCF lab protocols.

Materials and equipment

Materials:

- Polystyrene sulfate Particles (0.1 μ m) Interfacial Dynamics Co.
- *Snowtex*[®] (0.1 μ m) Nissan chemical
- Aldrich humic acid Sigma Aldrich
- Acid extractable organics CCF Lab
- Boiler blow down water SAGD plant
- DI Water *Purelab*[®] Ultra
- Acetone Fisher Scientific

Disposables:

- Erlene meyer flask Fisher Scientific
- Syringe (10ml) and Needle Fisher Scientific
- Microliter pipette with disposable tips Fisher Scientific

Equipment:

- TOC-VCPH analyzer ,(Shimadzu, Kyoto, Japan)

Sample preparation for baseline measurement

- Clean and dry 18 Erlenmeyer flasks.
- Label them from 1 to 18.
- Take 10 ml water using micro pipette in all flasks.
- Take 7.5, 18.75, 37.5, 7.5, 18.75, 37.5, 18.75, 37.5, 7.5 *Snowtex*[®] (100 nm) diameter for samples 1 to 9.
- Take 375,75,187.5,187.5,375,75,375,75,187.5 micro litre polystyrene latex sulfate (100nm) diameter for samples 10 to 18.
- Weight and dissolve 17.6, 175.5, 438.3,175.5, 17.6, 438.3 mg NaCl in samples 1, 4, 7,10, 13,16.
- Weight and dissolve 332.6, 831.6, 33.3, 831.6, 332.6, 33.3 mg *CaCl*₂ in samples 2, 5, 8,11, 14,17.
- Weight and dissolve 1015.13, 40.3, 405.98, 40.3, 1015.13, 405.98 mg *AlCl*₃ in samples 3,6, 9,12, 15,18.
- Add DI water to all the samples to make the volume 30 ml.
- Adjust pH of the samples 1 to 18 to 3,6,9,9,3,6, 6,9,3, 6,9,3, 9,3,6, 3,6,9 using 1N HCl and 12N and 0.1N NaOH solution.
- Put all the samples on a shaker and set the speed at 200 rpm.
- Set the shaker for 24 hours and start it.
- After 24 hours take down the samples from shaker and let them settle down for 24 hours.
- Take the supernatant carefully using micro pipette on a cleaned Petri dish.
- Use 0.22 μ m syringe driven filter to filter the samples.
- Take the filtrate in a cleaned and labeled TOC bottle.

Sample preparation for DOM removal measurement

- Clean and dry 18 Erlenmeyer flasks.
- Label them from 1 to 18.
- Take 10 ml water using micro pipette in all flasks, except for sample 3 and 10.
- Take 2 ml water for sample 3 and 10.
- Take 7.5, 18.75, 37.5, 7.5, 18.75, 37.5, 18.75, 37.5, 7.5 micro litre *Snowtex*[®] (100nm) diameter for samples 1 to 9.
- Take 375,75,187.5,187.5,375,75,375,75,187.5 micro litre polystyrene latex sulfate (100 nm) diameter for samples 10 to 18.
- Prepare stock solution of AHA by dissolving 0.2 gm of AHA in 100 ml DI water.
- Find out TOC value of AHA stock solution.
- Collect AEO and BBD, find out TOC value.
- Filter AHA, AEO, BBD through 0.45 μ m syringe driven filter.
- Add 5.1, 12.8, 25.5 ml AHA in samples 1 to 3 (using 588 mg/L TOC AHA).
- Add 1.0, 2.1, 0.4 ml AEO in samples 4 to 6 (using 8466 mg/L TOC AEO).
- Add 2.7, 6.8, 13.6 ml BBD in samples 7 to 9 (using 1100 mg/L TOC BBD).
- Add 25.5, 5.1, 12.8 ml AHA in samples 10 to 12 (using 588 mg/L TOC AHA).
- Add 2.1, 0.4 , 1.0 AEO in samples 13 to 15 (using 8466 mg/L TOC AEO).
- Add 6.8, 13.6, 2.7 ml BBD in samples 16 to 18 (using 1100 mg/L TOC BBD).

- Weight and dissolve 17.6, 175.5, 438.3, 175.5, 17.6, 438.3 mg NaCl in samples 1, 4, 7,10, 13,16.
- Weight and dissolve 332.6, 831.6, 33.3, 831.6, 332.6, 33.3 mg $CaCl_2$ in samples 2, 5, 8,11, 14,17.
- Weight and dissolve 1015.13, 40.3, 405.98, 40.3, 1015.13, 405.98 mg $AlCl_3$ in samples 3,6, 9,12, 15,18.
- Add DI water to all the samples to make the volume 30 ml.
- Adjust pH of the samples 1 to 18 to 3,6,9,9,3,6, 6,9,3, 6,9,3, 9,3,6, 3,6,9 using 1N HCl and 12N and 0.1N NaOH solution.
- Put all the samples on a shaker and set the speed at 200 rpm.
- Set the shaker for 24 hours and start it.
- After 24 hours take down the samples from shaker and let them settle down for 24 hours.
- Take the supernatants carefully using micro pipette on a cleaned Petri dish.
- Use 0.22 μ m syringe driven filter to filter the samples.
- Take the filtrate in a cleaned and labeled TOC bottle.
- Repeat the experiments at least twice.

TOC standard preparation

Accurately weight 2.125 g potassium hydrogen phthalate and take in a 1 L volumetric flask. Add DI water upto the 1 L mark and stir the solution properly.

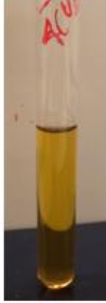
TOC analyzer Operating Procedure

- Open gas cylinder, check water levels and turn on the instrument.
- Turn on the computer and go to sample Table Editor.
- Go to new sample table , choose saline TOC, press ok, then press connect.
- Go to H/W setting in instrument tab, click TOC, choose Furnace temperature 680° and press ok.
- Go to monitor, wait at least for 30 minute to reach the temperature 680°.
- When instrument is ready all the options in monitor will be green press 1 in sample table , go to insert, then sample, then method, select appropriate method select multiple injection and auto correct of injection volume.
- Put the standard and labeled TOC bottles in sample holder.
- Select the vial and then start analysis.

Calculation

Correct all data based on calibration using TOC standard. Deduct baseline data 1 to 18 from organic containing samples 1 to 18. This is corrected data (Y). Deduct Y values from original organics concentration Z (column 6 of experimental matrix, table 4.3). This is X. Ratio of X over original organics concentration Z times 100 is the percentage removal. Analyze percentage removal data using ANOVA and MINITAB.

C.3 DOM removal through silica organic co-precipitation images

					
1 (unfiltered)	1 (filtered)	2 (unfiltered)	1 (filtered)	3 (unfiltered)	3 (filtered)
					
4 (unfiltered)	4 (filtered)	5 (unfiltered)	5 (filtered)	6 (unfiltered)	6 (filtered)
					
7 (unfiltered)	7 (filtered)	8 (unfiltered)	8 (filtered)	9 (unfiltered)	9 (filtered)

					
10 (unfiltered)	10 (filtered)	11 (unfiltered)	11 (filtered)	12 (unfiltered)	12 (filtered)
					
13 (unfiltered)	13 (filtered)	14 (unfiltered)	14 (filtered)	15 (unfiltered)	15 (filtered)
					
16 (unfiltered)	16 (filtered)	17 (unfiltered)	17 (filtered)	18 (unfiltered)	18 (filtered)

C.4 Minitab Prediction

Predicted values

Factor levels for predictions

Colloid type	Organics type	Salt type	Conc. colloid	Conc. org	Conc. salt	pH
1	1	1	1	1	1	1

S/N Ratio	Mean	StDev	Ln(StDev)
38.1171	71.375	1.47314	0.336758

Predicted values

Factor levels for predictions

Colloid type	Organics type	Salt type	Conc. colloid	Conc. org	Conc. salt	pH
1	1	3	2	1	3	1

S/N Ratio	Mean	StDev	Ln(StDev)
60.8131	129.708	-0.176777	0.173287

Predicted values

Factor levels for predictions

Colloid type	Organics type	Salt type	Conc. colloid	Conc. org	Conc. salt	pH
1	3	3	2	1	3	1

S/N Ratio	Mean	StDev	Ln(StDev)
41.4148	72.5	3.29983	0.645200

Predicted values

Factor levels for predictions

Colloid type	Organics type	Salt type	Conc. colloid	Conc. org	Conc. salt	pH
1	2	3	2	1	3	1

S/N Ratio	Mean	StDev	Ln(StDev)
60.6551	115.729	2.44541	1.13184

Predicted values

Factor levels for predictions

Colloid type	Organics type	Salt type	Conc. colloid	Conc. org	Conc. salt	pH
1	3	3	2	3	3	1

S/N Ratio	Mean	StDev	Ln(StDev)
34.0528	52.3333	2.59272	0.529676

Predicted values

Factor levels for predictions

Colloid type	Organics type	Salt type	Conc. colloid	Conc. org	Conc. salt	pH
1	1	3	1	1	3	1

S/N Ratio	Mean	StDev	Ln(StDev)
58.8524	125.313	0.677644	0.264273

Predicted values

Factor levels for predictions

Colloid type	Organics type	Salt type	Conc. colloid	Conc. org	Conc. salt	pH
1	3	3	1	3	3	1

S/N Ratio	Mean	StDev	Ln(StDev)
32.0922	47.9375	3.44715	0.620662

Predicted values

Factor levels for predictions

Colloid type	Organics type	Salt type	Conc. colloid	Conc. org	Conc. salt	pH
1	3	2	1	1	3	1

S/N Ratio	Mean	StDev	Ln(StDev)
23.0374	38.2292	4.56673	0.467006

Predicted values

Factor levels for predictions

Colloid type	Organics type	Salt type	Conc. colloid	Conc. org	Conc. salt	pH
1	3	2	2	1	3	1

S/N Ratio	Mean	StDev	Ln(StDev)
24.9980	42.625	3.71231	0.376019

Predicted values

Factor levels for predictions

Colloid type	Organics type	Salt type	Conc. colloid	Conc. org	Conc. salt	pH
1	3	2	2	3	3	1

S/N Ratio	Mean	StDev	Ln(StDev)
17.6360	22.4583	3.00520	0.260495

Predicted values

Factor levels for predictions

Colloid type	Organics type	Salt type	Conc. colloid	Conc. org	Conc. salt	pH
1	3	2	3	3	3	1

S/N Ratio	Mean	StDev	Ln(StDev)
8.17990	1.41667	7.18892	0.645200

Predicted values

Factor levels for predictions

Colloid type	Organics type	Salt type	Conc. colloid	Conc. org	Conc. salt	pH
1	3	2	1	3	3	1

S/N Ratio	Mean	StDev	Ln(StDev)
15.6754	18.0625	3.85962	0.351481

Predicted values

Factor levels for predictions

Colloid type	Organics type	Salt type	Conc. colloid	Conc. org	Conc. salt	pH
1	3	2	2	3	3	1

S/N Ratio	Mean	StDev	Ln(StDev)
17.6360	22.4583	3.00520	0.260495

Predicted values

Factor levels for predictions

Colloid type	Organics type	Salt type	Conc. colloid	Conc. org	Conc. salt	pH
1	3	2	2	2	3	1

S/N Ratio	Mean	StDev	Ln(StDev)
9.53068	11.7917	3.71231	-0.201603

Predicted values

Factor levels for predictions

Colloid type	Organics type	Salt type	Conc. colloid	Conc. org	Conc. salt	pH
1	3	2	2	1	3	1

S/N Ratio	Mean	StDev	Ln(StDev)
24.9980	42.625	3.71231	0.376019

Predicted values

Factor levels for predictions

Colloid type	Organics type	Salt type	Conc. colloid	Conc. org	Conc. salt	pH
1	3	1	1	1	3	1

S/N Ratio	Mean	StDev	Ln(StDev)
25.3810	15.2292	6.21665	1.20810

Predicted values

Factor levels for predictions

Colloid type	Organics type	Salt type	Conc. colloid	Conc. org	Conc. salt	pH
1	3	1	2	1	3	1

S/N Ratio	Mean	StDev	Ln(StDev)
27.3416	19.625	5.36223	1.11711

Predicted values

Factor levels for predictions

Colloid type	Organics type	Salt type	Conc. colloid	Conc. org	Conc. salt	pH
1	3	1	2	2	3	1

S/N Ratio	Mean	StDev	Ln(StDev)
11.8743	-11.2083	5.36223	0.539491

Predicted values

Factor levels for predictions

Colloid type	Organics type	Salt type	Conc. colloid	Conc. org	Conc. salt	pH
1	3	1	2	1	3	1

S/N Ratio	Mean	StDev	Ln(StDev)
27.3416	19.625	5.36223	1.11711

Predicted values

Factor levels for predictions

Colloid type	Organics type	Salt type	Conc. colloid	Conc. org	Conc. salt	pH
1	3	1	3	3	3	1

S/N Ratio	Mean	StDev	Ln(StDev)
10.5235	-21.5833	8.83883	1.38629

Predicted values

Factor levels for predictions

Colloid type	Organics type	Salt type	Conc. colloid	Conc. org	Conc. salt	pH
1	3	1	3	2	3	1

S/N Ratio	Mean	StDev	Ln(StDev)
2.41819	-32.25	9.54594	0.924196

Predicted values

Factor levels for predictions

Colloid type	Organics type	Salt type	Conc. colloid	Conc. org	Conc. salt	pH
1	2	3	2	1	3	1

S/N Ratio	Mean	StDev	Ln(StDev)
60.6551	115.729	2.44541	1.13184

Predicted values

Factor levels for predictions

Colloid type	Organics type	Salt type	Conc. colloid	Conc. org	Conc. salt	pH
1	2	2	2	1	3	1

S/N Ratio	Mean	StDev	Ln(StDev)
44.2383	85.8542	2.85789	0.862656

Predicted values

Factor levels for predictions

Colloid type	Organics type	Salt type	Conc. colloid	Conc. org	Conc. salt	pH
1	2	1	2	1	3	1

S/N Ratio	Mean	StDev	Ln(StDev)
46.5820	62.8542	4.50781	1.60375

Predicted values

Factor levels for predictions

Colloid type	Organics type	Salt type	Conc. colloid	Conc. org	Conc. salt	pH
1	2	1	2	2	3	1

S/N Ratio	Mean	StDev	Ln(StDev)
31.1146	32.0208	4.50781	1.02613

Predicted values

Factor levels for predictions

Colloid type	Organics type	Salt type	Conc. colloid	Conc. org	Conc. salt	pH
1	2	2	2	2	3	1

S/N Ratio	Mean	StDev	Ln(StDev)
28.7710	55.0208	2.85789	0.285033

Predicted values

Factor levels for predictions

Colloid type	Organics type	Conc. colloid	Conc. org	pH
1	1	3	3	1

S/N Ratio	Mean
36.2621	69

Predicted values

Factor levels for predictions

Colloid type	Organics type	Conc. colloid	Conc. org	pH
1	1	2	1	1

S/N Ratio	Mean
47.9680	101.917

Predicted values

Factor levels for predictions

Colloid type	Organics type	Conc. colloid	Conc. org	pH
1	1	3	3	2

S/N Ratio	Mean
29.0296	57.4167

Predicted values

Factor levels for predictions

Colloid type	Organics type	Conc. colloid	Conc. org	pH
1	1	3	3	3

S/N Ratio	Mean
30.3749	54.0833

Predicted values

Factor levels for predictions

Colloid type	Organics type	Conc. colloid	Conc. org	pH
1	2	2	1	1

S/N Ratio	Mean
44.9399	82.0833

Predicted values

Factor levels for predictions

Colloid type	Organics type	Conc. colloid	Conc. org	pH
1	3	2	1	1

S/N Ratio	Mean
33.5991	53

Predicted values

Factor levels for predictions

Colloid type	Organics type	Conc. colloid	Conc. org	pH
1	3	3	3	3

S/N Ratio	Mean
16.0061	5.16667

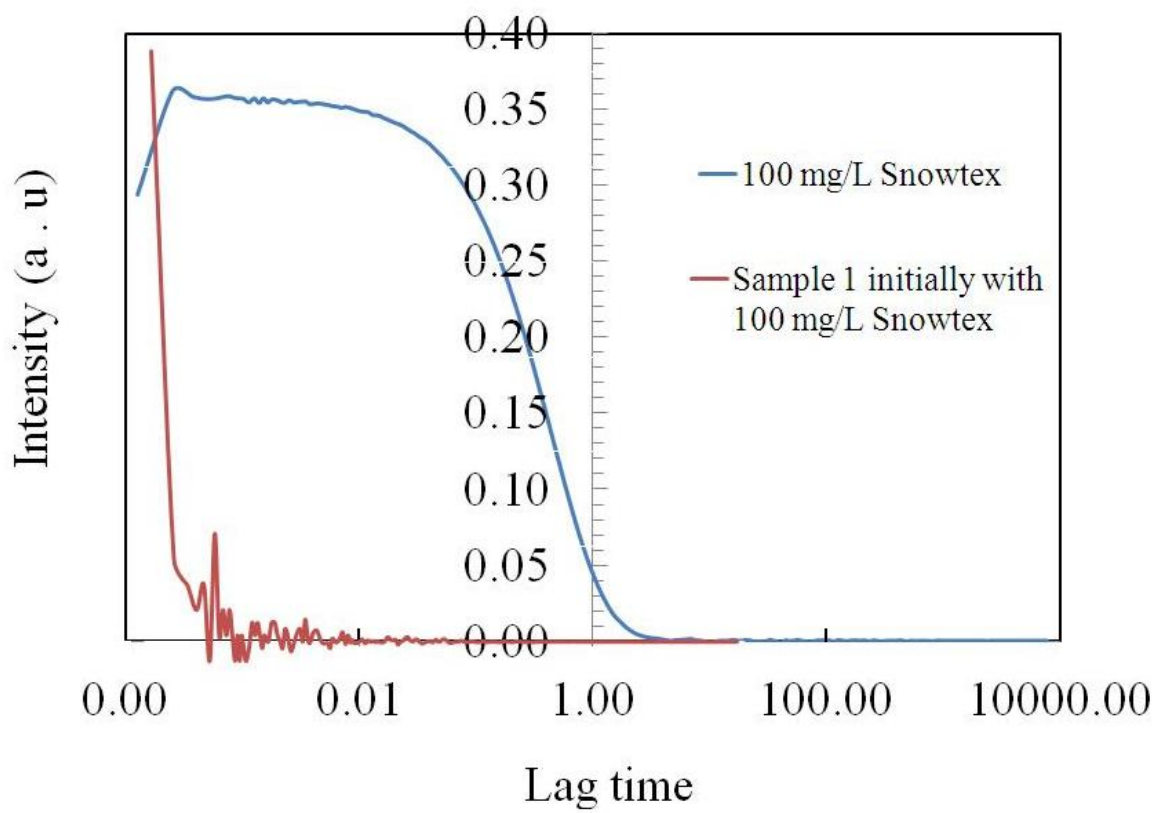
Predicted values

Factor levels for predictions

Colloid type	Organics type	Salt type	Conc. colloid	Conc. org	Conc. salt	pH
1	3	1	3	3	1	3

S/N Ratio	Mean
8.62892	-18.25

C.5 Comparison of autocorrelation functions



Appendix D

XPS analysis results

Quantification Report

/export/home/kratos/data/Sep19_2013-JannatFatema.dset Mon Sep 23 15:34:08 2013

State : Angle Name : Jannat#2

Peak	Position BE (eV)	FWHM (eV)	Raw Area (CPS)	RSF	Atomic Mass	Atomic Conc %	Mass Conc %
O 1s	529.500	3.275	31091.5	0.780	15.999	15.02	12.50
Ca 2p	345.500	2.665	42399.2	1.833	40.078	8.91	18.58
C 1s	282.500	2.846	41934.2	0.278	12.011	58.52	36.55
Cl 2p	196.500	3.281	39911.3	0.891	35.460	17.55	32.37

Quantification Report

/export/home/kratos/data/Sep19_2013-JannatFatema.dset Mon Sep 23 15:34:16 2013

State : Angle Name : Jannat#3

Peak	Position BE (eV)	FWHM (eV)	Raw Area (CPS)	RSF	Atomic Mass	Atomic Conc %	Mass Conc %
Na 1s	1069.000	2.542	81250.0	1.685	22.990	27.76	29.01
O 1s	529.000	2.729	7323.8	0.780	15.999	5.43	3.95
C 1s	282.500	3.698	17360.8	0.278	12.011	37.18	20.30
Cl 2p	196.500	3.267	39985.0	0.891	35.460	26.99	43.50
Al 2s	116.500	2.929	1871.7	0.426	26.982	2.65	3.25

Quantification Report

/export/home/kratos/data/Sep19_2013-JannatFatema.dset Mon Sep 23 15:33:43 2013

State : Angle Name : Jannat#6

Peak	Position BE (eV)	FWHM (eV)	Raw Area (CPS)	RSF	Atomic Mass	Atomic Conc %	Mass Conc %
Na 1s	1069.500	2.818	15879.6	1.685	22.990	3.29	4.40
O 1s	529.500	2.935	88310.0	0.780	15.999	39.74	36.99
C 1s	282.000	2.678	29182.5	0.278	12.011	37.94	26.51
Cl 2p	196.000	3.659	9309.2	0.891	35.460	3.81	7.87
Si 2p	100.500	2.797	4892.5	0.328	28.086	5.45	8.90
Al 2p	72.000	2.420	5173.7	0.193	26.982	9.77	15.33

Quantification Report

/export/home/kratos/data/Sep19_2013-JannatFatema.dset Mon Sep 23 15:33:43 2013

State : Angle Name : Jannat#9

Peak	Position BE (eV)	FWHM (eV)	Raw Area (CPS)	RSF	Atomic Mass	Atomic Conc %	Mass Conc %
Na 1s	1068.500	1.782	1526.0	1.685	22.990	0.28	0.39
O 1s	529.500	2.987	83367.5	0.780	15.999	33.20	31.94
C 1s	282.000	2.876	42162.5	0.278	12.011	48.51	35.04
Cl 2p	196.500	3.514	18182.5	0.891	35.460	6.59	14.06
Si 2p	100.000	1.214	577.5	0.328	28.086	0.57	0.96
Al 2p	72.500	2.563	6497.5	0.193	26.982	10.86	17.62

State : Angle Name : Jannat#12

Peak	Position BE (eV)	FWHM (eV)	Raw Area (CPS)	RSF	Atomic Mass	Atomic Conc %	Mass Conc %
Na 1s	1070.000	2.790	29843.8	1.685	22.990	7.79	10.84
O 1s	529.500	3.146	31666.2	0.780	15.999	17.94	17.37
C 1s	282.000	3.099	36836.2	0.278	12.011	60.29	43.83
Cl 2p	197.000	3.868	19223.8	0.891	35.460	9.91	21.28
Si 2p	100.500	1.840	349.0	0.328	28.086	0.49	0.83
Al 2p	72.000	2.661	1507.5	0.193	26.982	3.58	5.85

State : Angle Name : Jannat#15

Peak	Position BE (eV)	FWHM (eV)	Raw Area (CPS)	RSF	Atomic Mass	Atomic Conc %	Mass Conc %
Na 1s	1069.000	2.643	75932.5	1.685	22.990	30.77	31.10
O 1s	529.000	2.578	3442.5	0.780	15.999	3.03	2.13
C 1s	282.500	3.264	13655.0	0.278	12.011	34.69	18.32
Cl 2p	196.500	3.309	37102.5	0.891	35.460	29.71	46.31
Al 2s	117.500	3.051	1076.3	0.426	26.982	1.81	2.14

State : Angle Name : Jannat#18

Peak	Position BE (eV)	FWHM (eV)	Raw Area (CPS)	RSF	Atomic Mass	Atomic Conc %	Mass Conc %
Na 1s	1069.000	2.612	89102.5	1.685	22.990	35.76	34.73
O 1s	529.000	2.751	6852.5	0.780	15.999	5.97	4.03
C 1s	282.500	3.785	10065.0	0.278	12.011	25.32	12.85
Cl 2p	196.500	3.337	38222.5	0.891	35.460	30.31	45.39
Al 2s	116.500	2.902	1585.0	0.426	26.982	2.63	3.00